2014

MEASURING HEAD IMPACT CONTACT PRESSURE IN COLLEGIATE FOOTBALL GAMES TO CORRELATE HEAD KINEMATICS TO BRAIN KINETICS ELUCIDATING BRAIN INJURY DYNAMICS

Chandrika S. Abhang
Michigan Technological University

Follow this and additional works at: https://digitalcommons.mtu.edu/etds
Part of the Biomechanical Engineering Commons

MEASURING HEAD IMPACT CONTACT PRESSURE IN COLLEGIATE FOOTBALL GAMES TO CORRELATE HEAD KINEMATICS TO BRAIN KINETICS ELUCIDATING BRAIN INJURY DYNAMICS

By

Chandrika S. Abhang

A REPORT

Submitted in partial fulfillment of the requirements for the degree of

MASTER OF SCIENCE

In Mechanical Engineering

MICHIGAN TECHNOLOGICAL UNIVERSITY

2014

This report has been approved in partial fulfillment of the requirements for the Degree of MASTER OF SCIENCE in Mechanical Engineering.

Department of Mechanical Engineering – Engineering Mechanics

Report Advisor: *Dr. Gopal Jayaraman*

Committee Member: *Dr. Ibrahim Miskioglu*

Committee Member: *Dr. Mahesh Gupta*

Committee Member: *Dr. Allan Struthers*

Department Chair: *Dr. William Predebon*

To my mother and grandfather

Table of Contents

List of Figures

List of Tables

Acknowledgments

First of all, I would like to thank my mother, Manorama Abhang for recognizing and believing in my potential. Her courage to attain the difficult and belief in me has brought me this success today. Words are indeed less to appreciate her efforts and hardships she has gone through to bring me to the stage I am today. I am deeply grateful for her relentless support in all aspects of my life. I thank God for giving me such a great mother!

I am thankful to my advisor Dr. Gopal Jayaraman for his guidance and support in completion of my Master's program. I would like to thank David Labyak for his constant support and reviews on my work. I wouldn't have completed my work without the support of these two. Thanks to the rest of my defense committee, Dr. Allan Struthers, Dr. Mahesh Gupta and Dr. Ibrahim Miskioglu for taking time to review my work. I would like to thank my research colleague and lab-mate Krishnatej Bhamidipati for providing me with the essential data of drop tests and pressure films.

Thank you to Kohler Co. and my Kohler colleagues for supporting me during the end phase of my Master's program.

Last but not the least; a special thank you to my best friends at MTU: Ranjeeth Naik, Yogita Uplane and Jayesh Borde for emotionally supporting me throughout my research days. The discussions and chats I had with you all helped me resume my work with renewed enthusiasm!

Abstract

Does a brain store thoughts and memories the way a computer saves its files? How can a single hit or a fall erase all those memories? Brain Mapping and traumatic brain injuries (TBIs) have become widely researched fields today. Many researchers have been studying TBIs caused to adult American football players however youth athletes have been rarely considered for these studies, contradicting to the fact that American football enrolls highest number of collegiate and high-school children than adults. This research is an attempt to contribute to the field of youth TBIs.

Earlier studies have related head kinematics (linear and angular accelerations) to TBIs. However, fewer studies have dealt with brain kinetics (impact pressures and stresses) occurring during head-on collisions. The National Operating Committee on Standards for Athletic Equipment (NOCSAE) drop tests were conducted for linear impact accelerations and the Head Impact Contact Pressures (HICP) calculated from them were applied to a validated FE model. The results showed lateral region of the head as the most vulnerable region to damage from any drop height or impact distance followed by posterior region. The TBI tolerance levels in terms of Von-Mises and Maximum Principal Stresses deduced for lateral impact were 30 MPa and 18 MPa respectively. These levels were corresponding to 2.625 feet drop height. The drop heights beyond this value will result in TBI causing stress concentrations in human head without any detectable structural damage to the brain tissue. This data can be utilized for designing helmets that provide cushioning to brain along with providing a resistance to shear.

1. Introduction

Could your brain be accessed by a computer after you die? Is it possible to retain it with all its thoughts and feelings? How about uploading your brain into a robot? This is not a sci-fi movie plot but a thought from arguably, the most intelligent man on planet – Stephan Hawking. He believes that human brain is like a computer program of one's body. So, theoretically it can be synced to a computer. Technology could make it happen in future thus providing us a form of life after death [1]. Brain Preservation Foundation is trying to preserve the brain along with its memories, emotions and consciousness. They are working on chemical fixation, plastic embedding and three-dimensional structuring techniques for the same [2]. Dmitry Itskov wishes to attain cybernetic immortality through his 2045 Initiative. He believes someday he will be able to upload his brain into a robot [3]. Neurovigil Inc. has become successful in developing a device called as iBrain which analyzes brain signals and converts them into text-based speech reader. This device will be launched soon with its first demonstration by Stephan Hawking probably replacing his current infrared speech-reading device. iBrain will also be used to treat traumatic brain injuries and understand diseases like Alzheimer's, autism, epilepsy and other neuropathologies [4]. These ambitious projects, high-end technologies and intelligent minds are working towards finding answers to a few basic questions – What happens inside a brain when we think? How does it infer through logical reasoning and observations? To sum it up -- How exactly does a brain work?

Brain research has got a new boost with the BRAIN (Brain Research through Advancing Innovative Neurotechnologies) Initiative launched by National Institutes of Health (NIH) and the Obama government. Also known as the 'Brain Activity Map' project, it literally aims towards mapping activity of every neuron in the human brain. This initiative will generate a dynamic brain model explaining interaction of individual cells and complex neural circuits in both space and time [5]. This will help us to understand how brain functions ultimately helping us to treat and prevent brain disorders. Brain disorders, more specifically traumatic brain injuries (TBIs) have become a major cause of physical impairment, social disorder and death. Motorcycle and car accidental injuries, sports related injuries and injuries to military personnel due to war-like situations are few of the most discussed areas in the field of neurotrauma.

This research is an attempt to contribute to this field of sports related head injuries by finding a method to detect sites of traumatic brain injuries through experimental laboratory-based drop tests and finite element methods.

1.1 Head Injury Facts

To help understand the procedures carried out during this research a brief introduction to the field of head injuries is given in this section. Importance of studying traumatic brain injuries, its causes and effects on the quality of life are presented. Basic anatomy of human head is presented in Appendix D for further reading. Pros and cons of existing methods to detect the traumatic brain injuries and concussions are also discussed in this section. A summarized objective of the research and the strategy followed to achieve it is presented at the end of this section.

1.1.1. Epidemiology of head injury

In United States, about 1.4 million people [6] or 1 out 53 individuals [7] are exposed to traumatic brain injuries (TBIs) every year. Years 2001 to 2010 saw 70 percent increase in the rate of TBI-related emergency department visits and 11 percent increase in hospitalizations [8, 9]. An age-group based statistical data shows that a large proportion of children (92.7%) show TBI-related emergency department visits than older adults (59.7%) [10]. 75 percent [11] or 3 out of 4 of these injuries are mild traumatic injuries (mTBIs or concussions) [6] and yet the most ignored ones. People have common misconceptions that concussions are not serious injuries and that they get cured after a few days of rest. These misconceptions are evident from a research done by DeMatteo and her team at McMaster University. The research shows that children diagnosed for concussion were discharged early from the hospitals and resumed activity earlier than they should [12]. This might increase the risk of a repeat injury occurs to about 3.5 million people each year [13]. Contradictory to people's misconceptions, mild TBIs are responsible for lasting damage of white matter which closely resembles the brain pattern of Alzheimer's dementia [14]. Studies also show that abnormalities in gray matter of the frontal cortex last for four months after concussion [15]. Measurable global and regional brain atrophy is observed even after one year of head impact [11]. These effects might worsen after the repeated injury and might result in permanent impairment of cognitive senses. TBIs increase the risk of stroke by tenfold [7] and make the injured 30 percent [16] more likely to suffer from it. This is a grave situation since multiple areas of brain seem to get affected due to an impact.

Studies also show that approximately 15% of falls or blunt traumas are traced back to sports. These falls or blunt traumas are also the second leading cause of TBI [9]. Football being one of the most fan-followed sports in US [17], is also enlisted as one of the highest concussion-incident sport along with boxing, hockey, rugby, soccer and basketball [18]. Many studies have been conducted for studying the effects of TBIs on adult athletes but no substantial data is available for young athletes considering American football has most number of young participants from high school and college levels [17]. Diagnosis of depression due to TBI in children and adolescents has increased 4.9 fold [19]. Suicidal tendencies in children are also seen to increase. The children suffering from Attention Deficit Hyperactivity Disorder (ADHD) are more prone to the moderate disability [20] whereas the ones sensitive to light and sound might develop emotional symptoms like anxiety and irritability or aggression [21] due to mild TBI.

Despite the knowledge of risks involved in repeated TBI, young athletes are usually reluctant in reporting the concussions to their coaches or parents. Most of them continue playing even after concussion and few of them even think they have a responsibility to play important games inspite of concussions [22]. Thus, development of safe tackling techniques and awareness about concussion amongst athletes, coaches and parents is not enough to avoid risks involved. Method for detecting on-field concussions should be developed to understand the severity of the injury suffered by the brain during games and mostly during practice sessions.

1.1.2. Available Methods for mTBI or Concussion detection

For years, clinicians have used neurocognitive testing to detect concussions on-field. This method is based on measuring reaction time, attention span, working memory of the player before and after the impact. This measurement is carried out by recording the responses of athletes to simple questionnaires and vision and speech tests. It also depends on athletes self-reporting their symptoms accurately. These responses can be easily forged or go unreported from player's end in order to continue playing in the game. Thus this method involves subjective evaluation. Probability of error in detecting the severity of injury is more in these tests.

Earlier imaging studies like MRI and CT scans compared non-concussed brains with concussed brains but were not able to compare severity amongst the concussed individuals. Most researchers have assumed the concussed areas of brain to be same for all patients which is practically impossible considering the unique head anatomies and various angles of impacts. Imaging techniques have evolved a lot since then. A Diffusion Tensor Imaging (DTI) technique that gives a value called Fractional Anisotropy (FA) is developed. Fractional Anisotropy or FA is a value recorded based on the movement of water in the white matter. Uniform water movement signifies healthy white matter and gives a high value of FA whereas a damaged white matter has more random water movement giving a lower FA value. This technique is however detecting changes to the brain structure on a macroscopic level. It is detecting areas that might have lesions, bruising, blood clots or tissue tears due to severe impact [14, 11]. However, minor changes caused due to mild TBIs might go unregistered. Another disadvantage of this technique is that it cannot be made available rapidly on-field for diagnosis.

University of Virginia (UVA) School of Medicine has discovered a method that uses Positron Emission Tomography (PET) scans and body's immune response to a brain injury. It is called the 'Trojan Horse' technique. Neutrophils[1] respond to the TBI and reach the injured area through blood vessels in brain. Researchers of UVA have attached radioactive tracers on these neutrophils which can be detected through PET scans. This helps to trace the areas affected due to TBI at the cellular or molecular level. Similar technique exists to detect lung infections however this is an in-development process yet to be proven for various brain injuries [23]. A portable PET scanner and necessary on-field instrumentation can make this technique accessible and feasible.

S100B, a brain protein and a well-accepted biomarker for traumatic brain injury can be detected through an on-field blood test. However, it has been observed that levels of this protein increase even after physical exertion. Research is being done to differentiate these occurrences from actual concussions [24]. This test if developed would help gauge the severity of brain injury rapidly.

Another similar test conducted by George Mason researchers, analyses saliva of the players before and after concussion. Changes in the saliva protein might be able to predict occurrences of concussion. This tool if developed would be non-invasive, without any threat of infection, easy to use and rapid to give results [25].

[1] Neutrophils are the white blood cells which are a part of immune response of body to any injury.

Numerous efforts are being done to develop techniques that are on-field diagnostic, repeatable, reproducible, non-invasive, without any threat of infection and most importantly objectively evaluated i.e. independent of player response or doctor's judgment. Engineering biomechanics of brain injury is one of the solutions to this problem and the basis of this research.

Wayne State Tolerance (WST) Curve [26] (Figure 1.1) was developed by subjecting anaesthetized animals, embalmed cadavers and human volunteers to linear frontal head impacts. This was a preliminary attempt of relating linear impact accelerations of human head to pulse duration causing skull fracture and head injury. However, in this method since the tolerance limit for head injury was based off of skull fracture limit, a precise method to determine just the head injury tolerance level should be devised.

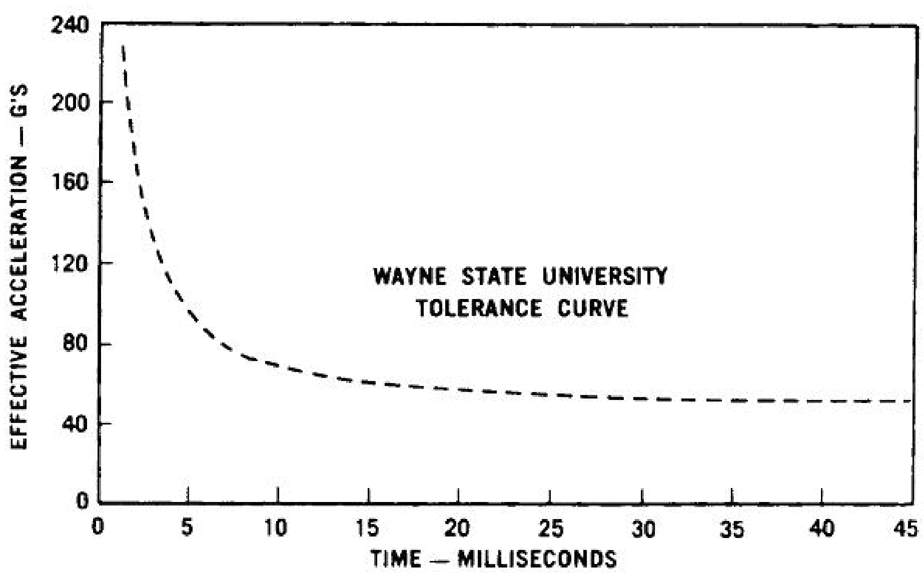

Figure 1.1Wayne State Tolerance Curve [26]

Anna Oeur and her research team at University of Ottawa have tried to determine these tolerance levels for non-persistent concussions, persistent concussions and TBIs through their study [27]. The linear and angular impact acceleration tolerance limits causing injuries are derived by her team as shown in Figure 1.2. These tolerance levels will be used as a basis in this research.

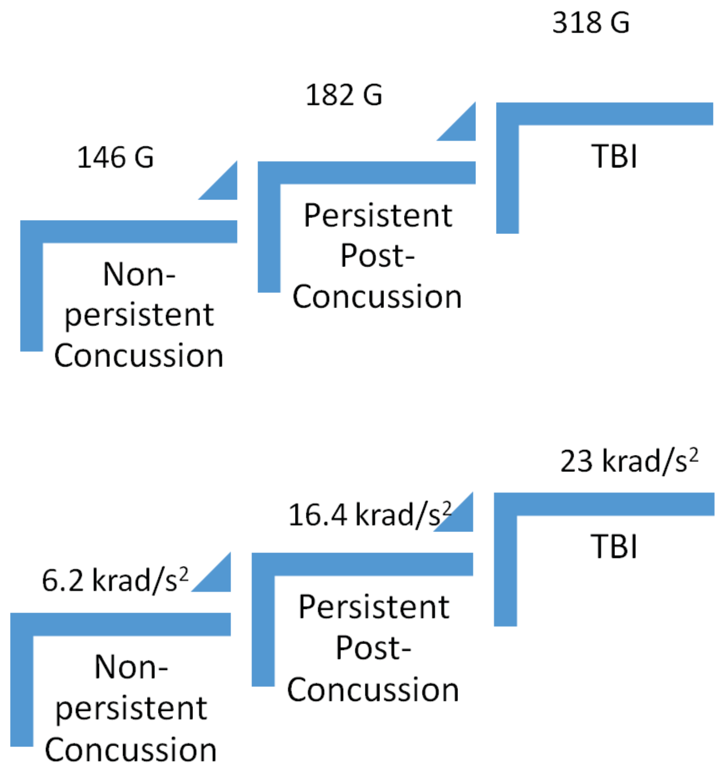

Figure 1.2 Linear (top) and Angular (bottom) Acceleration Tolerance levels of concussions and TBIs [27]

1.2 Scope of study

1.2.1 Objective

The main objective of this study is to contribute to the field of youth TBIs and correlate head kinematics with brain kinetics to explain brain injury dynamics. Specifically, this study will address the following questions:

- Do angular impact accelerations play a prominent role in causing TBI along with linear impact accelerations?
- Can a TBI criterion be derived through their relation?
- Do TBIs causing high stress concentrations also cause detectable structural damage in the brain tissue?
- Do impact tolerances with respect to impact regions on human head?

1.2.2 Strategy

To address these questions, following milestones were established:

- Conduct NOCSAE drop tests to acquire linear accelerations and impact pressures.
- Carry out analytical procedures to determine impact pressures and angular accelerations from available linear accelerations and headform dimensions.
- For various impact regions, determine relationship between linear and angular accelerations (at specific drop heights).
- Subject the validated FE model to impact pressures on frontal, 45 to frontal, lateral and posterior regions of head
- Correlate stress distributions from FE simulations to concussion tolerance levels and determine concussion-related pressures and stresses.

2. Methods and Materials

The aim of this research was to find a correlation between head impact pressure and linear - angular acceleration as well as to derive the effect of impact pressure in terms of Von-Mises and Maximum Principal Stresses on human head model. NOCSAE drop tests, analytical procedures and finite element simulations were carried out to obtain these correlations. In order to help understand the research procedures better, this section will start with a brief introduction to head injury mechanism and proceed with the details on procedures.

2.1 Head Injury Mechanism

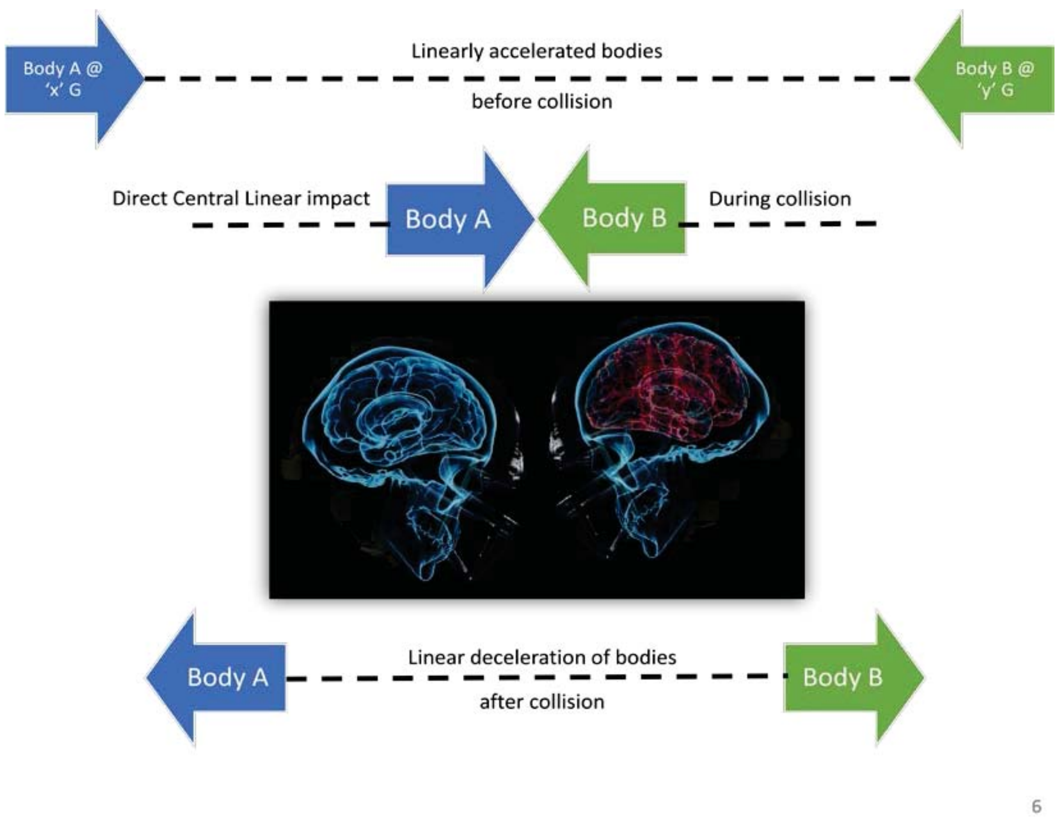

Figure 2.1 Pictorial representation of head-on collision in American football games to explain head injury mechanism

Referring to Figure 2.1, consider two football players running towards each other at different linear accelerations. Assuming that the impact is direct central linear impact i.e. both the bodies are hitting each other in a straight line then the transmission of energies from one body to other will occur. The two bodies will experience a reactive impact force pushing them in opposite directions and decelerating them.

To simulate the above (Figure 2.1) on-field conditions in the lab we conducted the National Operating Committee on Standards for Athletic Equipment (NOCSAE) drop tests.

2.2 NOCSAE Drop Tests for Linear Impact Accelerations

NOCSAE Drop Test instrumentation was setup in Michigan Technological University's Biomechanics Laboratory for experimentation. A NOCSAE Dummy Head Form was chosen for these tests. This head form was equipped with uniaxial accelerometers which were connected to Siglab data acquisition system. These accelerometers recorded linear acceleration values experienced by the headform due to drops from various heights.

NOCSAE Head form was oriented to focus various regions as impact locations; namely frontal, posterior, lateral & 45^0 to the frontal region. It was allowed to fall freely on an impactor[2] from four different heights: 2, 3, 4 and 5feet. A thin impactor was chosen for this study to incorporate the adverse impact conditions. Instantaneous linear impact acceleration values were recorded by the accelerometers for each location in X, Y and Z axes.

[2] Impactor is an anvil like cylindrical structure having padded top layer and solid steel base. It is used to simulate collision effect among the headform and a hard surface.

The NOCSAE drop test experimentation setup is shown in Figure 2.2

Figure 2.2 NOCSAE Drop Test: Photograph of Experimental Setup similar to that in MTU, MEEM Biomechanics Lab

(Image Courtesy : http://moravianequipment.blogspot.com/2013/05/this-is-how-football-helmets-are.html)

Linear impact accelerations were derived from these tests.

2.3 Analytical Calculations for Angular Impact Accelerations

NOCSAE drop tests yielded linear impact acceleration values as a function of time for entire drop cycle. Only major impact event spanning from 0 to 5.468 msec (Figure 2.3) was considered for this study and other acceleration values were ignored.

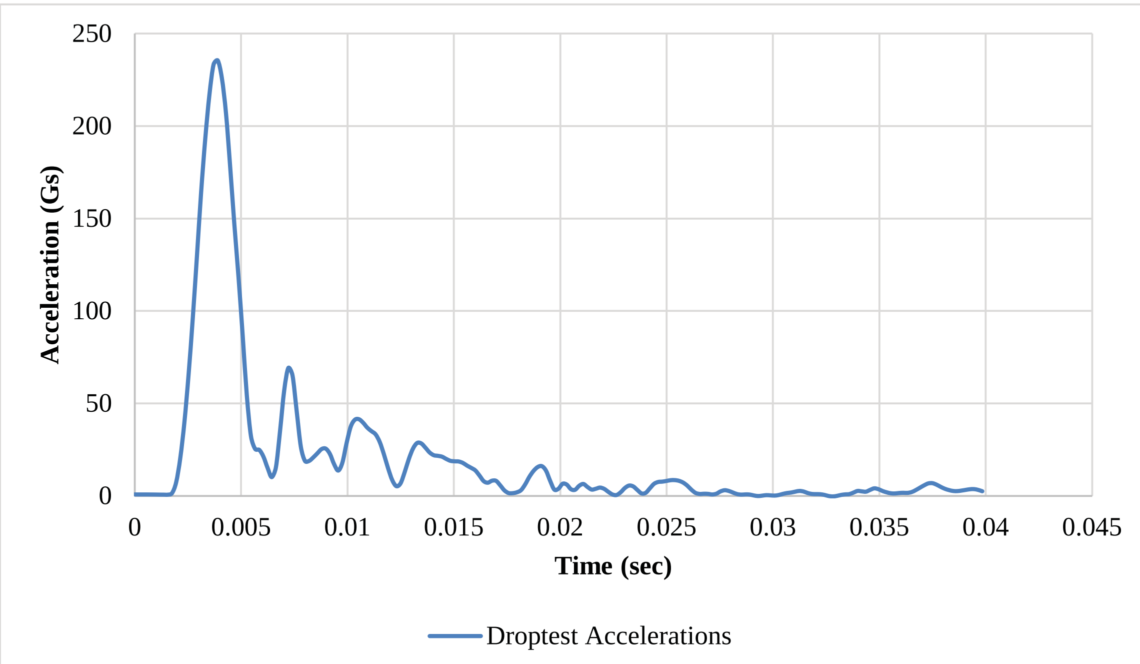

Figure 2.3 Plot of experimentally measured linear accelerations as a function of time

Newton's second law states, "The rate of change of momentum of a body is proportional to the impulse impressed on the body, and happens along the straight line on which that impulse is impressed". It is mathematically expressed as:

$$\vec{F} = \frac{d\,(m\,\overrightarrow{v})}{dt}$$

$$= m\left(\frac{d\vec{v}}{dt}\right)$$

$$\vec{F} = m\,\vec{a} \qquad \dots(E1)$$

Where 'F' is resultant force applied, 'm' is mass (constant) of the body and 'a' is acceleration of the body.

Applying the same equation to this case, impact force 'F_i' was calculated from acceleration acquired through drop tests and mass of head form which was 4.716 kg. The acceleration values were in 'Gs' which were converted to 'm/s^2' for calculation purposes. Thus equation (E1) modifies as:

$$\vec{F_i} = m_{headform} \,.\, \vec{a}_{droptest} \qquad \dots(E2)$$

In order to gauge the effect of an impact in terms of angular acceleration on human head, an attempt to quantify values of angular acceleration through analytical methods was done.

The procedure used for the same is as explained in the following section.

Newton's second law for rotational motion is mathematically expressed as,

$$\vec{T} = I \,.\, \vec{\alpha} \qquad \dots(E3)$$

Where, T = Torque or moment (in this case) the body is subjected to

I = Mass moment of inertia in $kg\text{-}m^2$

α = angular acceleration in rad /s^2

Torque or moment is also expressed as a cross product of moment arm and force vector and mathematically expressed as:

$$\vec{T} = \vec{r} \; x \; \vec{F_i} \qquad \dots(E4)$$

Where, r = position vector from the axis of rotation to the point of impact in meters

F_i = impact force in N

Substituting appropriate values of r_x, r_y, and r_z for corresponding F_x, F_y, and F_z, torque values can be determined about X, Y and Z axes.

Thus, equation E3 can also be written as:

$$\vec{\alpha} = \frac{\vec{T}}{I} \quad \ldots (E5)$$

Substituting appropriate values of torque (moment) from equation (E4) and moment of inertia for X, Y and Z axes in equation (E5) one gets:

$$\vec{\alpha}_{xx} = \frac{\overrightarrow{T_x}}{I_{xx}} \quad \ldots (E6)$$

$$\vec{\alpha}_{yy} = \frac{\overrightarrow{T_y}}{I_{yy}} \quad \ldots (E7)$$

$$\vec{\alpha}_{zz} = \frac{\overrightarrow{T_z}}{I_{zz}} \quad \ldots (E8)$$

Where, α_{xx}, α_{yy}, α_{zz} are angular accelerations with respect to X, Y and Z axes

Thus, the resultant angular acceleration will be

$$\alpha_R = \sqrt{a_{xx}^2 + a_{yy}^2 + a_{zz}^2} \quad \ldots (E9)$$

These values are calculated for frontal, posterior, lateral and 45 to frontal impacts from 2, 3, 4 and 5 feet drop heights. The tabulated calculations (excel calculator) can be referred in Appendix C

These results are used to plot linear and angular accelerations against various drop heights and locations and to propose a TBI criterion based on linear and angular impact accelerations.

2.4 Impact Pressure Measurement

Along with linear impact acceleration measurements, impact pressure measurements were also carried out simultaneously. In order to do that, NOCSAE drop test impactor was covered with medium scale pressure sensitive Fujifilm Prescale (or pressure films) provided by Sensor Products Inc.. These pressure films are mylar based films which contain a layer of tiny microcapsules which rupture with application of force in turn producing image of pressure variation across the contact area. Medium scale was chosen over lower scale pressure film in order to ensure that higher values of pressures get captured precisely. It also ensured that lower values do not superimpose the critical or required higher pressure values.

The cross-sectional image acquired from the website of Sensor Products Inc. (Figure 2.4) is shown below for better understanding.

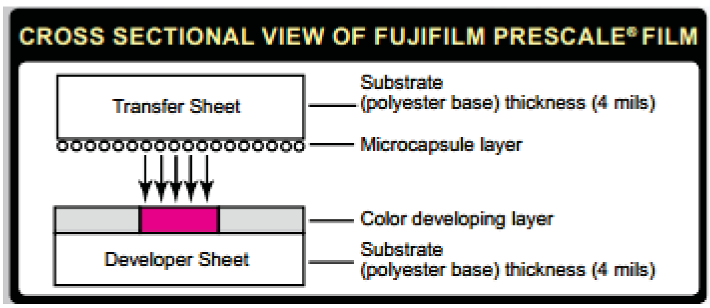

Figure 2.4 Cross section of a Fujifilm Prescale from Sensor Products Inc. website [28]

Actual physical pressure imprint caused on Fujifilm prescale due to Frontal 2feet impact is shown in Figure 2.5.

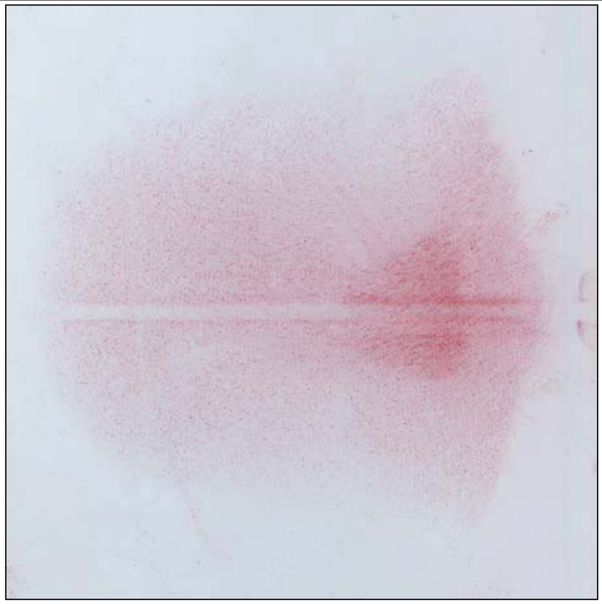

Figure 2.5 Sample Fujifilm prescale (pressure film) showing 2 feet drop impact

Topaq analyzer scanned these pressure films and displayed numerical values of pressure variations on the impacted area as shown in Figure 2.6.

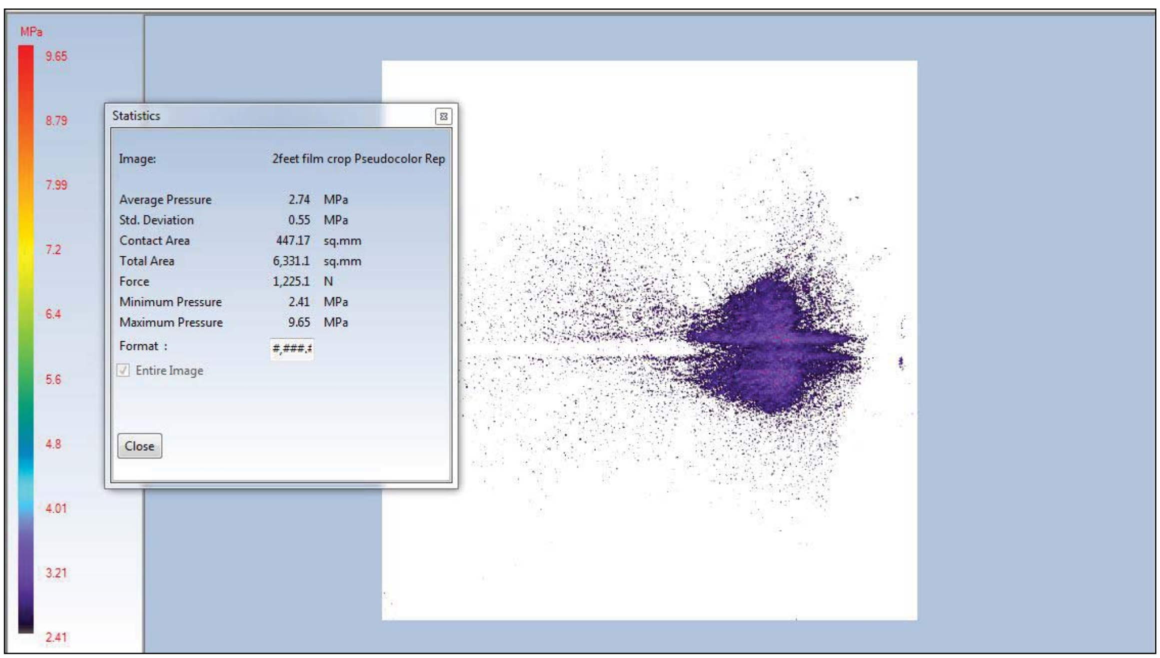

Figure 2.6 Analysis through Topaq scanner and software showing pressure readings (left) and pseudo image (right) for 2 feet drop height

In order to validate this procedure the impact pressures obtained from these pressure films were put in equation E10 to calculate impact force

$$P = \frac{\vec{F}}{\vec{A}} \qquad \ldots(E10)$$

Where P = Impact Pressure obtained from pressure films in Pa

F = Impact force vector on impact area 'A'

This impact force was then put as an input in equation E1 to get linear impact accelerations obtained from pressure films. These values were compared with linear impact acceleration values of drop tests ($\vec{a}_{droptest}$) for validation.

But as you can see in Figure 2.6, this analyzer was unable to provide a pressure curve and provides us with a single average pressure value per drop height and location. Thus, one cannot put these values as input to FE simulations. Another drawback of pressure films was that they were suitable for single impacts. Multiple impacts caused due to rebound of head after impact might have incorporated some errors in readings. However, after considering these error margins we did get substantial data of average pressure values from these pressure films which can be compared with analytically calculated impact pressures.

Hence impact pressures and linear impact accelerations obtained from pressure films were used only for comparison with analytical values of impact pressures and impact accelerations obtained from drop tests. This method can be developed more by eliminating approximations and errors of measurements.

2.5 Finite Element Simulations with Impact Pressures

2.5.1 Introduction

Traumatic brain injuries are basically caused due to transmission of impact pressures from the outer layer (scalp) to the inner layers (skull, Dura and brain) of the human head. If one is able to measure these pressures or impact forces on-field and at the time of impact then through this research concept one will be able to predict whether that individual will have a concussion or any other type of brain injury. A relationship between accelerations causing concussion and consequent impact pressures can be used for above prediction. Thus head kinematics and brain kinetics are correlated to explore brain injury dynamics.

2.5.2 Input to FE model

The impact pressure aptly named as 'Head Impact Contact Pressure or HICP' by this research group is calculated through equation E11

Using equations E2 and E10 we get,

$$P_i = \frac{m \,. \vec{a}_{droptest}}{\vec{A_i}} \qquad \ldots (E11)$$

Where P_i is Head Impact Contact Pressure or HICP,

$\vec{a}_{droptest}$ is the linear impact acceleration obtained from NOCSAE drop tests

A_i is area of impact recorded from pressure films.

These values of HICP were used as an input to validated FE model of human head.

The calculations and HICP data are presented in the Appendix A

2.5.3 Importing a validated FE model

A validated FE model of human head was taken from David Labyak's thesis [29]. It had the impactor and contact surfaces created for his simulations. Those were removed through Hypermesh software. The validated FE model is an orphan mesh in ABAQUS (.inp) format. Skull is created through geometry however scalp, dura and brain are generated by offsetting the mesh from the skull. Hence, one cannot import it as a geometry file in any analysis software. Solidworks, ABAQUS and ANSYS were the available options. File was made compatible to be imported in Solidworks however the model did not get imported as parts (for layers of head) and was unable to generate separate mesh for each layer of human head model. Though setup was correct in ABAQUS, multiple errors and discrepancies while importing the model were observed.

ANSYS was chosen considering the availability of software licenses in the university and compatibility of the software to import the available head model (ABAQUS) file. The validated FE human head model was imported using FEModeler feature (refer to Appendix B for more details) of ANSYS 14.5 [30].

The details of imported model are as follows:

Table 2.1 Modeling Details of Human Head FE Model [29]

Body Name	Nodes	Elements	Generic Element Type
SCALP	3762	3665	Linear Wedge
SKULL	6847	22930	Linear Tetrahedron
DURA	4158	4154	Linear Wedge
BRAIN TISSUE	3971	17088	Linear Tetrahedron

The impact regions were created on the FE head model by creating components in FEModeler. The areas of impact as measured from the pressure film analysis were tried to replicate on FE model. This replication involved approximation of areas to match the mesh and element sizes since any change in mesh properties would deviate us from validated FE model.

The impact regions are shown in Figure 2.7

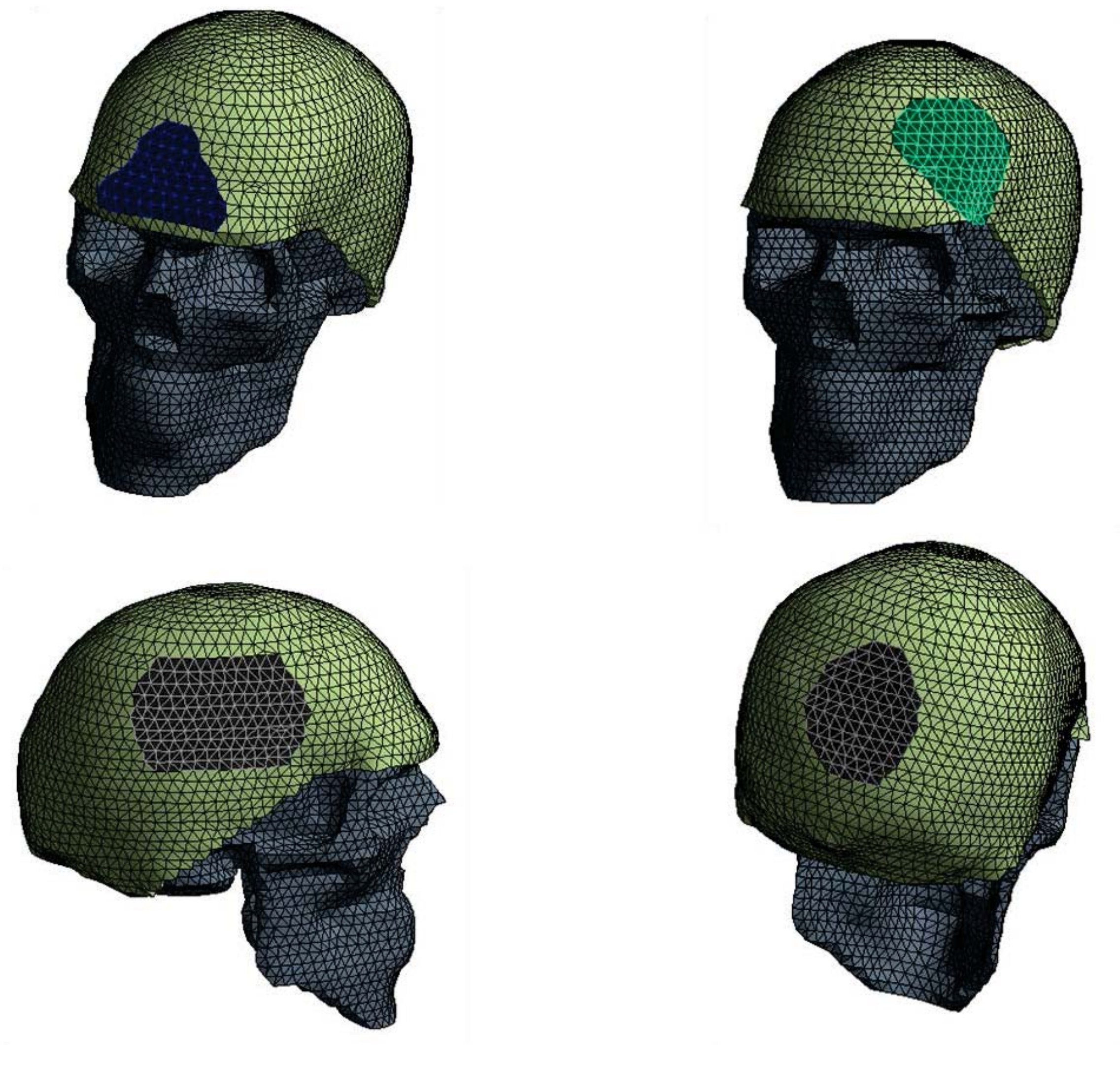

Figure 2.7 Screenshots of Impact areas marked on FE model, Frontal region (left-top); Posterior region (right-top), Lateral region (left-bottom); 45 to frontal region (right-bottom)

2.5.4 Analysis module: Transient Structural

Transient Structural Analysis module (also called time-history analysis) was chosen for the study. This type of analysis is used to determine dynamic response of structure caused due to these time-dependent loads. In this study, dynamic response of human head model due to time dependent pressure loads was determined.

2.5.5 Material Assignments

The imported model was grouped according to layers of human head and named accordingly. Appropriate materials were assigned. Material properties were kept same as that of the validated model which are enlisted in Table 2.2

Table 2.2 Material Properties of Human Head (validated FE model) [29]

Layer Name	Density (kg/m^3)	Young's Modulus (MPa)	Poisson's Ratio
SCALP	1412	8.05	0.42
SKULL	2700	6500	0.22
DURA	1040	0.148	0.49
BRAIN TISSUE	1040	0.533	0.49

2.5.6 Mesh

Mesh was kept consistent with the validated model [29]. The details are in Table 2.3

Table 2.3 Mesh of imported validated FE model

Defaults	
Physics Preference	Mechanical
Solver Preference	Mechanical APDL
Sizing	
Relevance Center	Coarse
Element Size	Default
Initial Size Seed	Active Assembly
Smoothing	Medium
Transition	Fast
Span Angle Center	Coarse
Maximum Layers	5
Statistics	
Nodes	12719
Elements	47837

2.5.7 Boundary Conditions

Since the FE model does not have a neck region the stem of skull was assumed as the region to be constrained. A remote point was created and connected it to the skull stem via spring as shown in Figure 2.8

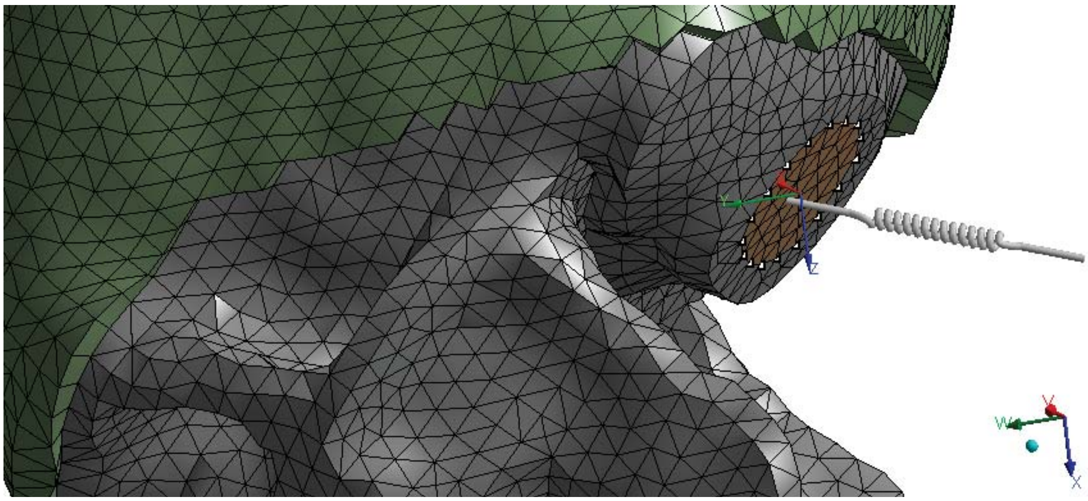

Figure 2.8 Screenshot of spring connection from remote point

Remote point offers a single point association without over constraining a portion of the geometry having multiple boundary conditions scoped to it. It also gives choice of Degrees of Freedom thus facilitating boundary conditions similar to actual experimental setup. A coordinate system was created on a flat surface of the brain stem and a remote point at (0, -0.005, 0.002) was chosen from it. The coordinate system on the brain stem was created to facilitate easy measurement of the distance from the skull stem. It was not used in any of the applied boundary conditions. This remote point was named as ‘Fixed Point’ and connected to multiple set of points (named selection) called ‘Fixed_points’ located on the skull stem. These connections appear as shown in Figure 2.9.

The Degrees of freedom were manually selected constraining translation in X, Y and Z axes and allowing rotation about X, Y and Z axes as shown in Table 2.4.

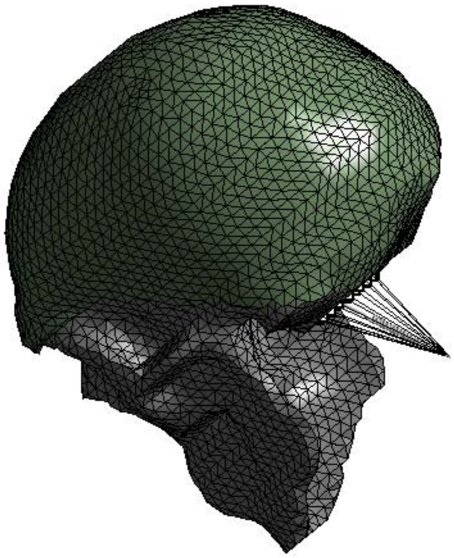

Figure 2.9 Screenshot of Remote point connecting to skull stem

Table 2.4 Remote Point Controls

Object Name	*Remote Points*
State	Fully Defined
Display	
Show Connection Lines	Yes
Object Name	*Fixed Point*
State	Fully Defined
Scope	
Scoping Method	Named Selection
Named Selection	Fixed_points
Coordinate System	Fixed area
X Coordinate	0. m
Y Coordinate	-5.e-002 m
Z Coordinate	2.e-002 m
Location	Defined
Definition	
Suppressed	No
Pinball Region	All
DOF Selection	Manual
X Component	Inactive
Y Component	Inactive
Z Component	Inactive
Rotation X	Active
Rotation Y	Active
Rotation Z	Active

Spring connection (Figure 2.8) offers elastic and flexible connection between the skull stem and fixed remote point. This avoids over-constraint by removing the rigidness of a connection along with giving a strong support to the model.

As shown in Table 2.5, the deformability of this longitudinal connection (spring) was governed through spring stiffness which was chosen as 10000N/m making it stronger than skull yet not rigid. The spring length automatically gets calculated after the source and destination points are specified, in this case remote point and fixed faces on the skull stem were chosen. Remote point is immobile and hence was chosen as a reference. The fixed faces on the brain stem will have motion after load application hence they were chosen under Mobile Components. Both the connections were made deformable in order to avoid over constraints.

Table 2.5 Spring Controls

Object Name	*Longitudinal*
State	Fully Defined
Definition	
Type	Longitudinal
Spring Behavior	Both (Linear)
Longitudinal Stiffness	10000 N/m
Longitudinal Damping	0. N·s/m
Preload	None
Suppressed	No
Spring Length	5.4863e-002 m
Scope	
Scope	Body-Body
Reference	
Scoping Method	Remote Point
Remote Points	Fixed Point
Body	Multiple
Coordinate System	Fixed area
Reference X Coordinate	0. m
Reference Y Coordinate	-5.e-002 m
Reference Z Coordinate	2.e-002 m
Behavior	Deformable
Pinball Region	All
Mobile	
Scoping Method	Named Selection
Mobile Component	Fixed_faces
Body	Skull
Coordinate System	Global Coordinate System
Mobile X Coordinate	1.5271e-002 m
Mobile Y Coordinate	-0.11884 m
Mobile Z Coordinate	0.10406 m
Mobile Location	Defined
Behavior	Deformable
Pinball Region	All

2.5.8 Analysis Settings and Load Conditions

Referring to the time span of major impact event in Figure 2.3, the cycle has 21 time steps starting from 0 sec and ending at 0.00546sec. These were put as analysis settings so that results on each time step would be recorded. 2 sub steps were optimally chosen for uniform distribution yet reduced processing time. Since these time steps were gained from data acquisition systems not much convergence was required.

The pressure (HICP) curves derived for various locations in Section 2.4 were put on FE model as time dependent load conditions.

This setup was then solved to get results in post processor of ANSYS 14.5.

(Refer to Appendix B for entire procedure details)

3. Results and Discussions

In this chapter, the results derived from methods described in Chapter 2 are discussed. This chapter will go over the following:

a) Comparison between linear accelerations derived from pressure films and droptests with angular accelerations (on secondary axis) from drop test derived through analytical methods

b) Von-Mises, Maximum shear and Maximum Principal stress contours on the FE human head model

c) Von-Mises, Maximum shear and Maximum Principal stress values calculated from Concussion tolerance acceleration values and its comparison with FE results

3.1 Head Kinematics: Comparison of Accelerations

3.1.1 Introduction

In this section, a comparison between linear impact accelerations from pressure films and linear impact accelerations from drop tests is done. The angular impact accelerations calculated through analytical procedures are also plotted simultaneously.

The FE human head model was used as a reference to find centroids of the impact areas. It was oriented in ANSYS to match with the head form drop test orientation. Positive X-axis passes through the nose of the head form which is in perpendicular to the forehead and is assumed to be perpendicular to frontal and posterior impact region. Y-axis passes through the superior region of the head form. Positive Z-axis passes through the left ear and is assumed to be perpendicular to the lateral or side impact region. 45 to frontal plane is located approximately midway between X and Z axes and is assumed to be perpendicular to the 45 to frontal impact region. The pictorial representation of the above mentioned orientations can be seen in Figure 3.1.

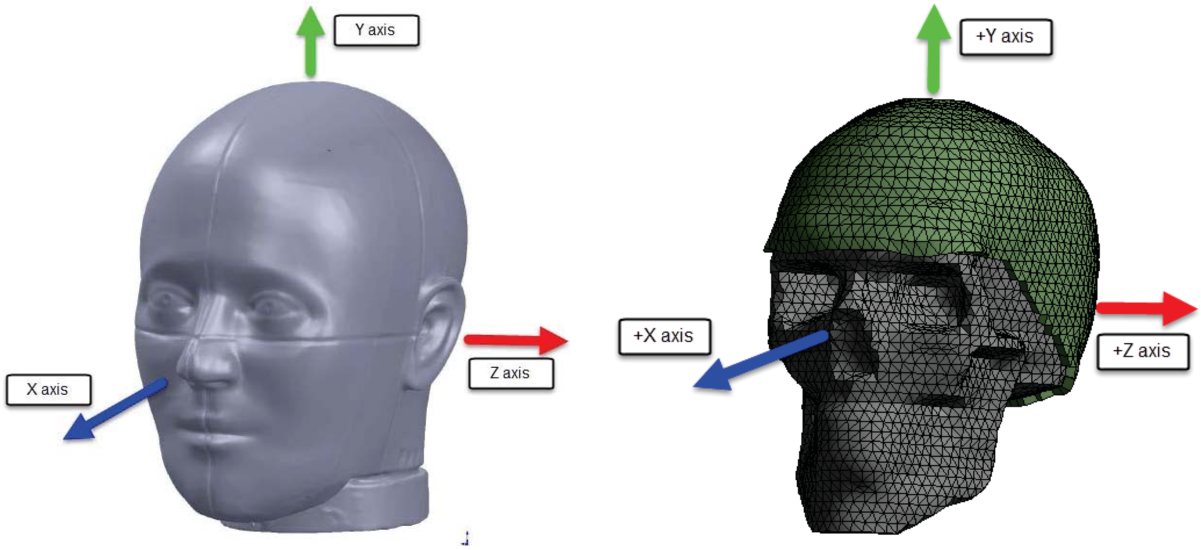

Figure 3.1 Screenshots showing orientation of FE head model aligned with drop test head form

Center of mass of FE human head model was assumed to be same as that of center of mass of headform. Since, areas are replicated on the FE model, centroids of areas on FE human head model were also assumed to be same as centroids of areas of impacts on NOCSAE head form. Distance between two centroids namely center of mass of head and centroid of impact region was calculated.

Extending on the methods discussed in Chapter 2, a calculator was created in excel to generate results of linear and angular accelerations based on equations (E1- E12) (refer to Appendix C for excel calculator and calculation details)

3.1.2 Pressure Films and Topaq Analyzer

Following were the linear acceleration results for impact regions: frontal, 45 to frontal, posterior and lateral generated using pressure films, topaq analyzer and equation (E2) (Refer to Table 3.1)

(Blue color signifies that these results will be used for comparison in later steps)

Table 3.1 Linear acceleration values from pressure films and Topaq analyzer

Impact Regions	Height (feet)	Average Pressure (MPa)	Area measured through chalk markings (m^2)	Linear Acceleration (m/s^2)
Front	2	2.79	0.0028	1588.8
	3	2.84	0.0030	1768
	4	3.25	0.0033	2068.8
	5	3.42	0.0035	2483
45° to Frontal	2	3.85	0.0030	2364.6
	3	4.04	0.0030	2481
	4	4.26	0.0036	3144.9
	5	4.63	0.0036	3418
Lateral / Side	2	3.32	0.0052	3524.6
	3	3.49	0.0057	4095.5
	4	3.55	0.0060	4360.7
	5	3.64	0.0064	4745
Posterior / Rear	2	2.77	0.0034	1921
	3	3.9	0.0039	3085
	4	4.01	0.0040	3311
	5	4.2	0.0041	3553

3.1.3 NOCSAE drop test analyzer

Following were the maximum linear acceleration values for impact regions: frontal, 45 to frontal, posterior and lateral generated using NOCSAE drop test analyzer and Siglab Data Acquisition System (refer to Table 3.2)

(Blue color signifies that these results will be used for comparison in later steps)

Table 3.2 Maximum linear acceleration values from NOCSAE drop tests

Impact Regions	Height (feet)	Maximum Linear Acceleration (m/s^2)
Front	2	2309.5
	3	3030
	4	3634.7
	5	4219
45° to Frontal	2	2019.8
	3	2502.7
	4	3017.9
	5	3427
Lateral / Side	2	2561.8
	3	3386.8
	4	3909
	5	4544
Posterior / Rear	2	2489.5
	3	3243
	4	3923.5
	5	4516.8

3.1.4 Analytical angular accelerations

Following were the maximum calculated values of angular acceleration for impact regions: frontal, 45 to frontal, posterior and lateral generated using linear acceleration values from drop tests, dimension details of headform & FE model and equations (E5-E9) (Refer to Table 3.3)

(Blue color signifies that these results will be used for comparison in later steps)

Table 3.3 Maximum angular acceleration values calculated analytically from linear accelerations of drop tests

Impact Regions	Height (feet)	Maximum Angular Acceleration (rad/s^2)
Front	2	29273.3
	3	36129.8
	4	43318.6
	5	47785.3
45° to Frontal	2	18391
	3	22254
	4	26185.6
	5	29433
Lateral / Side	2	8065.8
	3	9331.5
	4	10254
	5	10410
Posterior / Rear	2	18874.5
	3	23401
	4	29268
	5	31407

3.1.5 Results: Graphical comparison of all accelerations

Refer to Figures 3.2, 3.3, 3.4, 3.5

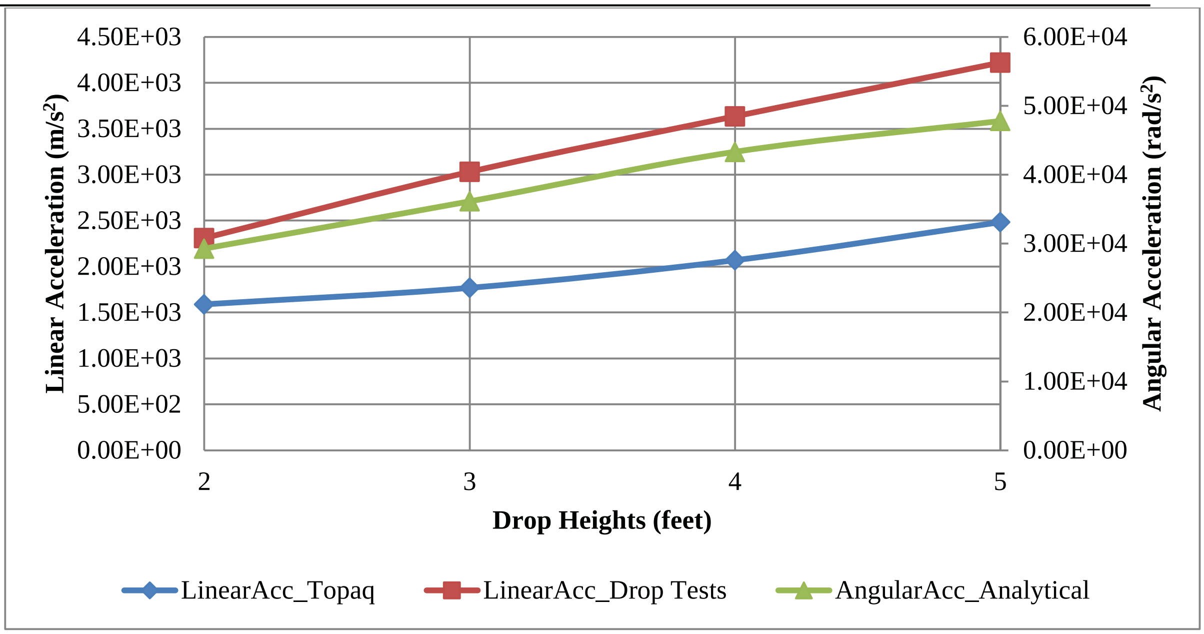

Figure 3.2 Plot of experimentally measured linear acceleration and analytically calculated angular acceleration as a function of drop heights (Frontal Impact)

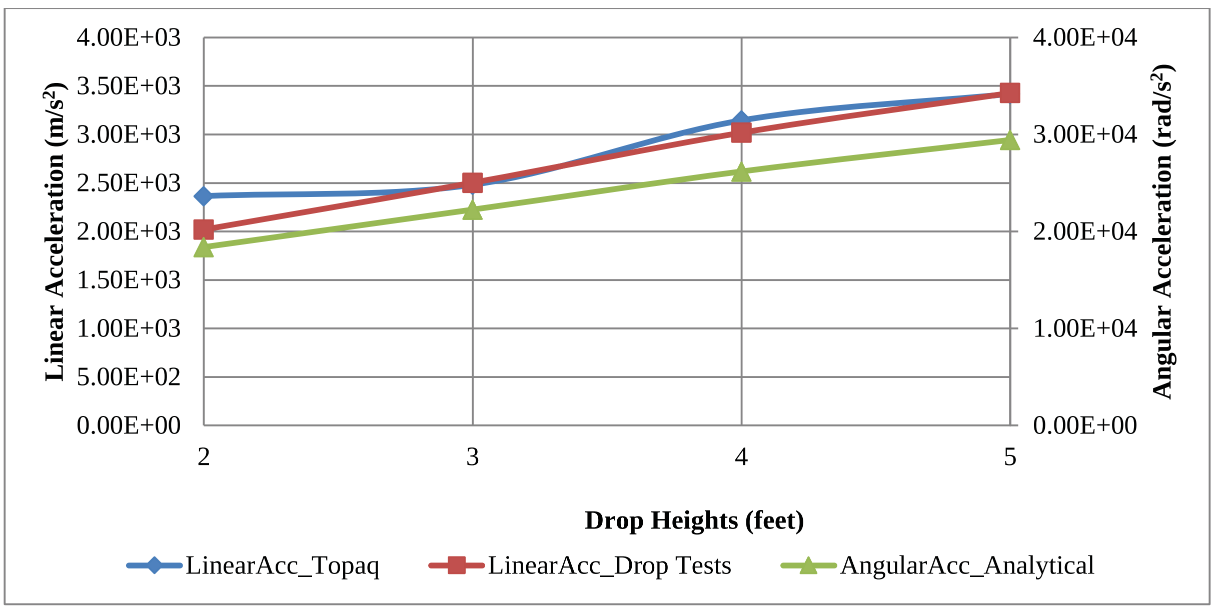

Figure 3.3 Plot of experimentally measured linear acceleration and analytically calculated angular acceleration as a function of drop heights (45 to Frontal Impact)

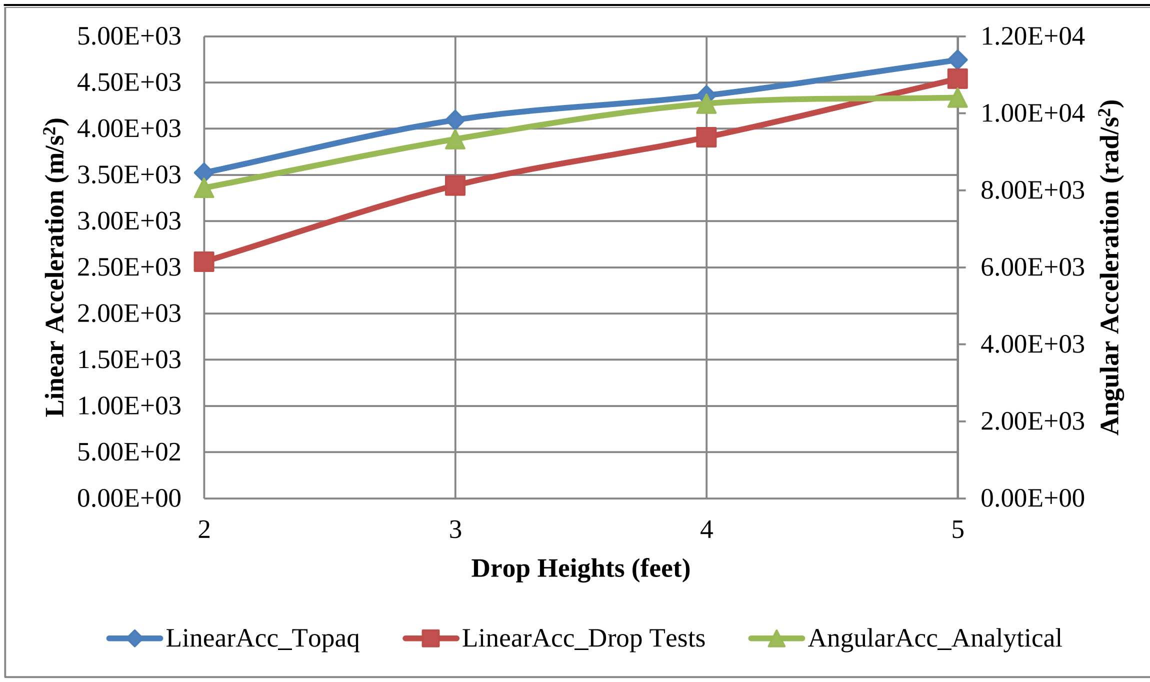

Figure 3.4 Plot of experimentally measured linear acceleration and analytically calculated angular acceleration as a function of drop heights (Lateral Impact)

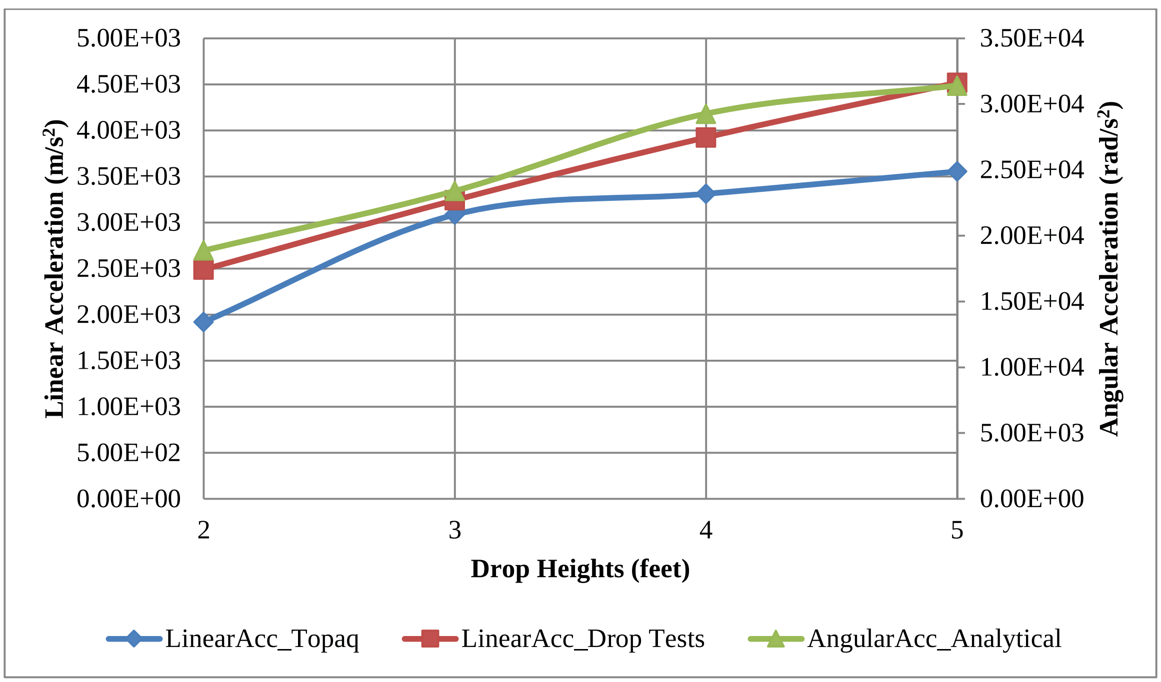

Figure 3.5 Plot of experimentally measured linear acceleration and analytically calculated angular acceleration as a function of drop heights (Posterior Impact)

3.1.6 Discussions

1. Numerical values of linear accelerations for various impact regions calculated from pressure films are quite close to maximum linear accelerations acquired from NOCSAE drop tests except for frontal region. This deviation might have come in due to approximations in area measurements through chalk dust markings. The frontal region on the headform has an eye-brow line which sometimes interferes with measurement of actual area of impact thus adding into the error in area measurement. As mentioned in Section 2.4 (in description of Figure 2.6), the values acquired from pressure films are average pressure values which also adds the deviation in maximum acceleration values.
2. Maximum linear acceleration is observed for 5 feet lateral (side) impact. This observation is consistent for both pressure films (4745 m/s^2) and NOCSAE drop test (4541 m/s^2) readings. Minimum linear acceleration for NOCSAE drop tests is observed for 2 feet 45 to frontal impact region whereas through pressure films minimum linear acceleration observed is for 2 feet frontal impact closely followed by 3 feet frontal and 2 feet posterior impacts.
3. Maximum analytical angular acceleration amongst all impact regions and drop heights is observed for 5 feet frontal impact (47.7 $krad/s^2$).
4. Amongst all 5 feet impacts (since 5 feet drop height observations will be used in helmet design), maximum angular acceleration is observed in frontal region (47.7 $krad/s^2$) whereas minimum is observed in lateral region (10 $krad/s^2$). Posterior (31 $krad/s^2$) and 45-to-frontal (29 $krad/s^2$) regions show angular accelerations on the higher end as well.

5. Maximum linear acceleration is observed on lateral impact region whereas maximum angular acceleration is observed on frontal impact region. Minimum linear acceleration is observed on frontal and 45-to-frontal impact regions whereas minimum angular acceleration is observed on lateral impact region.

   Thus one can conclude,

   - Relationship between impact accelerations and drop heights depends on impact regions
   - Impact acceleration sensitivity to drop heights differs from region to region

3.1.7 Formula Proposition

From above analysis it is evident that both linear and angular impact accelerations contribute towards causing TBIs. Thus, this research group is proposing a formula relating acceleration values to the TBI.

$$\frac{a_{regional}}{a_{TBI-max}} + \frac{\alpha_{regional}}{\alpha_{TBI-max}} \leq 1 \ then\ no\ TBI \qquad \ldots(E12)$$

Where,

$a_{regional}$ = linear impact accelerations for a particular impact region and drop height

$a_{TBI-max}$ = TBI tolerant linear impact acceleration measured individually (value = 318 G) [27]

$\alpha_{regional}$ = angular impact accelerations for a particular impact region and drop height

$\alpha_{TBI-max}$ = TBI tolerant angular impact acceleration measured individually (value = 23krad/s^2) [27]

This formula has to be used only when $\frac{a_{regional}}{a_{TBI-max}}$ or $\frac{\alpha_{regional}}{\alpha_{TBI-max}}$ is less than one. When those values are greater than 1 then this formula is not required to determine which type of acceleration plays a prominent role in causing TBI. For example, consider case 1 of Frontal 2feet impact. Linear TBI tolerance $\left(\frac{a_{regional}}{a_{TBI-max}}\right)$ value is 0.74 however angular TBI tolerance $(\frac{\alpha_{regional}}{\alpha_{TBI-max}})$ is 1.27 (refer to Table 3.4) which signifies that angular impact acceleration prominently causes TBI and above formula is not required. Now, consider case 2 of Lateral 2feet impact. Linear TBI tolerance $\left(\frac{a_{regional}}{a_{TBI-max}}\right)$ value for this impact is 0.82 however angular TBI tolerance $(\frac{\alpha_{regional}}{\alpha_{TBI-max}})$ is 0.35 (refer to Table 3.4). Though, Linear TBI value is below 1 and won't cause TBI if measured individually, if combined with angular TBI value of 0.35 it will go beyond 1 which will cause TBI.

Thus, linear impact accelerations combined with angular impact accelerations can cause TBIs even though they won't cause TBI if occurred individually. Football head-on collisions always have a combination of linear as well as angular impact accelerations.

Table 3.4 TBI acceleration criterion for frontal, 45-to-frontal, lateral and posterior regions based on equation E12

	Frontal					45-to-frontal				
Drop Height	Linear Acc (Gs)	Linear TBI Tolerance	Ang Acc (rad/s²)	Angular TBI Tolerance	TBI Condition	Linear Acc (Gs)	Linear TBI Tolerance	Ang Acc (rad/s²)	Angular TBI Tol	TBI tol
2	235	0.74	29273	1.27	-	206	0.65	20888	0.91	1.56
3	309	0.97	36129	1.57		255	0.80	25118	1.09	
4	370	1.16	43319	1.88		308	0.97	29575	1.29	
5	430	1.35	47785	2.08		349	1.10	33220	1.44	
	Lateral					Posterior				
	Linear Acc (Gs)	Linear TBI Tolerance	Ang Acc (rad/s²)	Angular TBI Tolerance	TBI Condition	Linear Acc (Gs)	Linear TBI Tolerance	Ang Acc (rad/s²)	Angular TBI Tol	TBI tol
2	261	0.82	8066	0.35	1.17	254	0.80	18875	0.82	1.62
3	345	1.08	9331	0.41		331	1.04	23401	1.02	
4	399	1.25	10254	0.45		400	1.26	29268	1.27	
5	463	1.46	10410	0.45		460	1.45	31407	1.37	

3.2 Brain Kinetics: Stress Distributions

The validated FE model, its material properties, boundary conditions and the entire setup for all the drop heights and impact regions was maintained according to the Section 2.2.

3.2.1 Frontal Impact - Introduction

HICP or impact pressure curves (for respective drop heights) used as inputs to the validated FE model are shown in Figures 3.7-3.10. Refer to Appendix A for detailed data.

3.2.2 Frontal Impact – Summary of Results

Table 3.5 Results of Frontal Impact for 2, 3, 4 and 5 feet drop heights

	Drop Heights	**Max. HICPressure (Pa)**	**Max. Principal Stress (Pa) (tension)**	**Peak Von-Mises Stress (Pa)**	**Peak Max. Shear Stress (Pa)**
Frontal Impact	2	4.06E+06	4.46E+06	7.80E+06	4.20E+06
	3	4.87E+06	5.40E+06	9.39E+06	5.13E+06
	4	5.40E+06	6.09E+06	1.04E+07	5.70E+06
	5	5.81E+06	6.59E+06	1.12E+07	6.13E+06

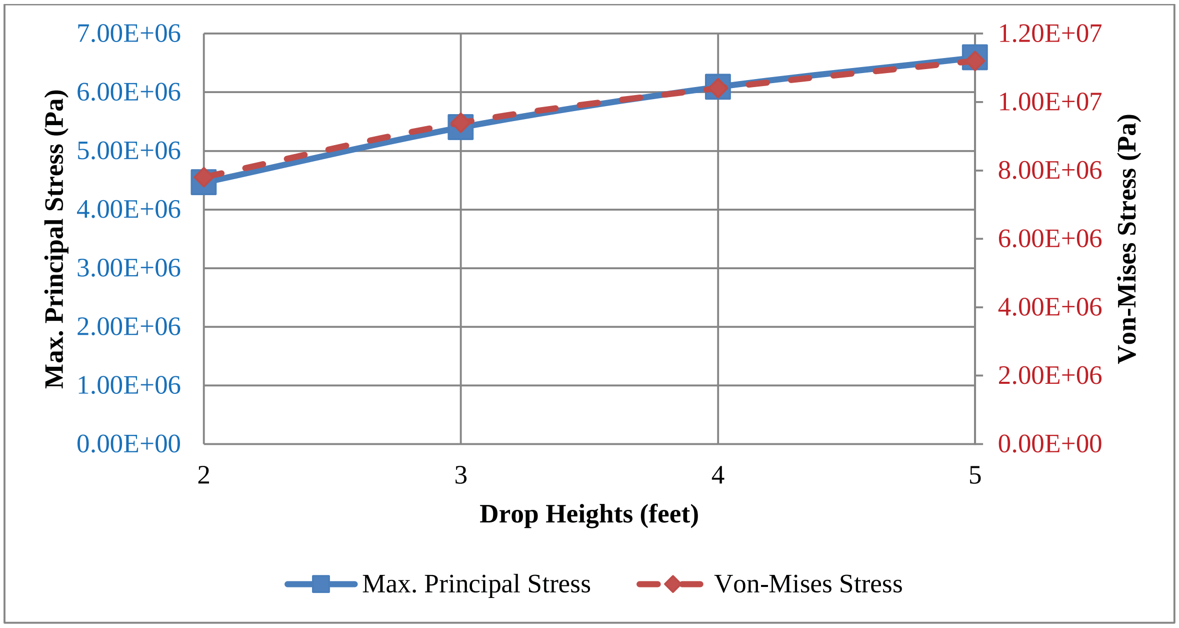

Figure 3.6 Plot of Maximum Principal Stress and Von-Mises Stress for Frontal impact obtained from ANSYS simulations as a function of drop heights

3.2.3 Frontal Impact – Result Discussions

- Peak values of Von-Mises stresses were observed in the frontal impact region, entire superior region of head model (scalp and skull), facial areas of skull and areas surrounding brain stem. For all drop heights the time locations of peak Von-Mises Stress values were at 3.9msec except for 5 feet frontal impact which occurred early at 3.7 msec. (Figures 3.11, 3.13, 3.15, 3.17)
- Observed Von-Mises stress contours for the entire time cycle were such that impact pressure wave has initiated from the frontal impact region of the scalp, translated through skull, dura & brain and bounced back from the posterior wall of skull. This observation matches with the Coup and Contre-Coup injury mechanisms of TBI. (Coup injury is caused at the site of impact which deforms the skull and translates the impact to the brain. Brain bounces off from the opposite wall of skull causing ContreCoup injury.)
- Peak (tension) values of Maximum Principal Stress were observed in parietal lobe that extends around frontal side of ears and few areas of brain stem (Figure 3.19). This seems structurally similar to cerebral aneurysm, a phenomenon in which arteries in brain bulge out due to their weakening and hypertension (increase in blood pressure) on them. Minimum (compression) value of Maximum Principal Stress was observed in the impact region which signifies maximum compression at the impact region. (Figures 3.12, 3.14, 3.16, 3.18)
- Peak values of Maximum Shear stress were observed in parietal lobe that extends around frontal side of ears and some areas surrounding the impact region in a lesser magnitude than maximum.

3.2.4 Frontal Impact – Pressure Curves

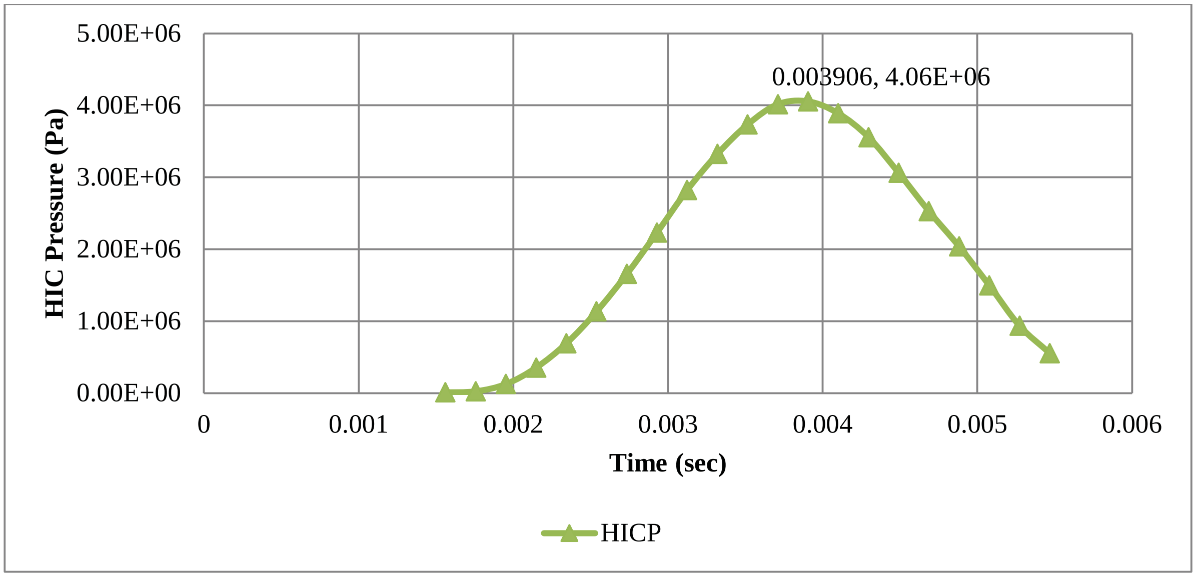

Figure 3.7 Plot of analytically calculated impact pressures as a function of time (frontal impact 2 feet drop height)

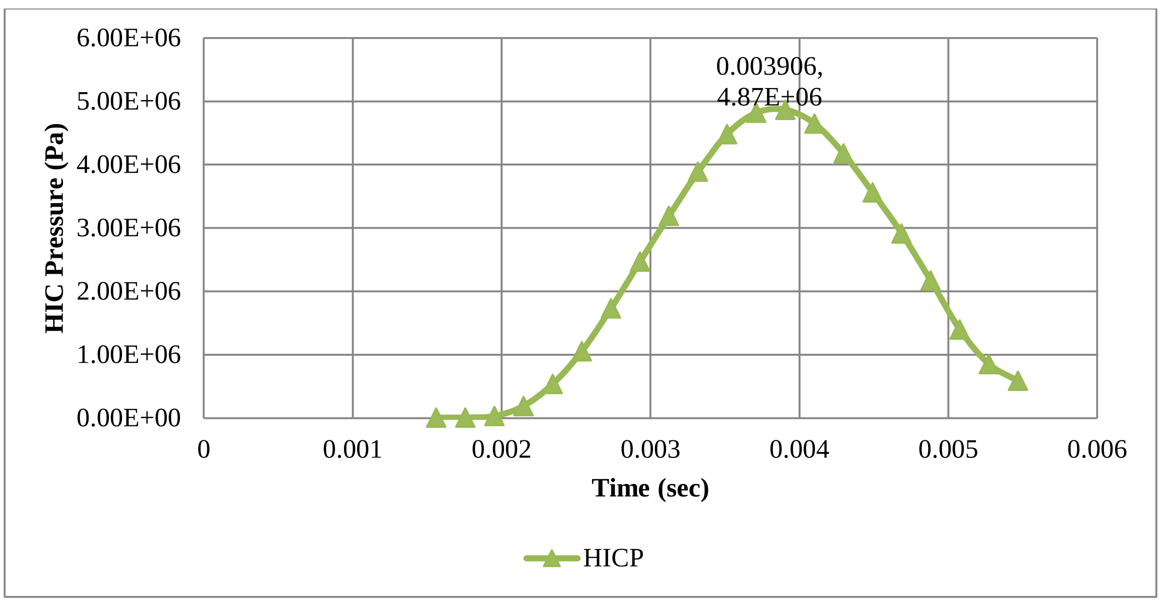

Figure 3.8 Plot of analytically calculated impact pressures as a function of time (frontal impact 3 feet drop height)

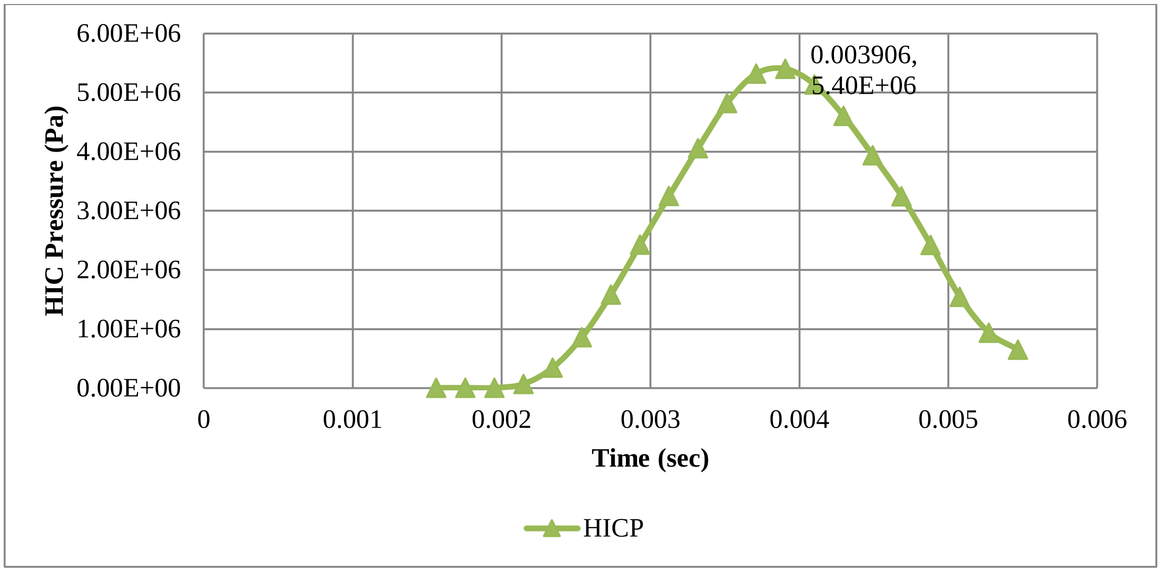

Figure 3.9 Plot of analytically calculated impact pressures as a function of time (frontal impact 4 feet drop height)

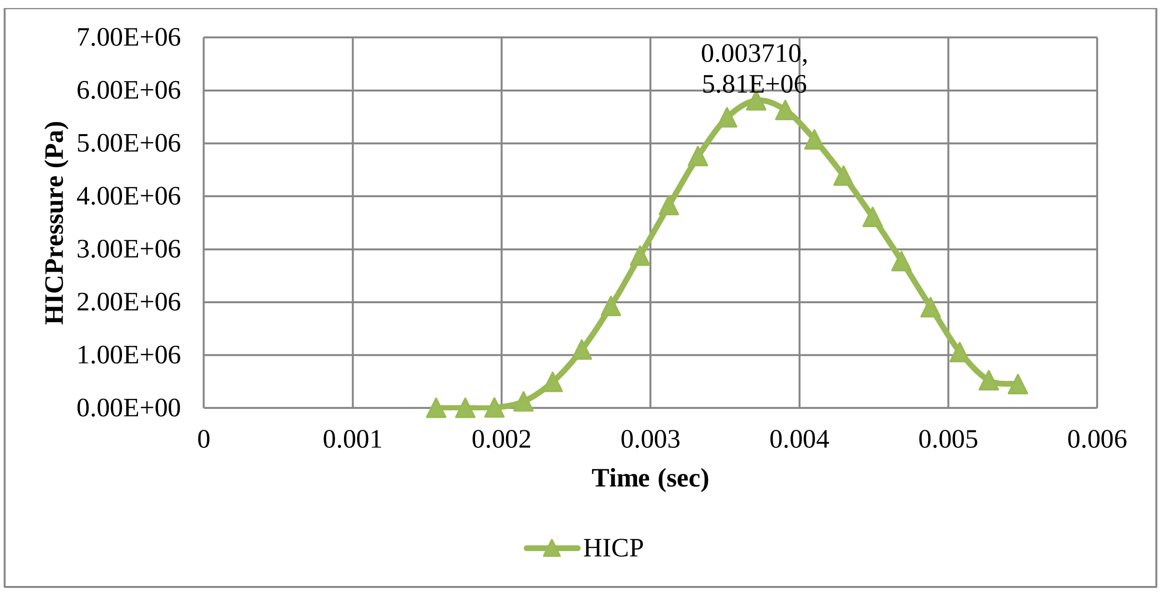

Figure 3.10 Plot of analytically calculated impact pressures as a function of time (frontal impact 5 feet drop height)

3.2.5 Frontal Impact – Simulation Results (Pressure Contours)

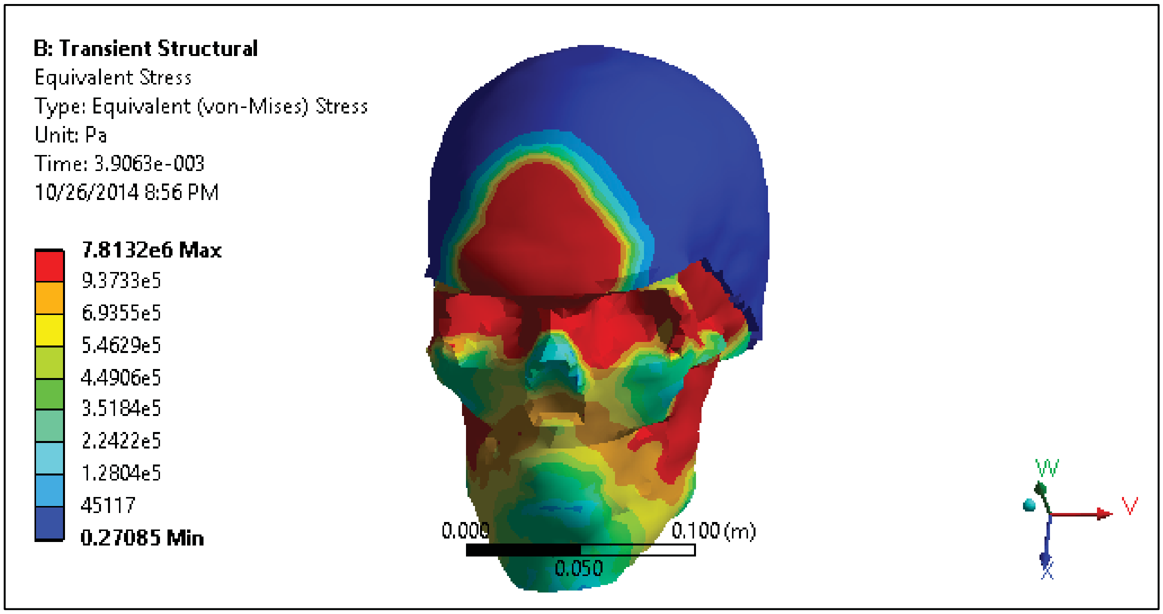

Figure 3.11 Von Mises Stress Distribution Contours - Frontal Impact 2 feet

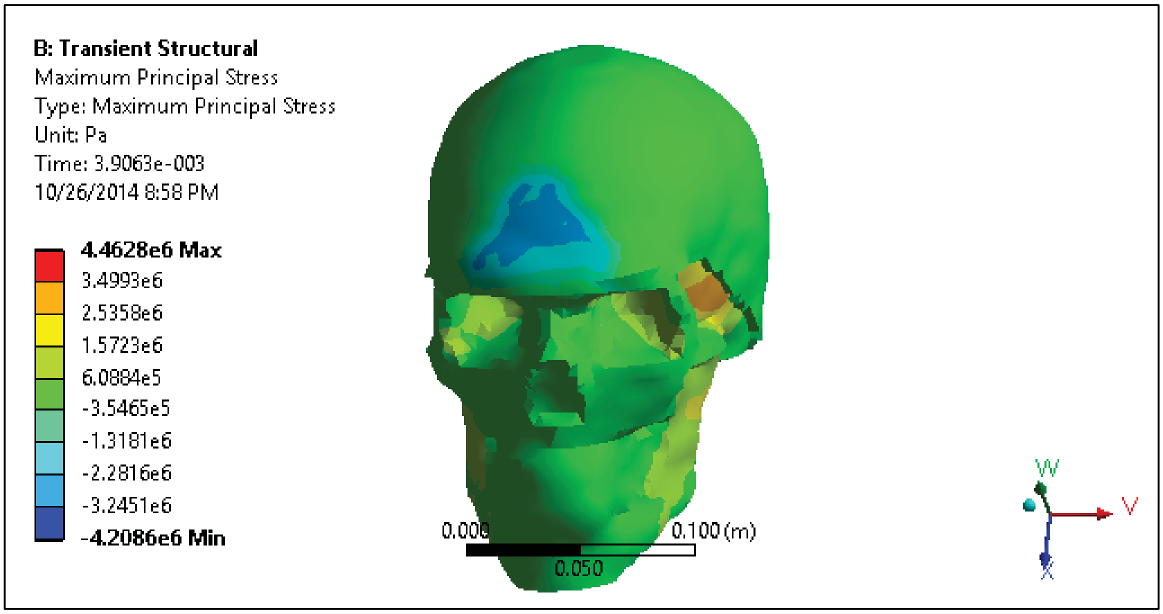

Figure 3.12 Maximum Principal Stress Distribution Contours - Frontal Impact 2 feet

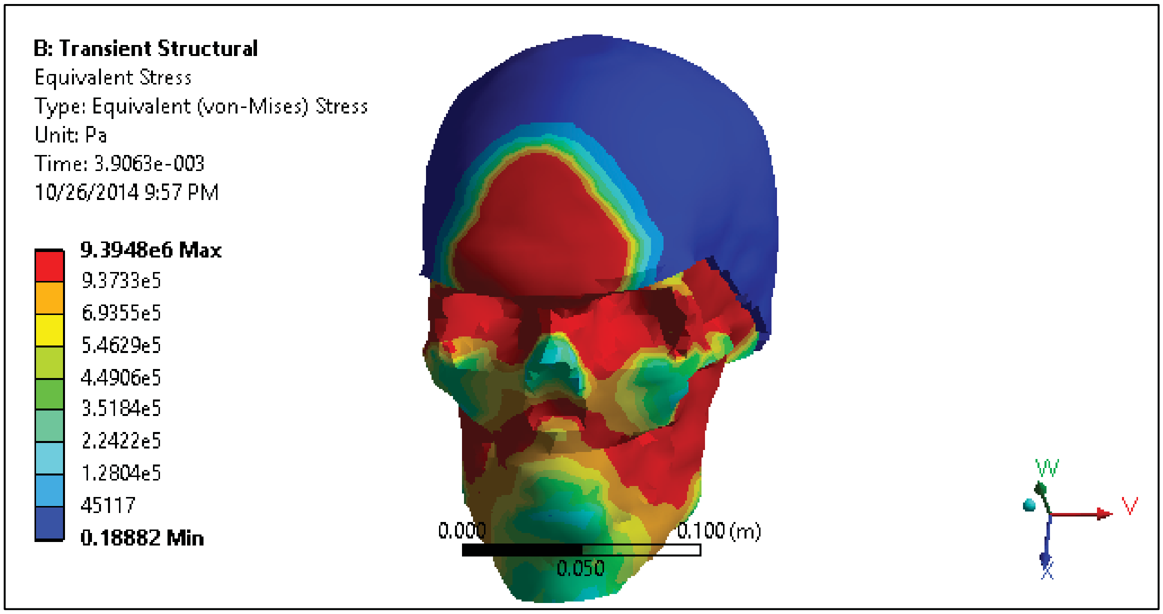

Figure 3.13Von Mises Stress Distribution Contours - Frontal Impact 3 feet

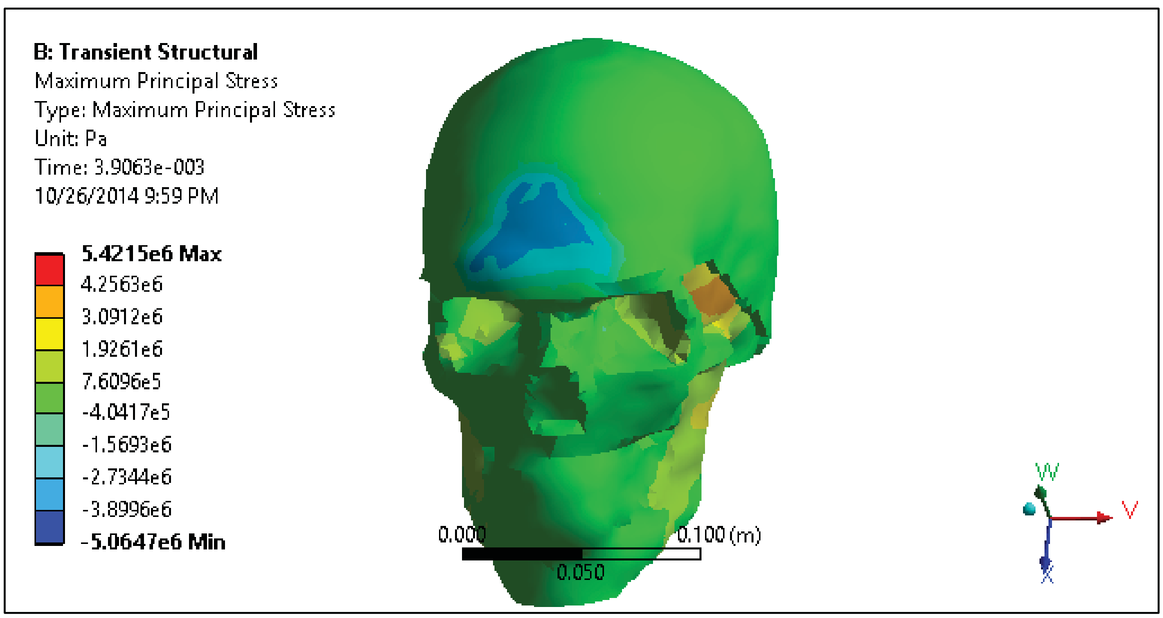

Figure 3.14 Maximum Principal Stress Distribution Contours - Frontal Impact 3 feet

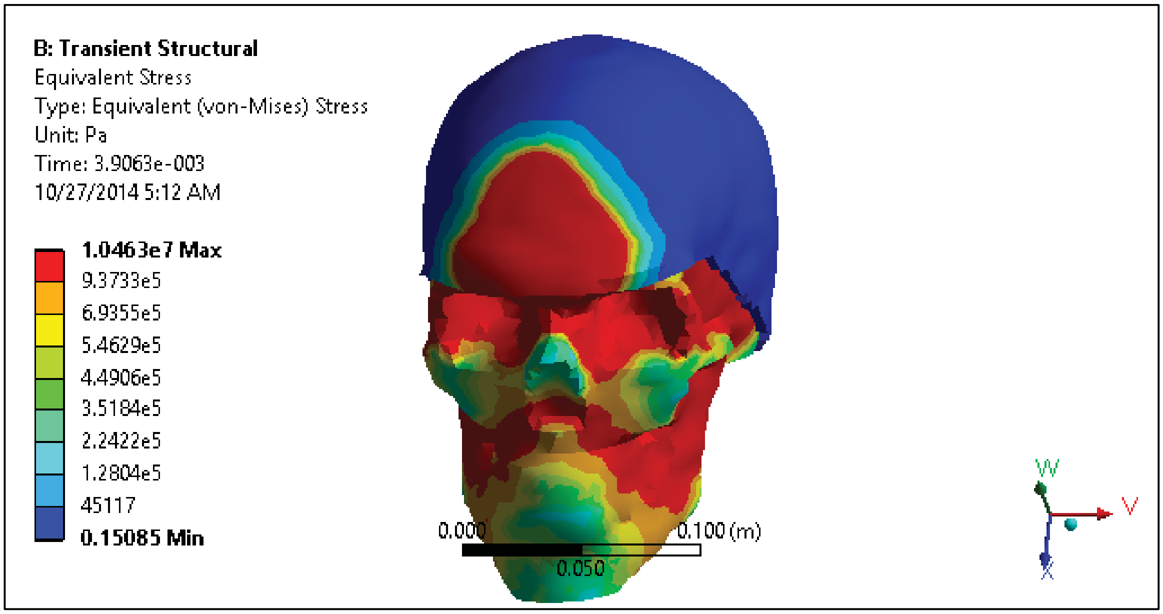

Figure 3.15 Von Mises Stress Distribution Contours - Frontal Impact 4 feet

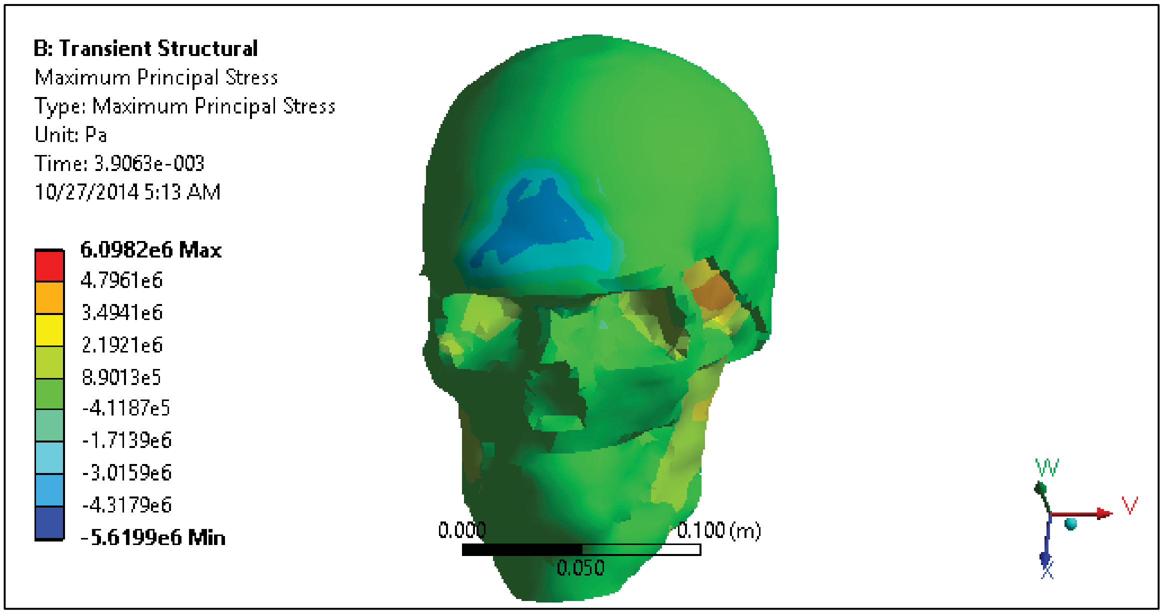

Figure 3.16 Maximum Principal Stress Distribution Contours - Frontal Impact 4 feet

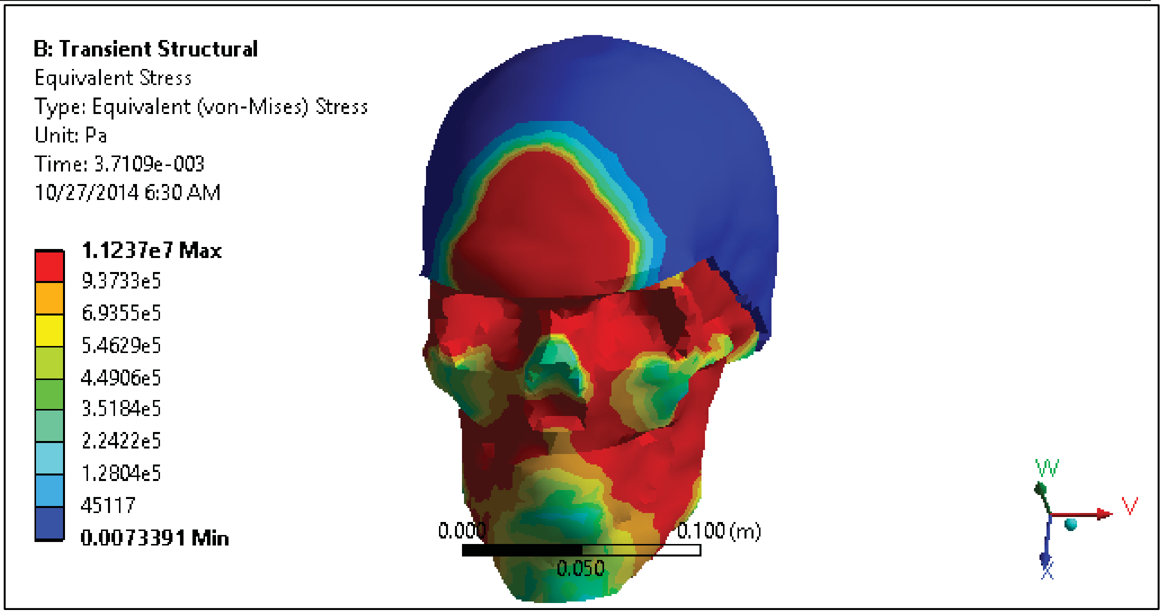

Figure 3.17 Von Mises Stress Distribution Contours - Frontal Impact 5 feet

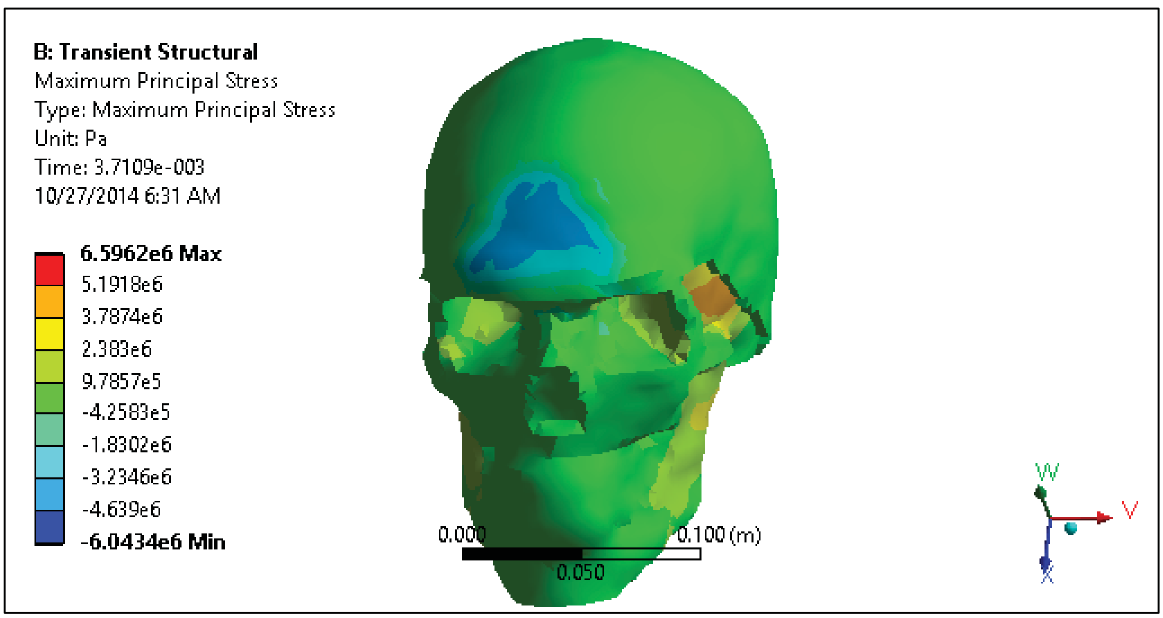

Figure 3.18 Maximum Principal Stress Distribution Contours - Frontal Impact 5 feet

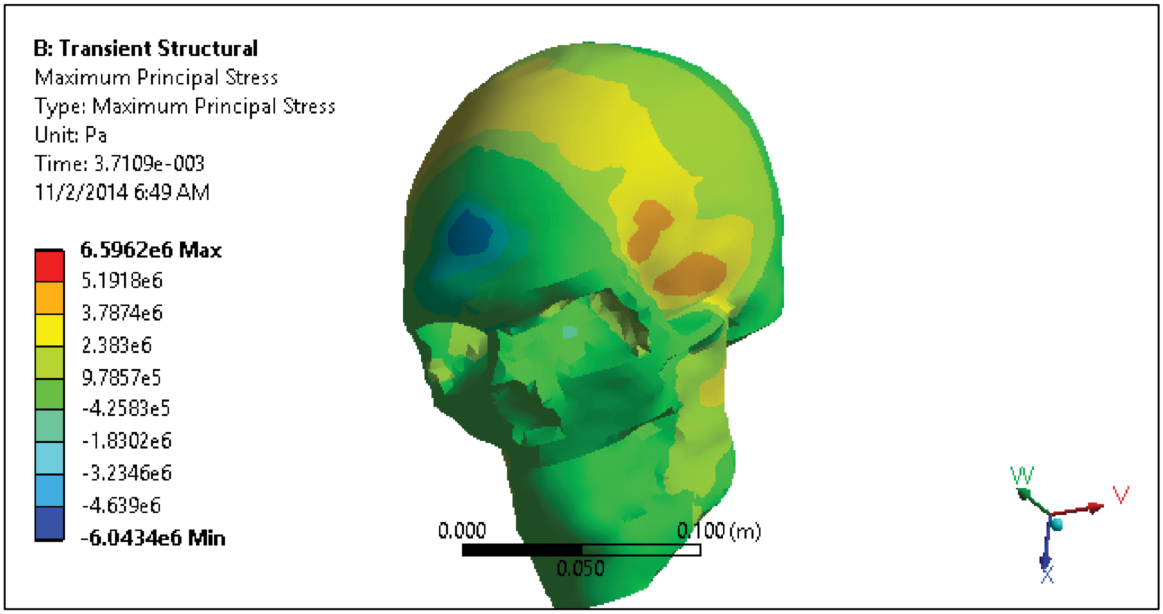

Figure 3.19 Location of peak value of Maximum Principal Stress on skull (without scalp) for Frontal 5 feet impact

3.2.6 45 to Frontal Impact – Introduction

HICP or impact pressure curves (for respective drop heights) used as inputs to the validated FE model are shown in Figures 3.21-3.24 of Section 3.2.9. Refer to Appendix A for detailed data.

3.2.7 45 to Frontal Impact – Summary of Results

Table 3.6 Results of 45-to-Frontal Impact for 2, 3, 4 and 5 feet drop heights

	Drop Heights	Max. HICPressure (Pa)	Max. Principal Stress (Pa) (tension)	Peak Von-Mises Stress (Pa)	Peak Max. Shear Stress (Pa)
45 to Frontal	2	3.29E+06	5.27E+06	1.60E+07	9.47E+06
	3	4.07E+06	6.50E+06	2.10E+07	1.17E+07
	4	4.09E+06	6.59E+06	2.12E+07	1.18E+07
	5	4.65E+06	7.64E+06	2.42E+07	1.35E+07

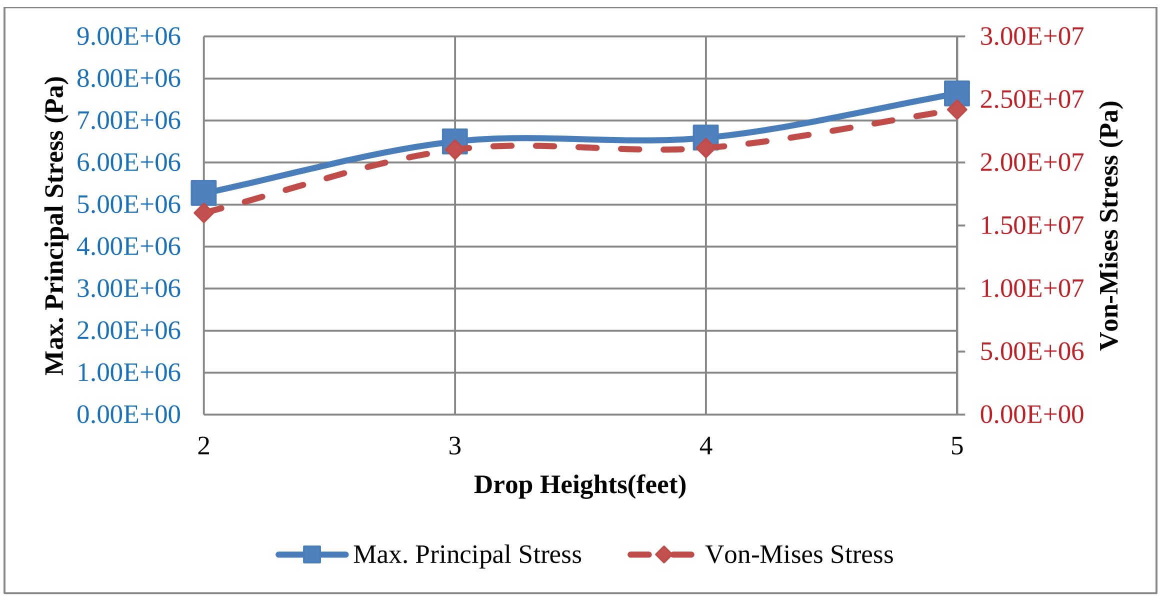

Figure 3.20 Plot of Maximum Principal Stress and Von-Mises Stress for 45-to-frontal impact obtained from ANSYS simulations as a function of drop heights

3.2.8 45 to Frontal Impact – Result Discussions

- Peak values of Von-Mises stresses were observed in 45-to-frontal impact region, entire superior region of head model (scalp and skull), facial areas of skull and areas surrounding brain stem. For all drop heights the time locations of peak Von-Mises Stress values were at 3.7msec. (Figures 3.25, 3.27, 3.29, 3.31)
- Observed Von-Mises stress contours for entire time cycle were such that impact pressure wave has initiated from the 45-to-frontal impact region of the scalp, translated through skull, dura & brain and bounced back from the parietal-occipital wall of the skull. This observation matches with the Coup and Contre-Coup injury mechanisms of TBI. (Coup injury is caused at the site of impact which deforms the skull and translates the impact to the brain. Brain bounces off from the opposite wall of skull causing ContreCoup injury.)
- Peak (tension) values of Maximum Principal Stress were observed on occipital lobe behind the left ear (besides impact region) and on the exact opposite end of the impact region i.e. on superior parietal region (Figure 3.33). This seems structurally similar to cerebral aneurysm, a phenomenon in which arteries in brain bulge out due to their weakening and hypertension (increase in blood pressure) on them. Minimum (compression) value of Maximum Principal Stress was observed in the impact region which signifies maximum compression at the impact region (Figures 3.26, 3.28, 3.30, 3.32). Compressive values increased with increase in drop heights.

- Peak values of Maximum Shear stress were observed in in parietal lobe besides the left eye (near impact region) and spanned entire superior region with lesser magnitude than maximum.

3.2.9 45 to Frontal Impact – Pressure Curves

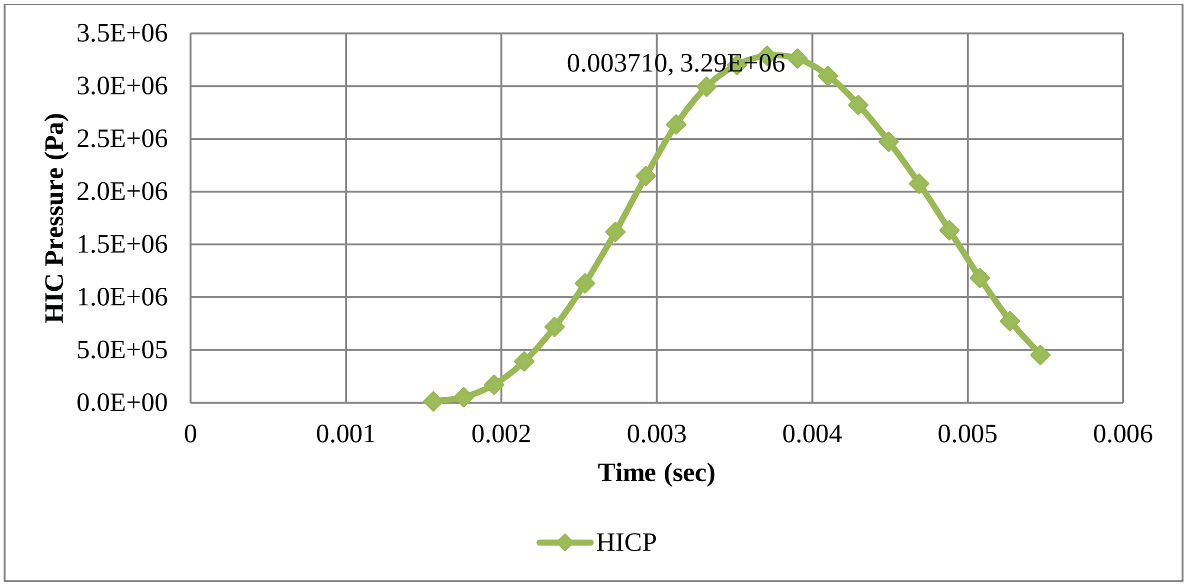

Figure 3.21 Plot of analytically calculated impact pressures as a function of time (45 to frontal impact 2 feet drop height)

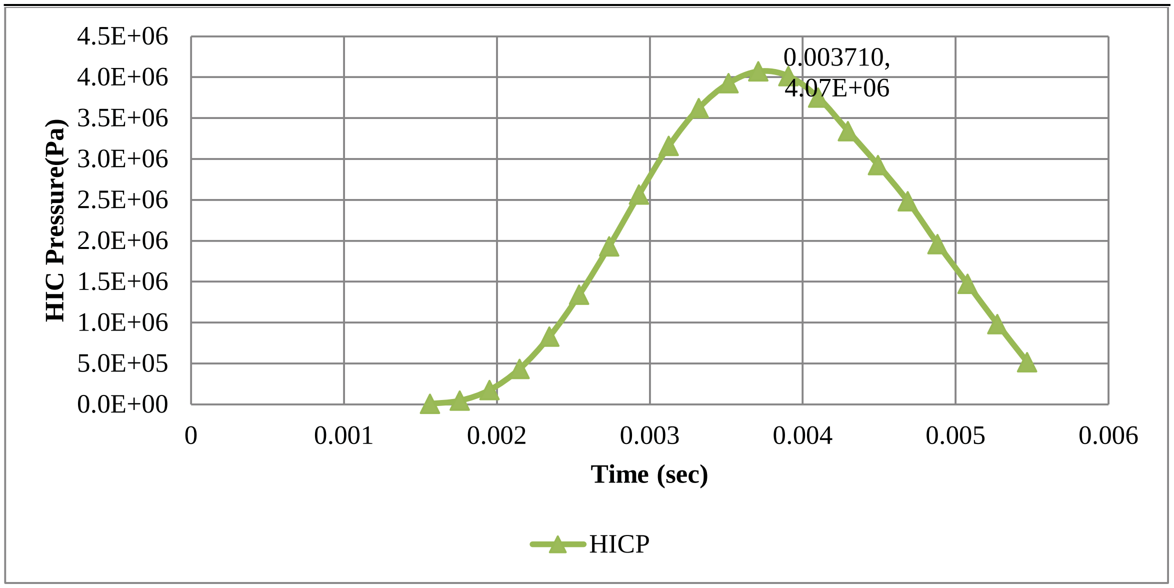

Figure 3.22 Plot of analytically calculated impact pressures as a function of time (45 to frontal impact 3 feet drop height)

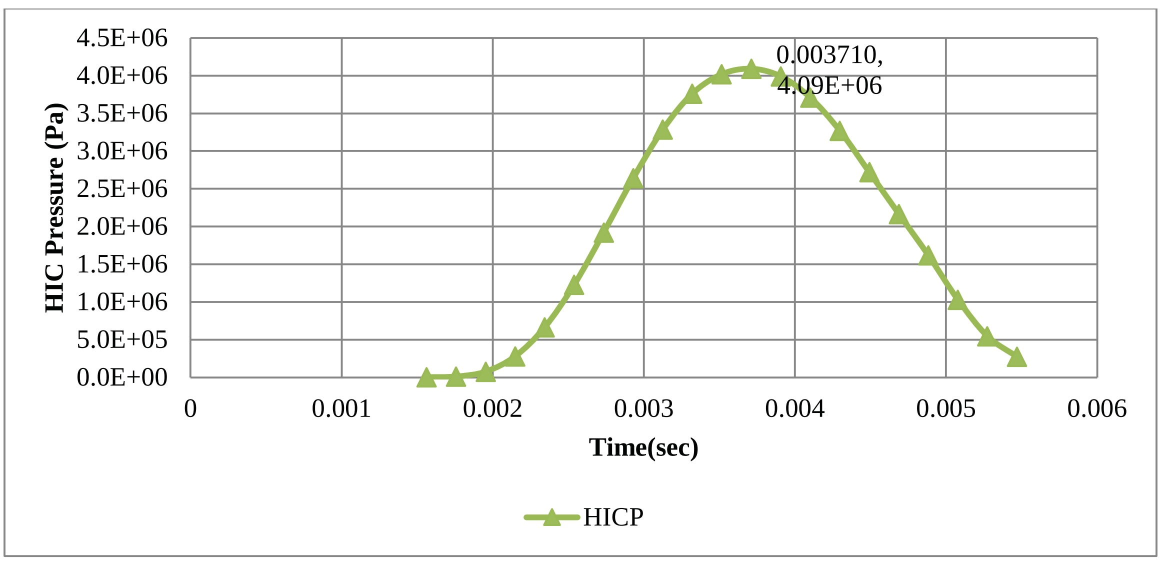

Figure 3.23 Plot of analytically calculated impact pressures as a function of time (45 to frontal impact 4 feet drop height)

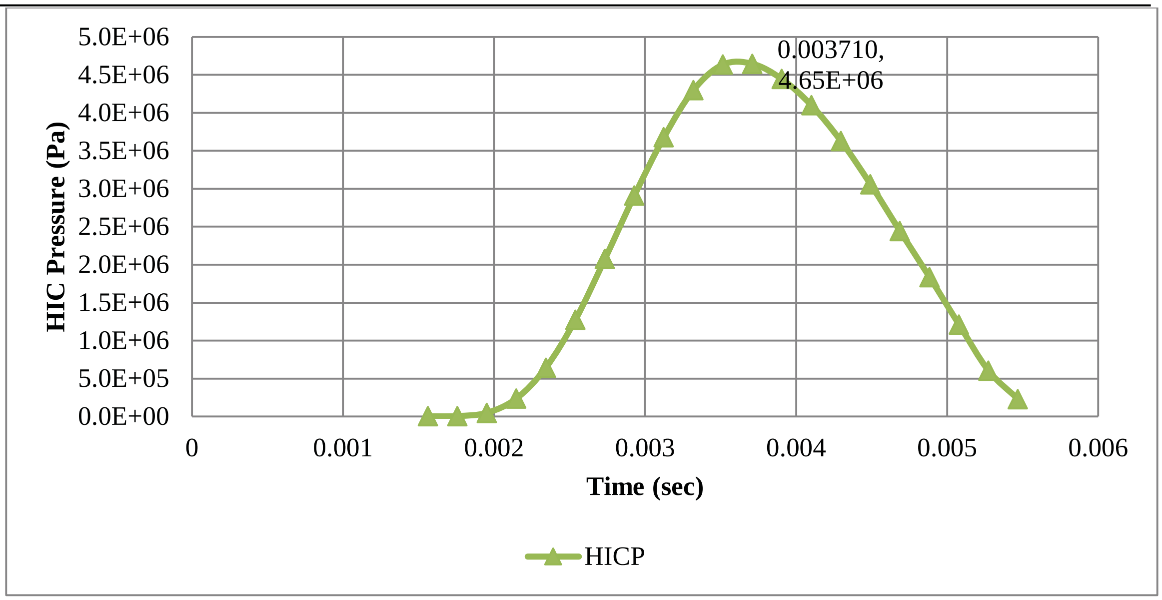

Figure 3.24 Plot of analytically calculated impact pressures as a function of time (45 to frontal impact 5 feet drop height)

3.2.10 45-to-Frontal Impact – Simulation Results (Pressure Contours)

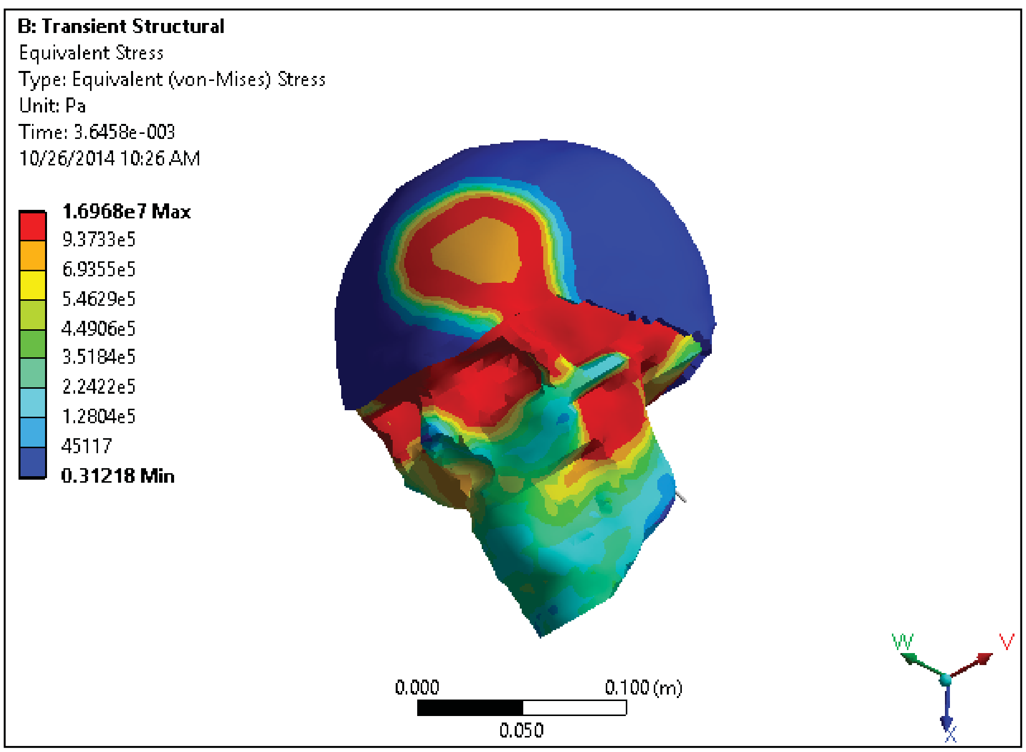

Figure 3.25 Von Mises Stress Distribution Contours – 45 to Frontal Impact 2 feet

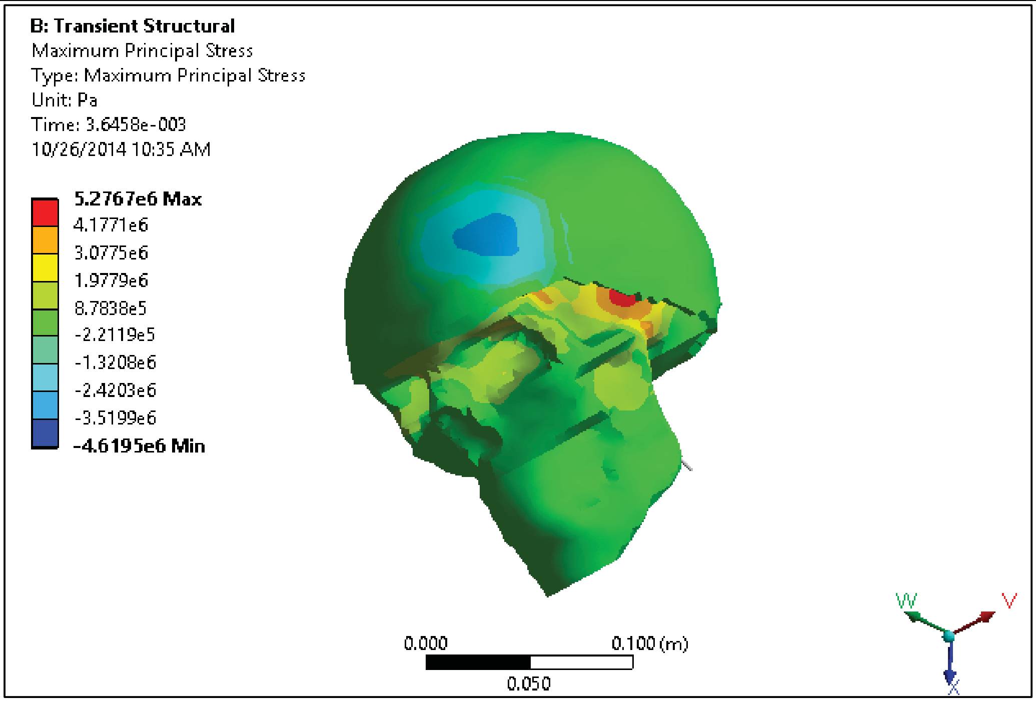

Figure 3.26 Maximum Principal Stress Distribution Contours – 45 to Frontal Impact 2 feet

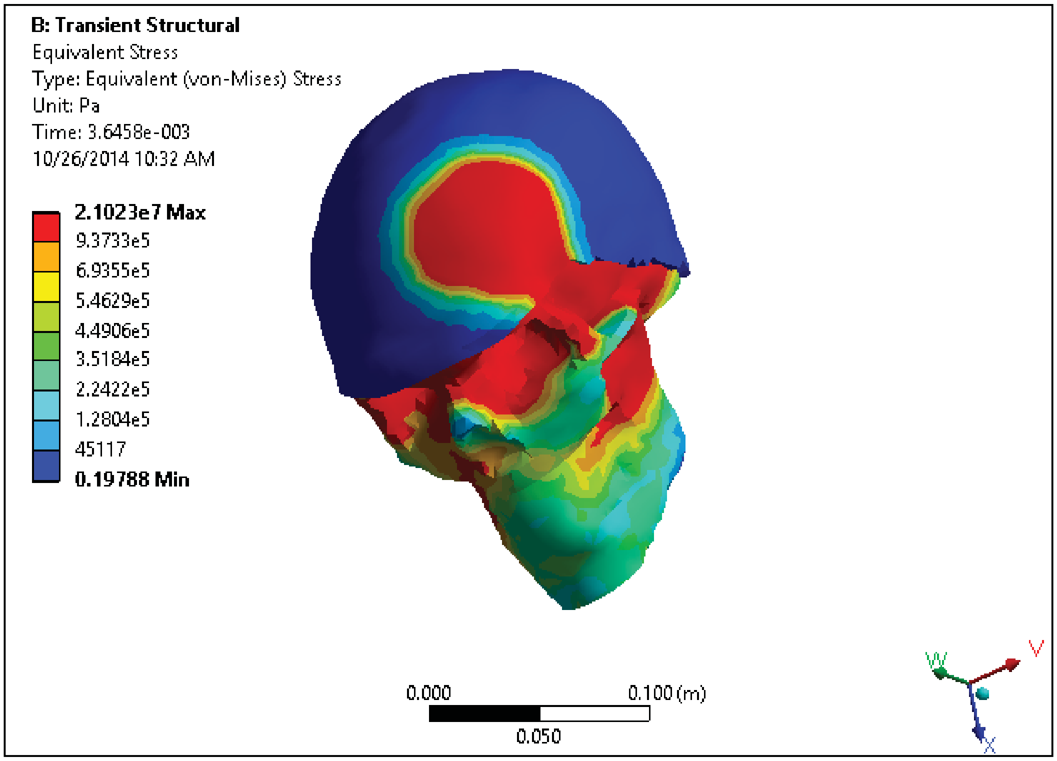

Figure 3.27 Von Mises Stress Distribution Contours – 45 to Frontal Impact 3 feet

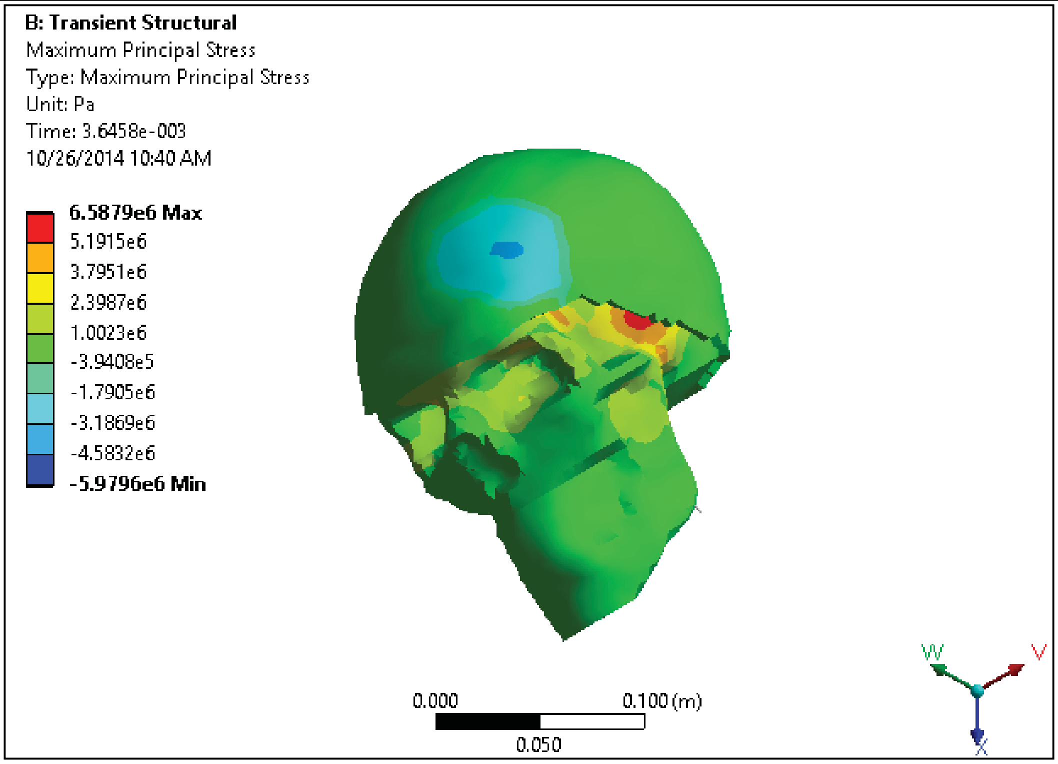

Figure 3.28 Maximum Principal Stress Distribution Contours – 45 to Frontal Impact 3 feet

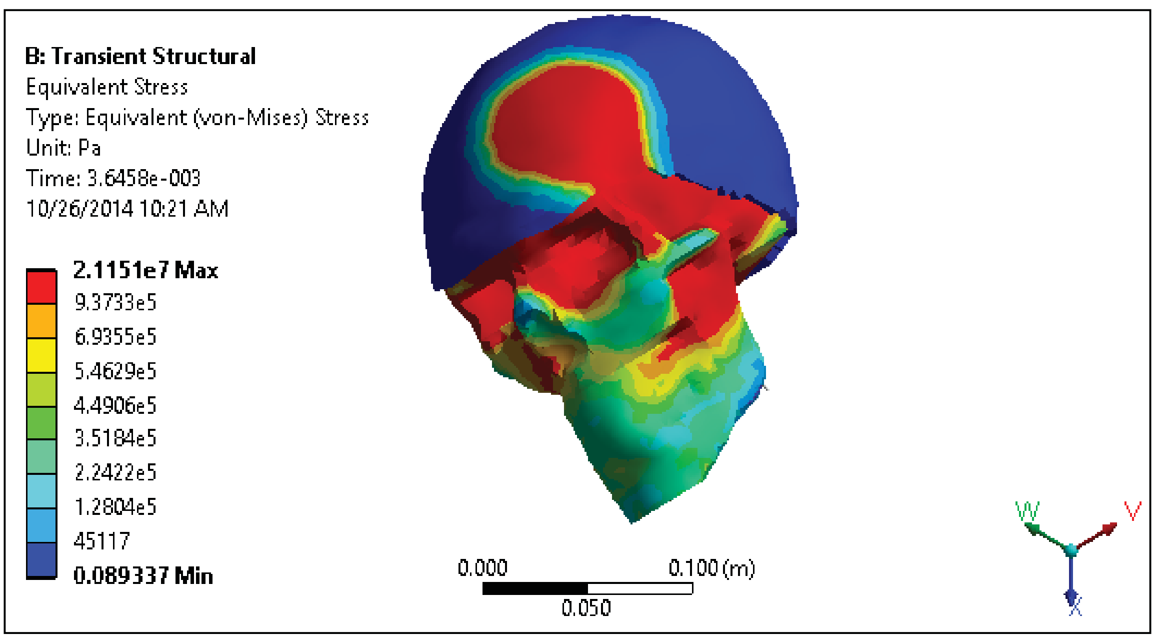

Figure 3.29 Von Mises Stress Distribution Contours – 45 to Frontal Impact 4 feet

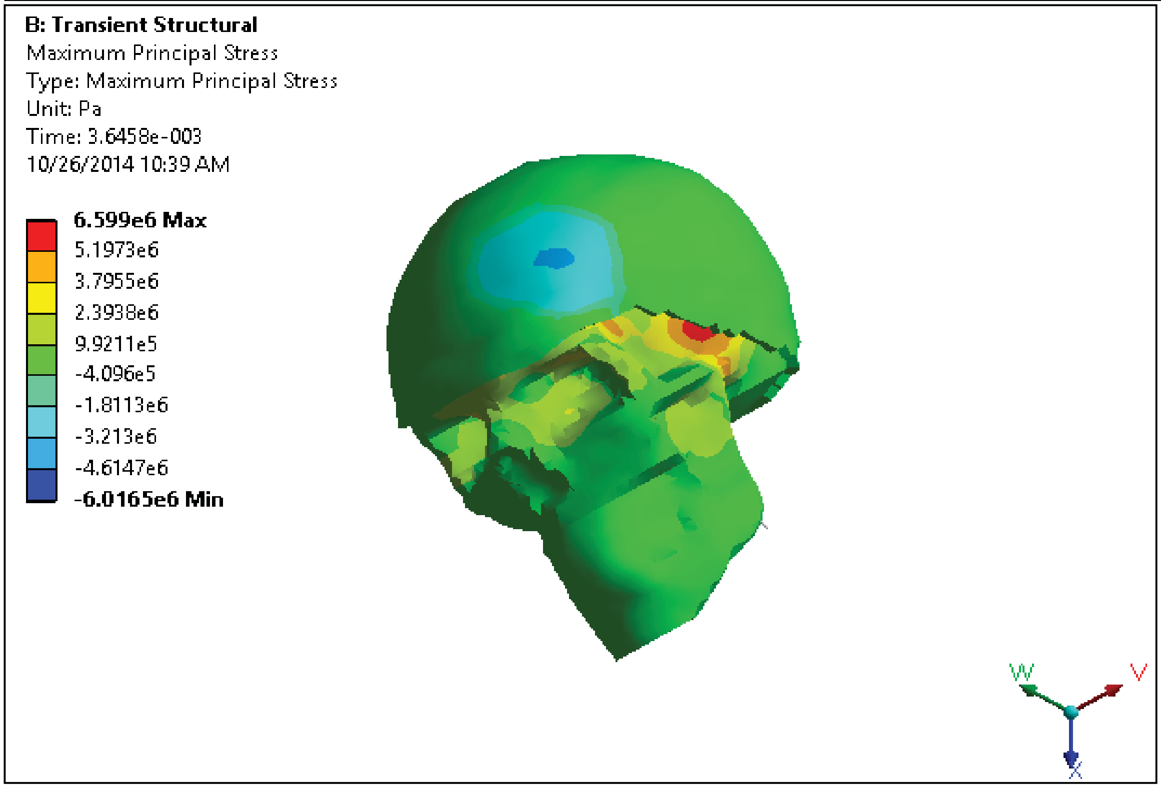

Figure 3.30Maximum Principal Stress Distribution Contours - 45 to Frontal Impact 4 feet

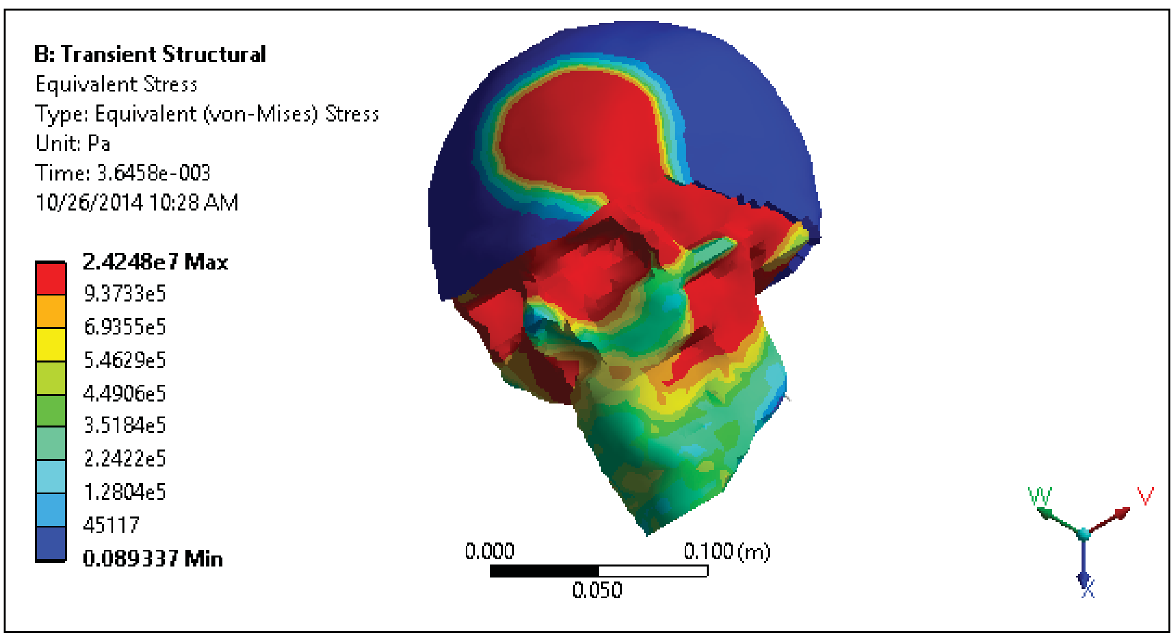

Figure 3.31 Von Mises Stress Distribution Contours - 45 to Frontal Impact 5 feet

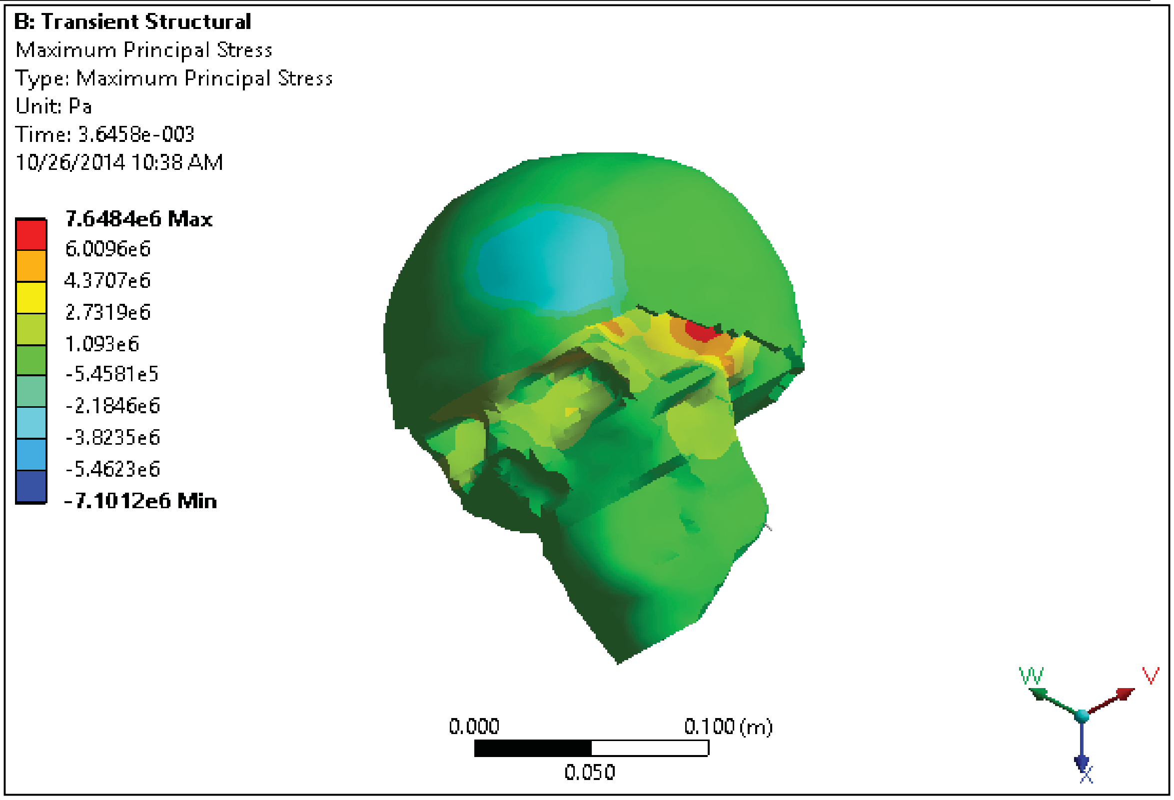

Figure 3.32 Maximum Principal Stress Distribution Contours - 45 to Frontal Impact 5 feet

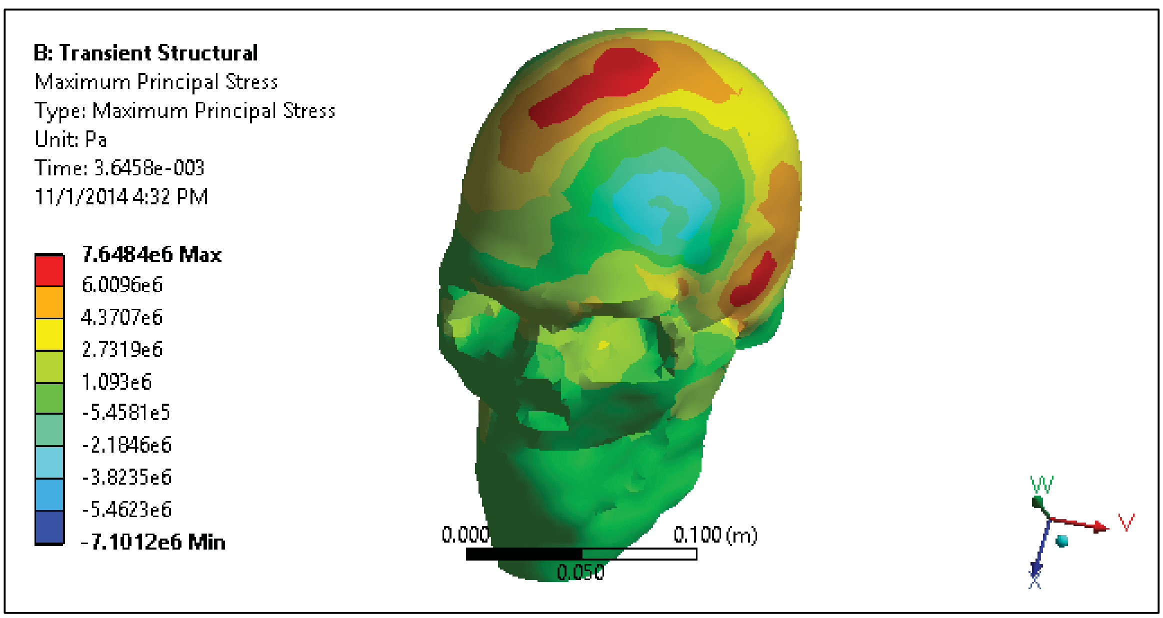

Figure 3.33 Location of peak value of Maximum Principal Stress on skull (without scalp) for 45-to-frontal 5 feet impact

3.2.11 Lateral Impact – Introduction

HICP or impact pressure curves (for respective drop heights) used as inputs to the validated FE model are shown in Figure 3.35-3.38 of Section 3.2.14. Refer to Appendix A for detailed data.

3.2.12 Lateral Impact – Summary of Results

Table 3.7 Results of Lateral Impact for 2, 3, 4 and 5 feet drop heights

	Drop Heights	Max. HICPressure (Pa)	Max. Principal Stress (Pa) (tension)	Peak Von-Mises Stress (Pa)	Peak Max. Shear Stress (Pa)
Lateral Impact	2	2.35E+06	1.60E+07	2.50E+07	1.30E+07
	3	2.89E+06	2.02E+07	3.14E+07	1.60E+07
	4	3.18E+06	2.25E+07	3.45E+07	1.77E+07
	5	3.49E+06	2.49E+07	3.80E+07	1.96E+07

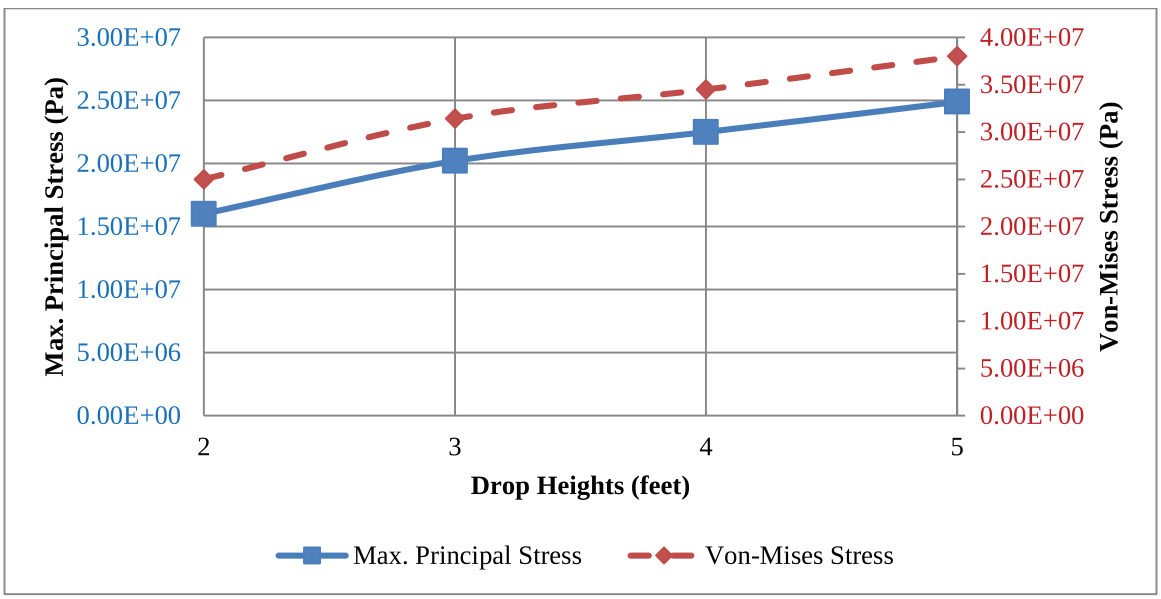

Figure 3.34 Plot of Maximum Principal Stress and Von-Mises Stress for lateral impact obtained from ANSYS simulations as a function of drop heights

3.2.13 Lateral Impact – Result Discussions

- Peak values of Von-Mises stresses were observed in lateral impact region, entire superior region of head model (scalp and skull), facial areas of skull and areas surrounding brain stem. For all drop heights the time locations of peak Von-Mises Stress values were at 3.64msec. (Figures 3.39, 3.41, 3.43, 3.45).
- Observed Von-Mises stress contours for entire time cycle were such that impact pressure wave has initiated from the right lateral (impact) region of the scalp, translated through skull, dura & brain and bounced back from the left lateral wall of the skull. This observation matches with the Coup and Contre-Coup injury mechanisms of TBI. (Coup injury is caused at the site of impact which deforms the skull and translates the impact to the brain. Brain bounces off from the opposite wall of skull causing ContreCoup injury.)
- Peak (tension) values of Maximum Principal Stress were observed in the regions near right ear (just below the impact region) and the superior region of skull. Higher values were also observed on the opposite end i.e. left lateral region. (Figures 3.47, 3.48) This seems structurally similar to cerebral aneurysm, a phenomenon in which arteries in brain bulge out due to their weakening and hypertension (increase in blood pressure) on them. Minimum (compression) value of Maximum Principal Stress was observed in the impact region which signifies maximum compression at the impact region. (Figures 3.40, 3.42, 3.44, 3.46)
- Peak values of Maximum Shear stress were observed at smaller points near impact region edges between scalp and skull. They also spanned over right parietal region with lesser magnitude than maximum.

3.2.14 Lateral Impact – Pressure Curves

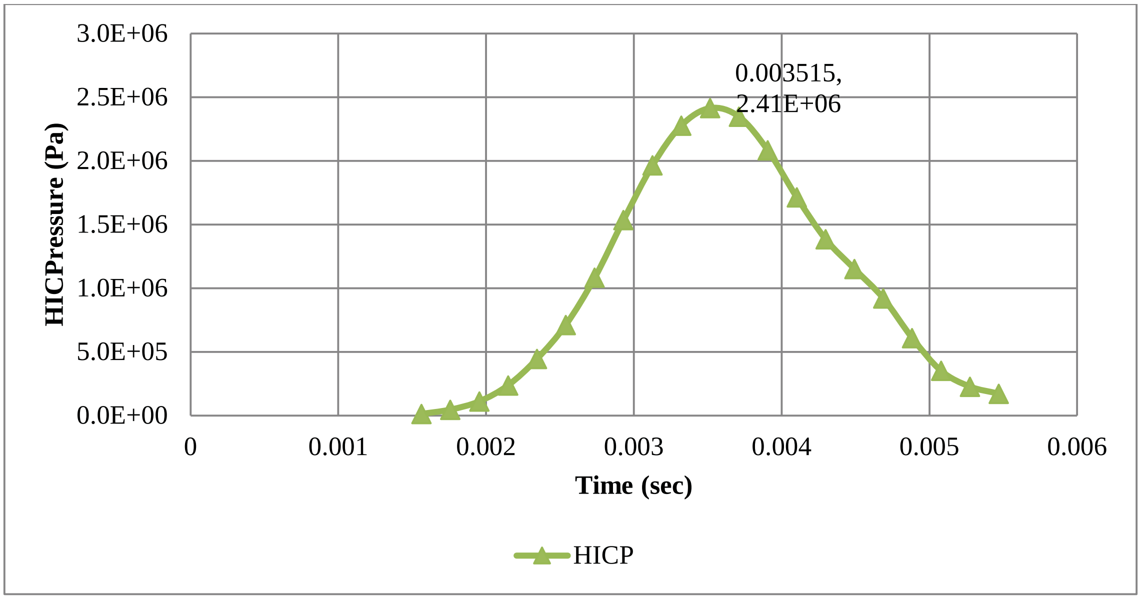

Figure 3.35 Plot of analytically calculated impact pressures as a function of time (lateral impact 2 feet drop height)

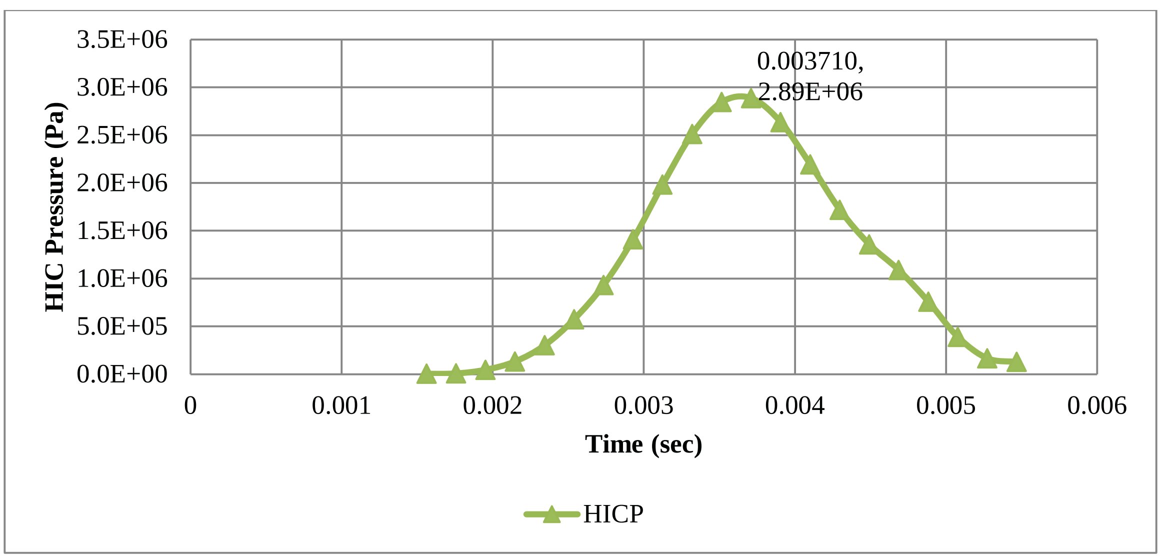

Figure 3.36 Plot of analytically calculated impact pressures as a function of time (lateral impact 3 feet drop height)

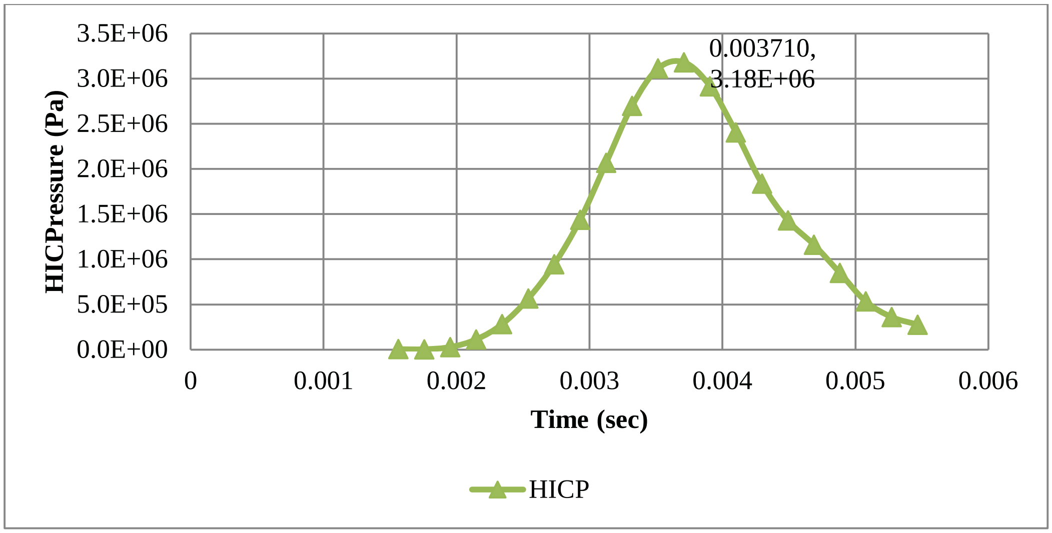

Figure 3.37 Plot of analytically calculated impact pressures as a function of time (lateral impact 4 feet drop height)

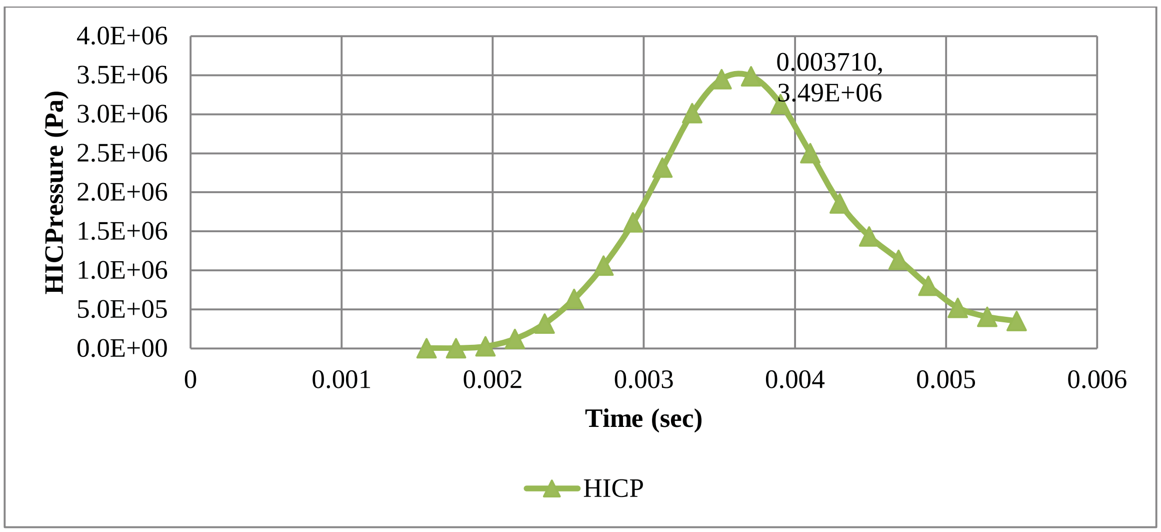

Figure 3.38 Plot of analytically calculated impact pressures as a function of time (lateral impact 5 feet drop height)

3.2.15 Lateral Impact – Simulation Results (Pressure Contours)

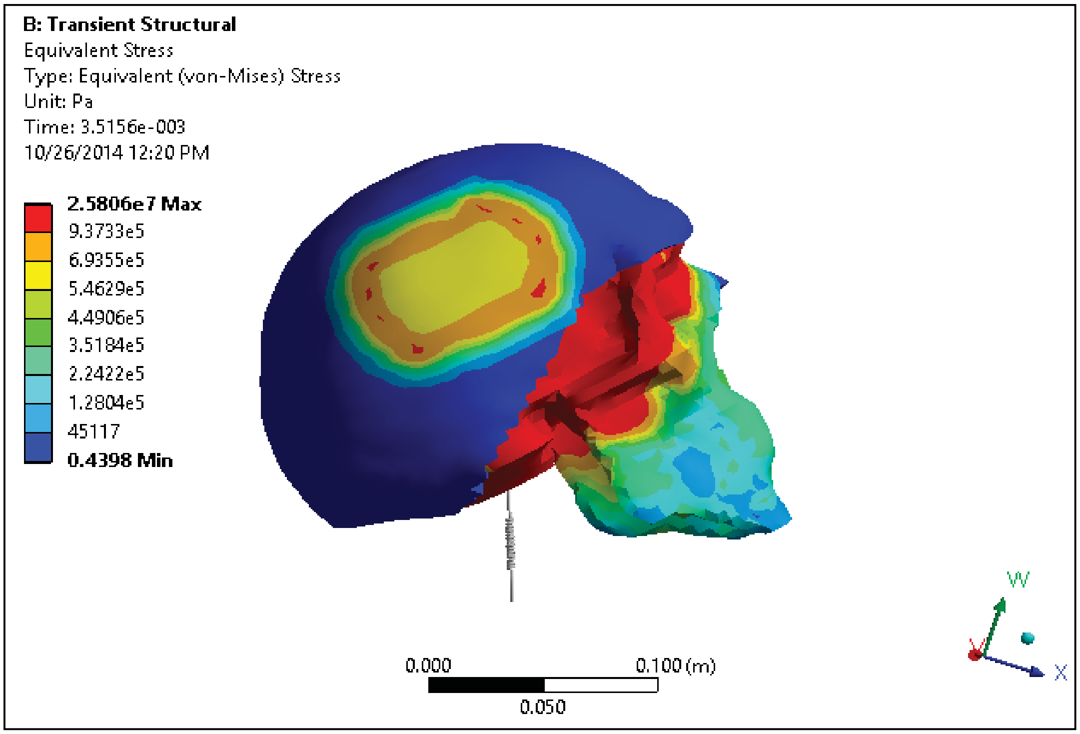

Figure 3.39 Von Mises Stress Distribution Contours - Lateral Impact 2 feet

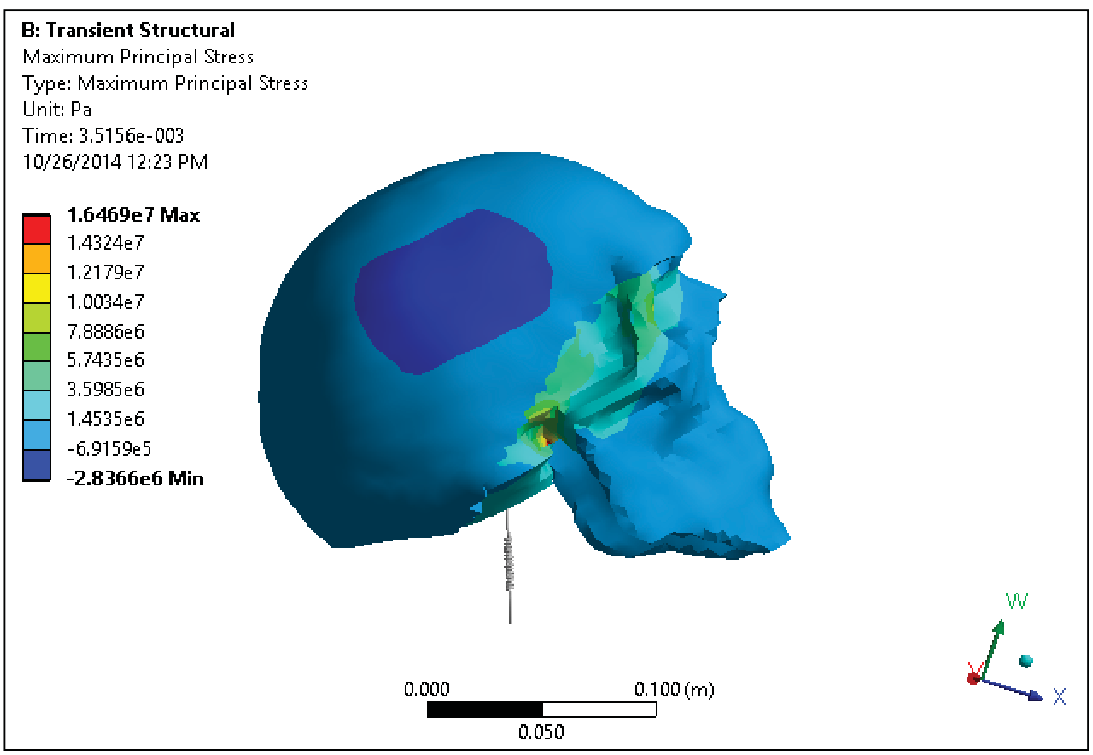

Figure 3.40 Maximum Principal Stress Distribution Contours - Lateral Impact 2 feet

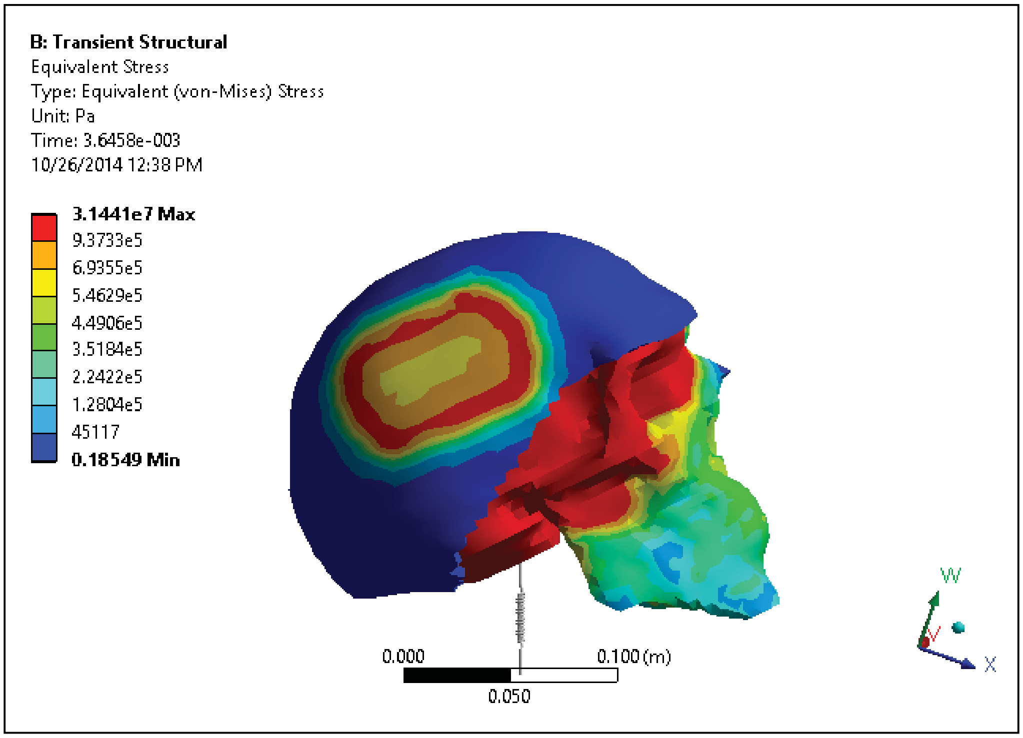

Figure 3.41 Von Mises Stress Distribution Contours - Lateral Impact 3 feet

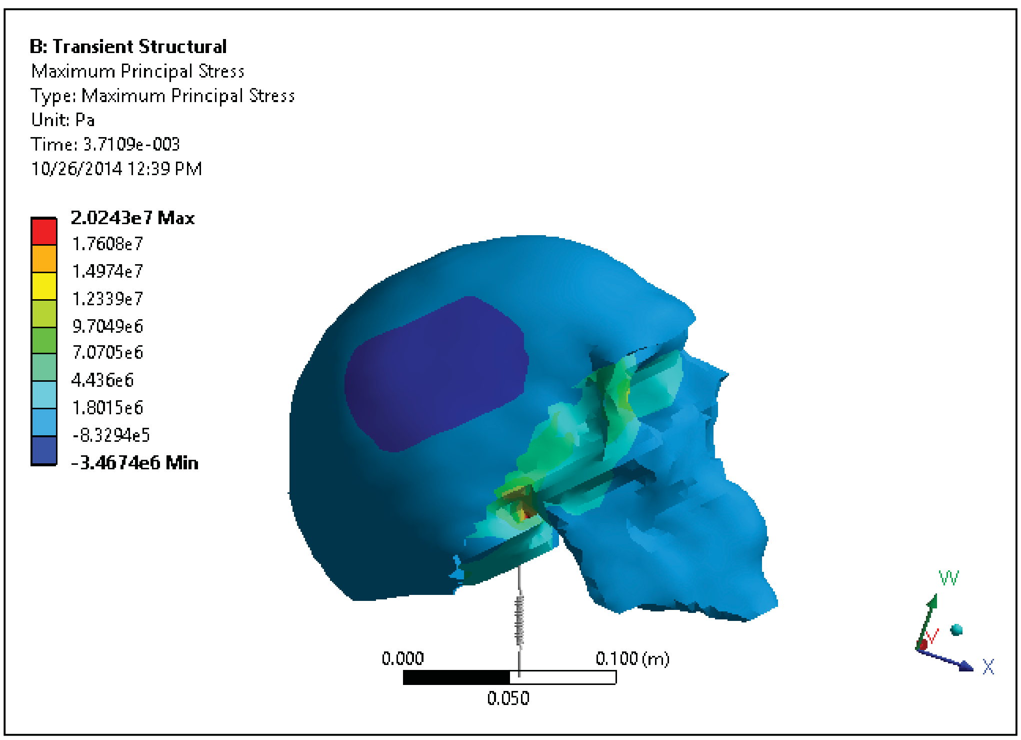

Figure 3.42 Maximum Principal Stress Distribution Contours - Lateral Impact 3 feet

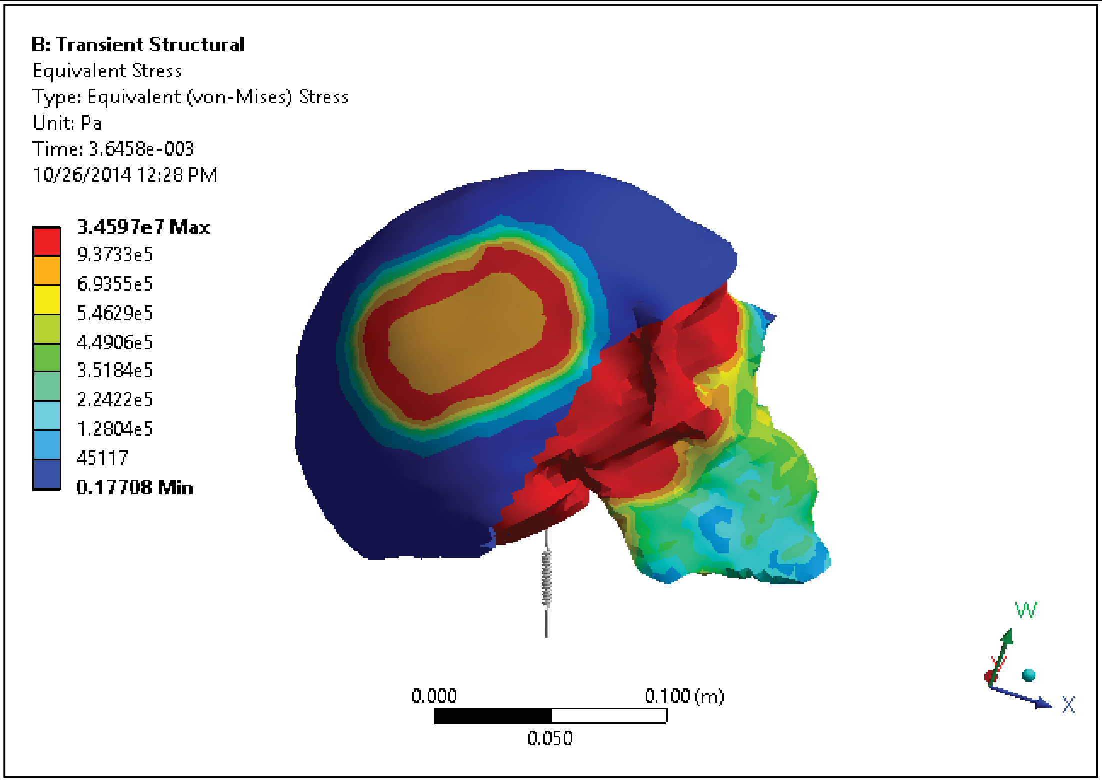

Figure 3.43 Von Mises Stress Distribution Contours - Lateral Impact 4 feet

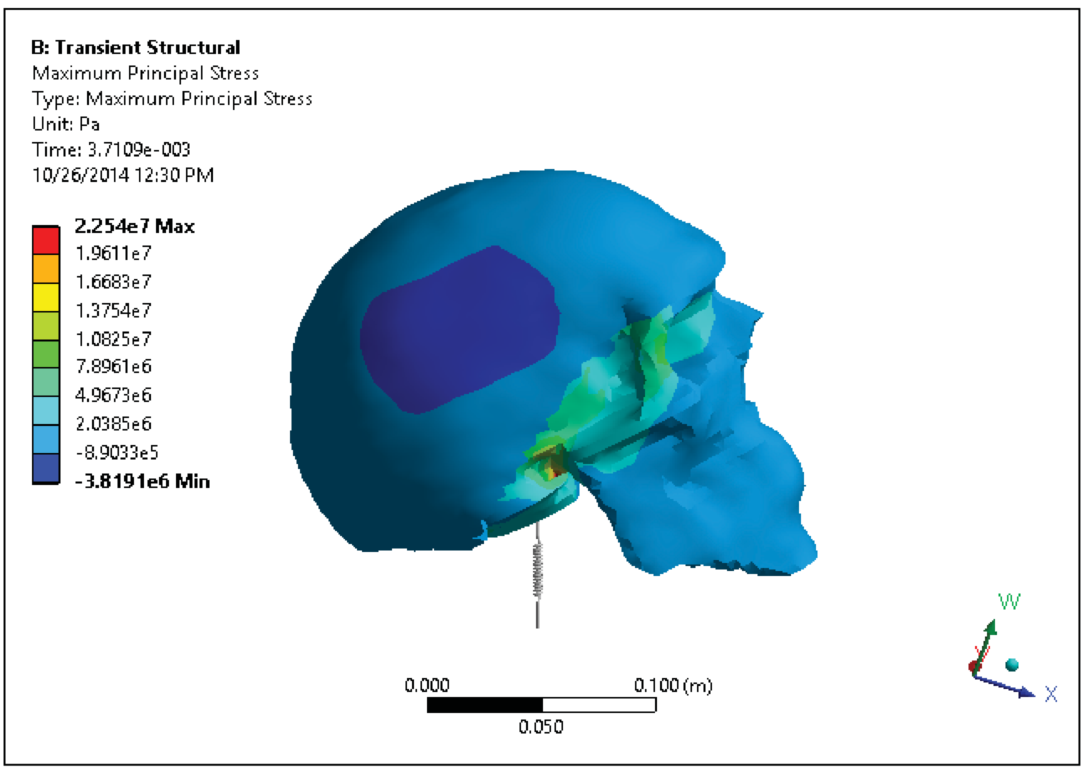

Figure 3.44 Maximum Principal Stress Distribution Contours - Lateral Impact 4 feet

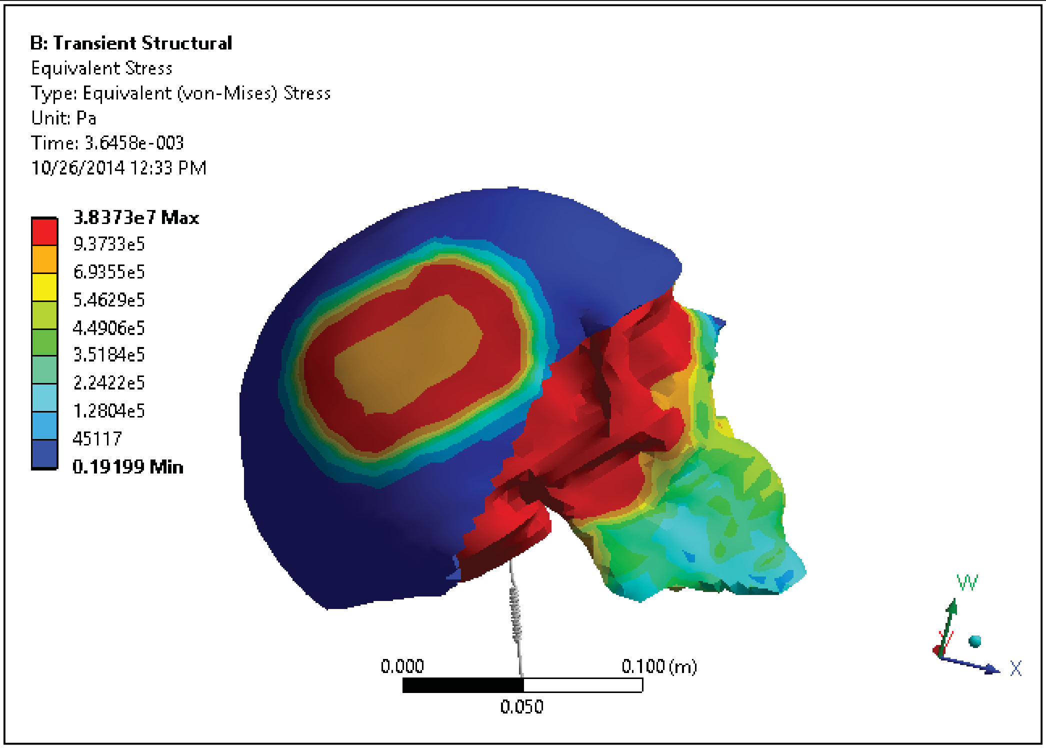

Figure 3.45 Von Mises Stress Distribution Contours - Lateral Impact 5 feet

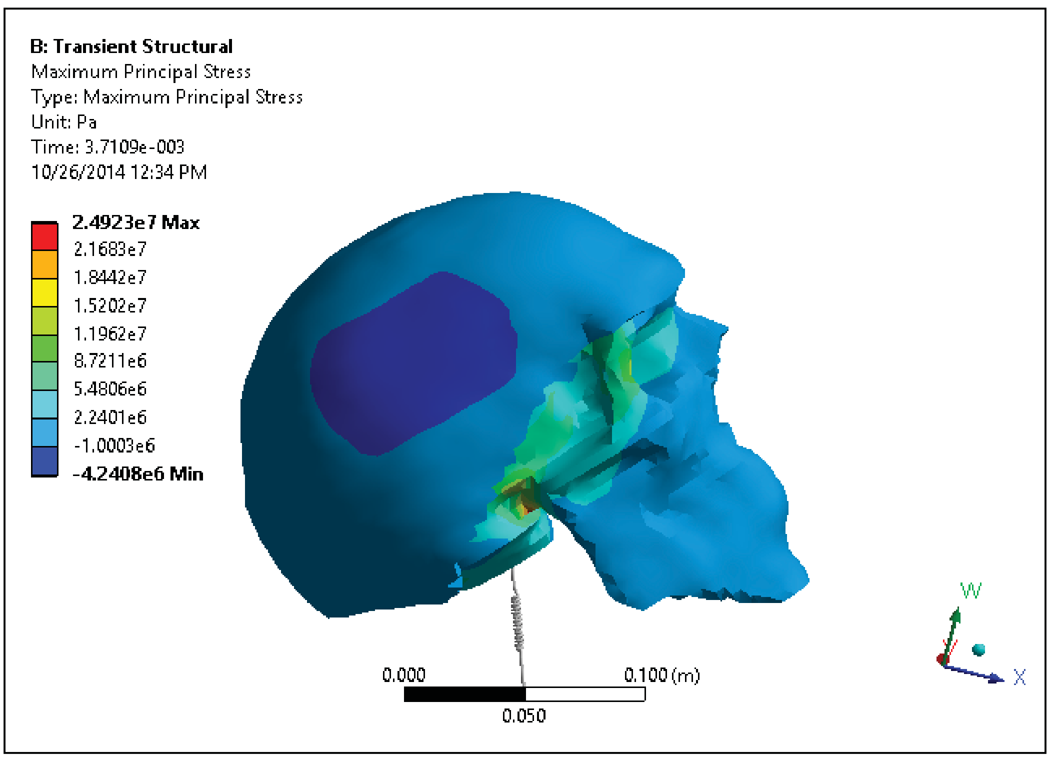

Figure 3.46 Maximum Principal Stress Distribution Contours - Lateral Impact 5 feet

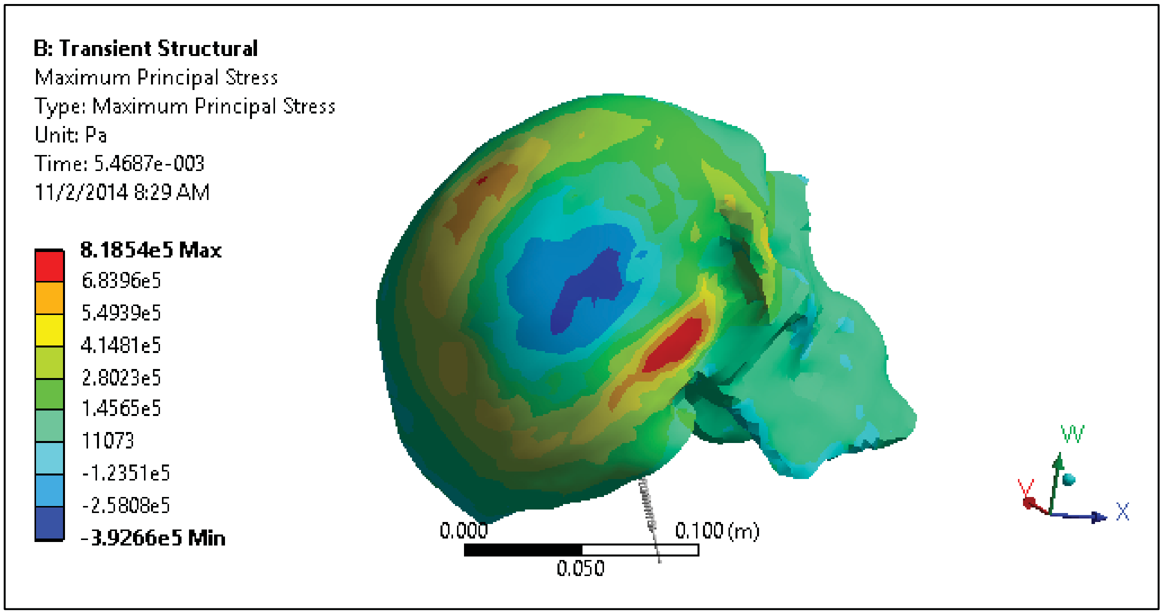

Figure 3.47 Location of peak value of Maximum Principal Stress near impact region on skull (without scalp) for Lateral 5 feet impact

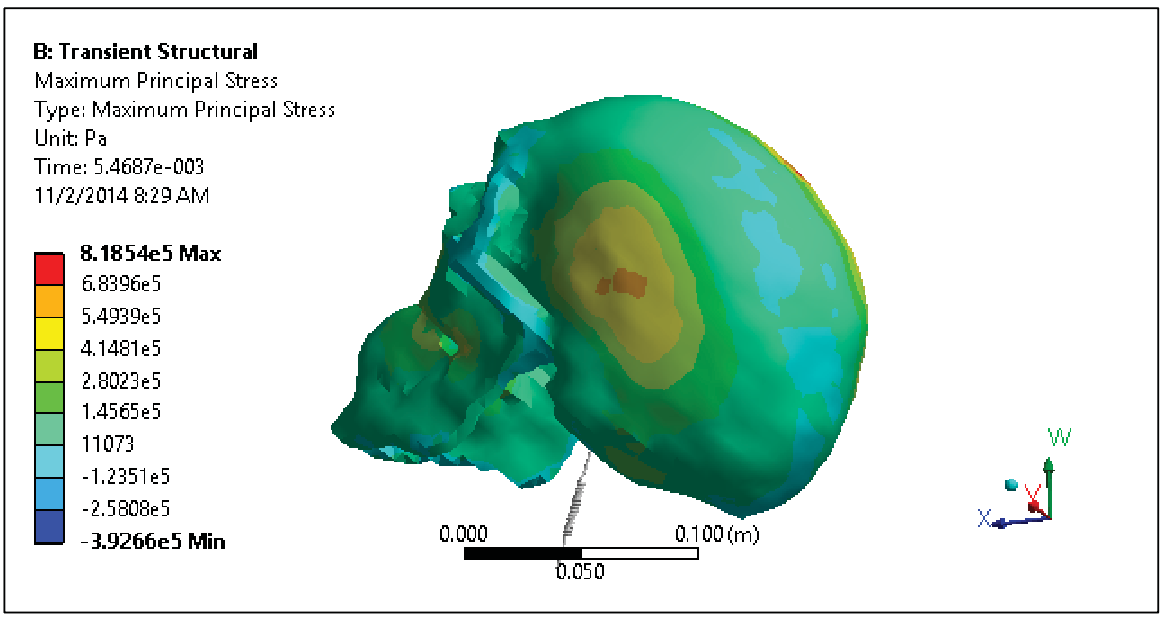

Figure 3.48 Location of peak value of Maximum Principal Stress opposite to impact region on skull (without scalp) for Lateral 5 feet impact

3.2.16 Posterior Impact – Introduction

HICP or impact pressure curves (for respective drop heights) used as inputs to the validated FE model are shown in Figure 3.50-3.53 in Section 3.19. Refer to Appendix A for detailed data.

3.2.17 Posterior Impact – Summary of Results

Table 3.8 Results of Posterior Impact for 2, 3, 4 and 5 feet drop heights

	Drop Heights	Max. HICPressure (Pa)	Max. Principal Stress (Pa) (tension)	Max. Von-Mises Stress (Pa)	Peak Max. Shear Stress (Pa)
Posterior Impact	2	3.50E+06	1.13E+07	1.74E+07	8.93E+06
	3	4.10E+06	1.28E+07	1.98E+07	1.01E+07
	4	4.76E+06	1.49E+07	2.30E+07	1.18E+07
	5	5.33E+06	1.68E+07	2.60E+07	1.33E+07

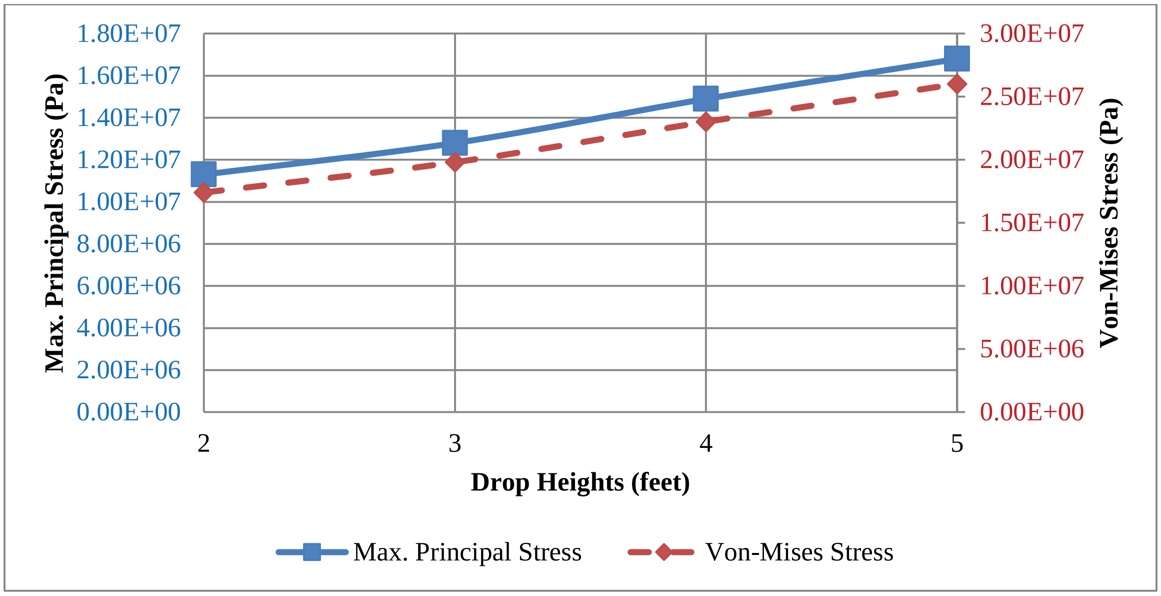

Figure 3.49 Plot of Maximum Principal Stress and Von-Mises Stress for posterior impact obtained from ANSYS simulations as a function of drop heights

3.2.18 Posterior Impact – Result Discussions

- Peak values of Von-Mises stresses were observed in posterior impact region, entire superior region of head model (scalp and skull), facial areas of skull and areas surrounding brain stem. For all drop heights the time locations of peak Von-Mises Stress values were at 3.64msec. (Figures 3.54, 3.56, 3.58, 3.60).
- Observed Von-Mises stress contours for entire time cycle were such that impact pressure wave has initiated from the posterior (impact) region of the scalp, translated through skull, dura & brain and bounced back from the frontal wall of the skull. This observation matches with the Coup and Contre-Coup injury mechanisms of TBI. (Coup injury is caused at the site of impact which deforms the skull and translates the impact to the brain. Brain bounces off from the opposite wall of skull causing ContreCoup injury.)
- Peak (tension) values of Maximum Principal Stress were observed in the posterior occipital regions behind both the ears and areas closer to brain stem (Figures 3.62). This seems structurally similar to cerebral aneurysm, a phenomenon in which arteries in brain bulge out due to their weakening and hypertension (increase in blood pressure) on them. Minimum (compression) value of Maximum Principal Stress was observed in the impact region which signifies maximum compression at the impact region (Figures 3.55, 3.57, 3.59, 3.61) Compressive value increased with height increase.
- Peak values of Maximum Shear stress were observed in smaller areas at the center of impact region between scalp and skull layers. They also spanned over occipital region with lesser magnitude than maximum.

3.2.19 Posterior Impact – Pressure curves

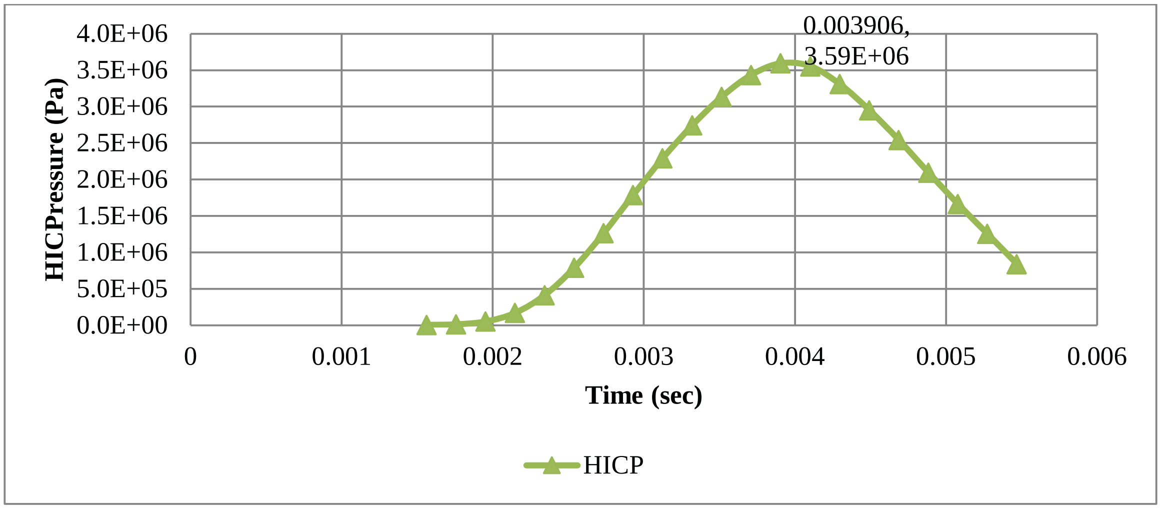

Figure 3.50 Plot of analytically calculated impact pressures as a function of time (posterior impact 2 feet drop height)

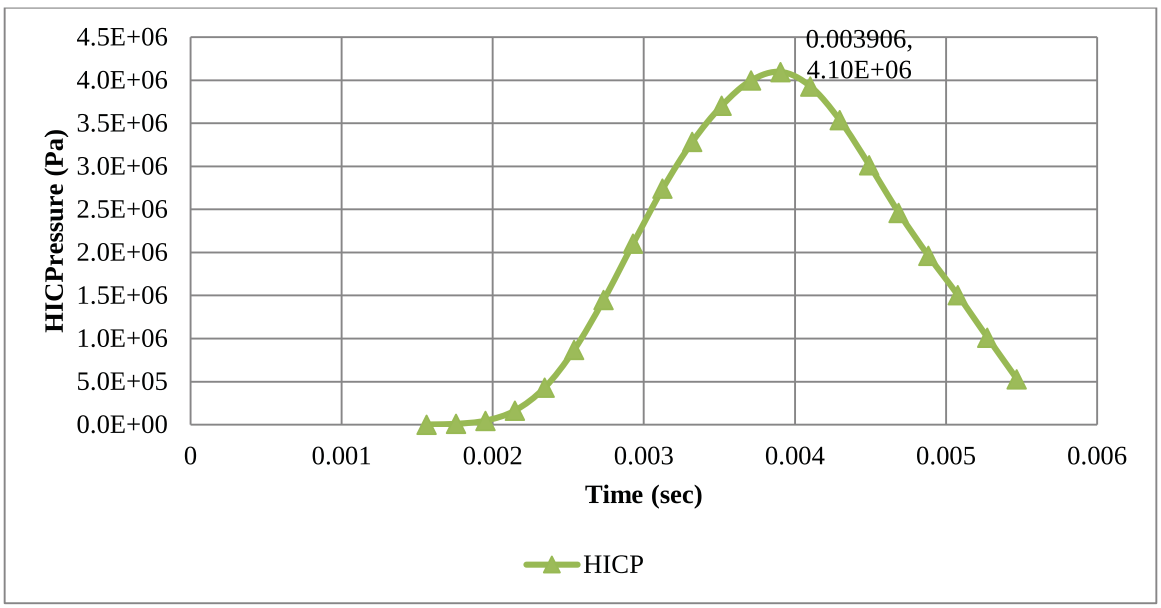

Figure 3.51 Plot of analytically calculated impact pressures as a function of time (posterior impact 3 feet drop height)

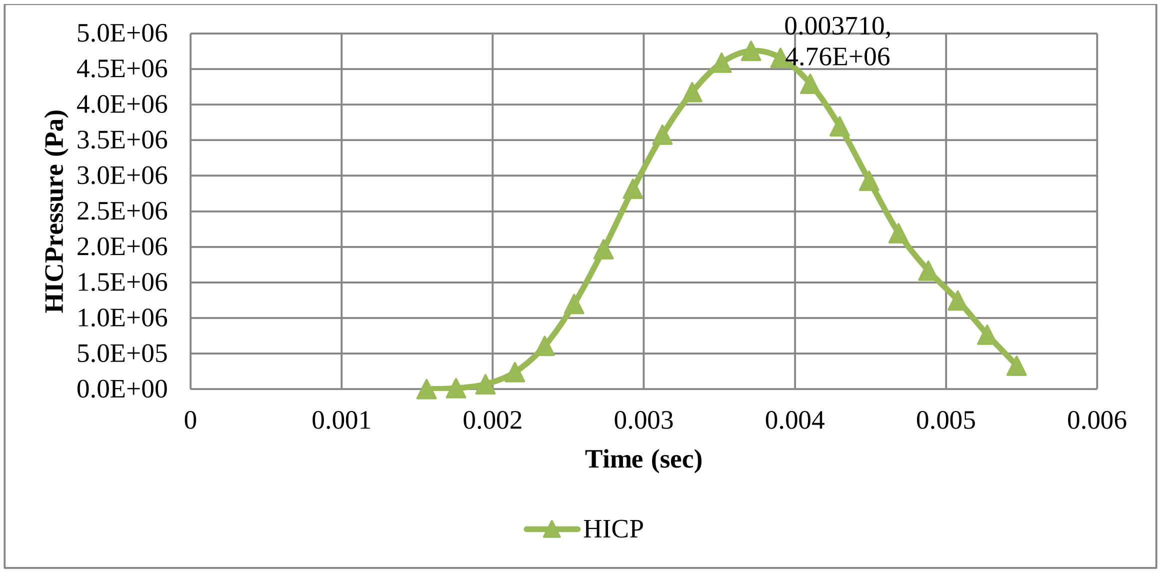

Figure 3.52 Plot of analytically calculated impact pressures as a function of time (posterior impact 4 feet drop height)

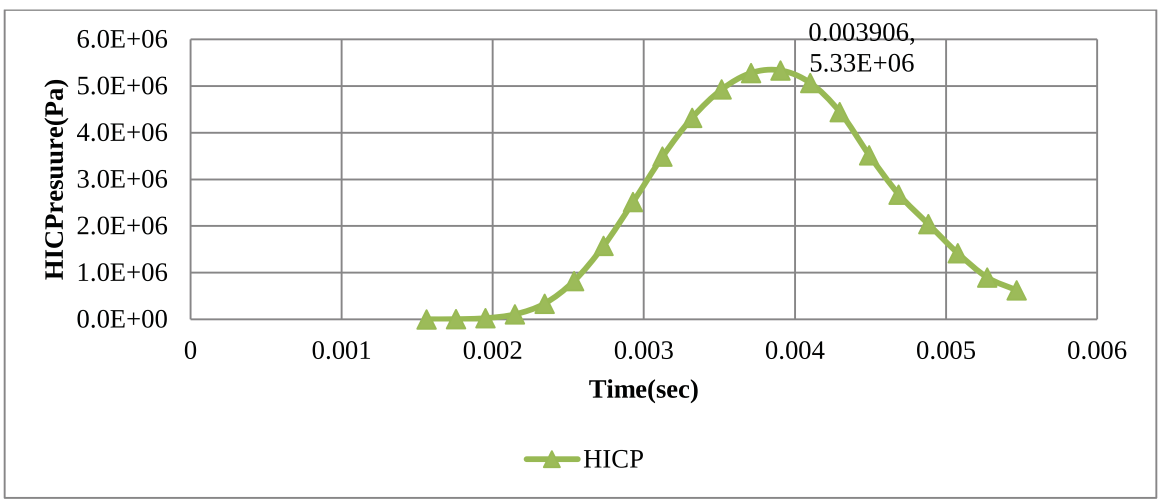

Figure 3.53 Plot of analytically calculated impact pressures as a function of time (posterior impact 5 feet drop height)

3.2.20 Posterior Impact – Simulation Results (Pressure Contours)

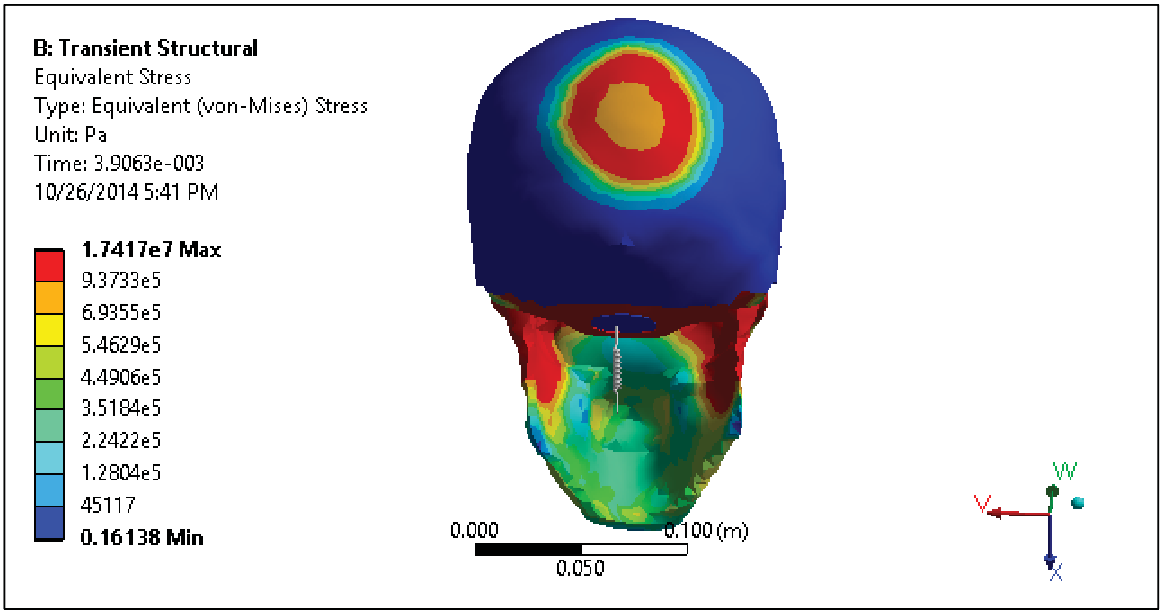

Figure 3.54 Von Mises Stress Distribution Contours - Posterior Impact 2 feet

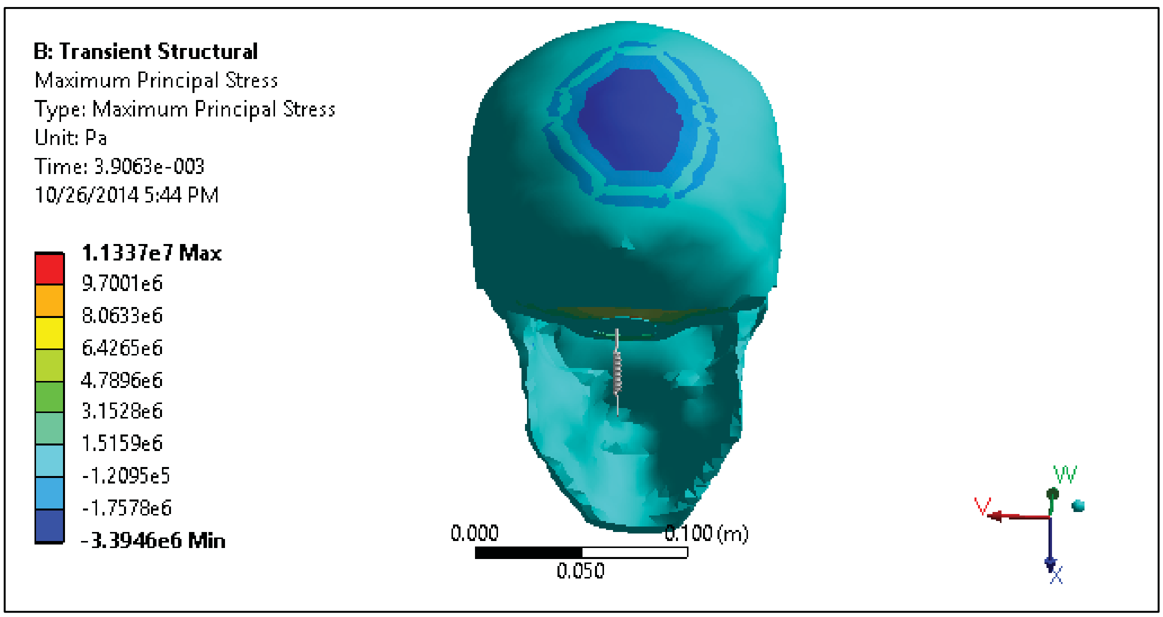

Figure 3.55 Maximum Principal Stress Distribution Contours - Posterior Impact 2 feet

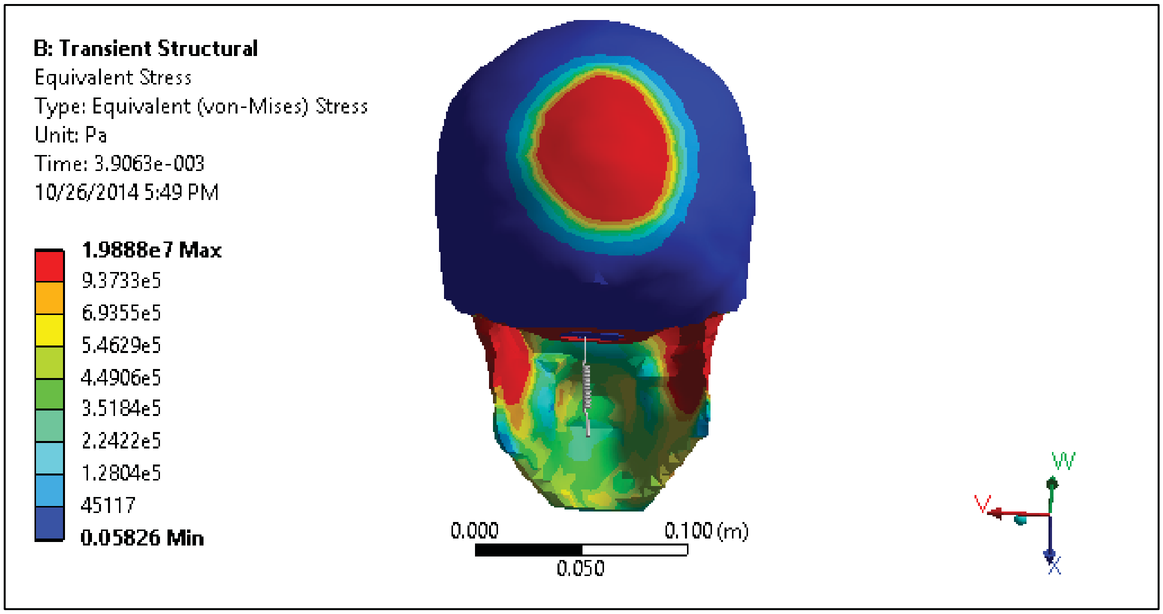

Figure 3.56 Von Mises Stress Distribution Contours - Posterior Impact 3 feet

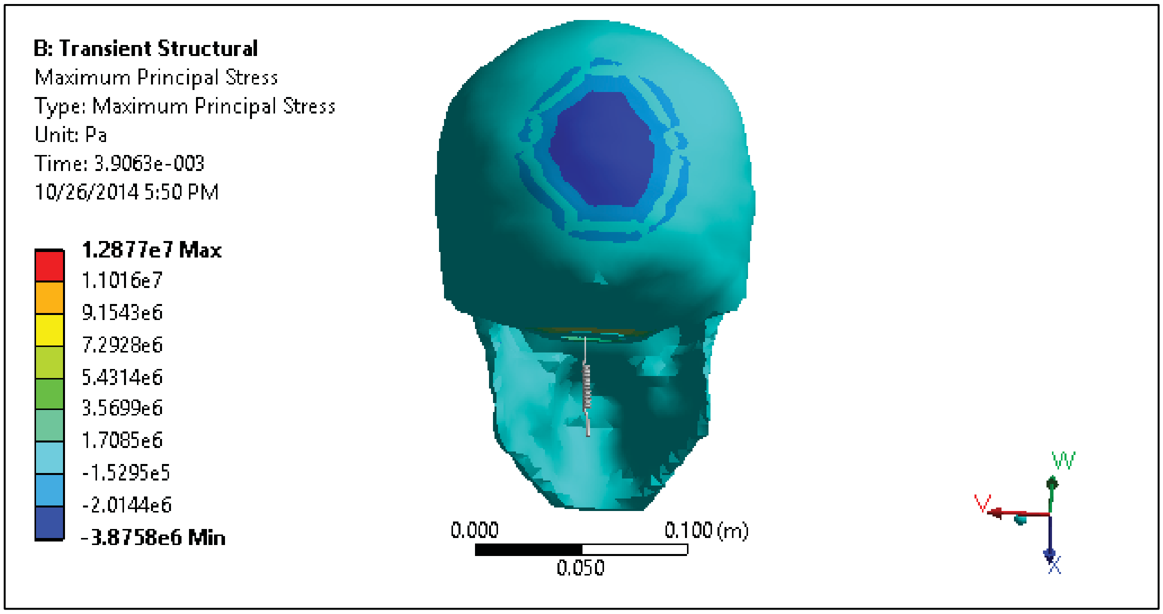

Figure 3.57 Maximum Principal Stress Distribution Contours - Posterior Impact 3 feet

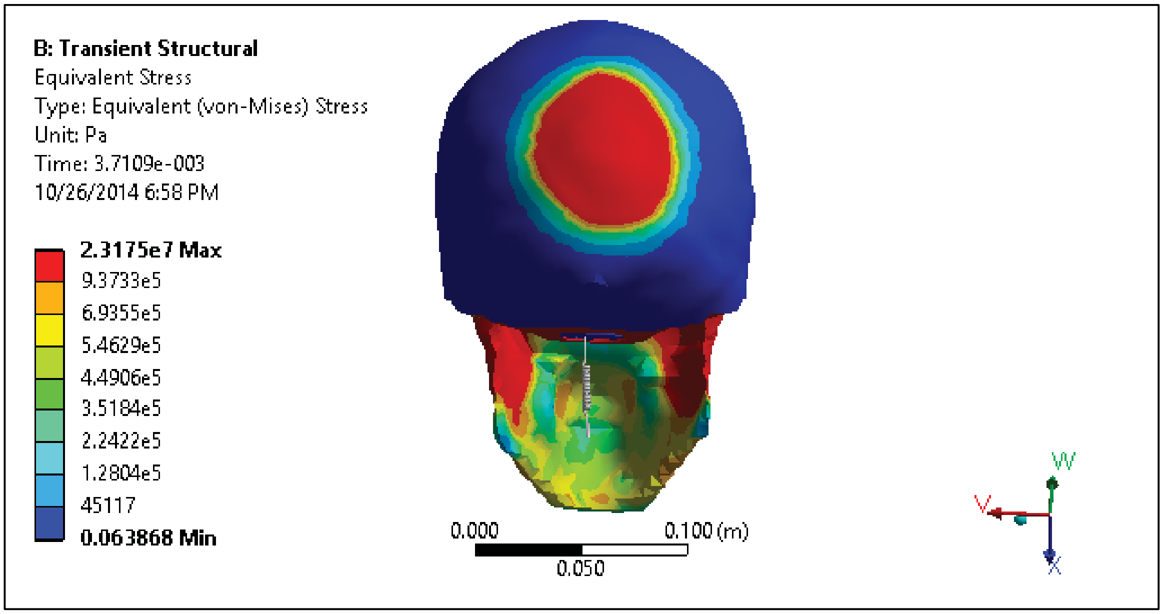

Figure 3.58Von Mises Stress Distribution Contours - Posterior Impact 4 feet

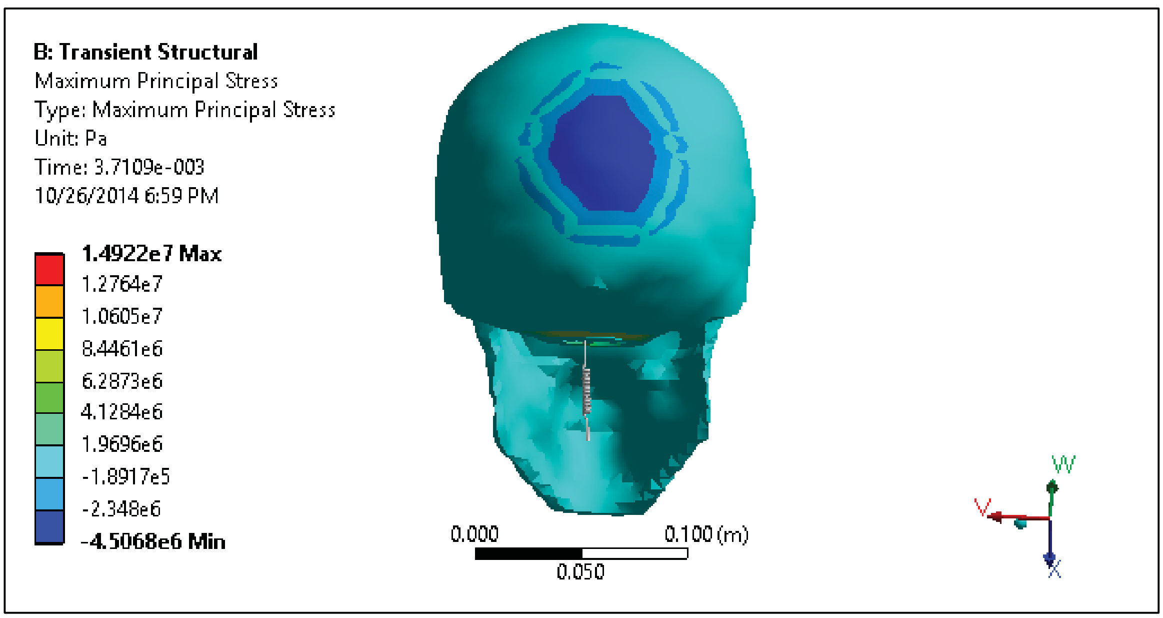

Figure 3.59 Maximum Principal Stress Distribution Contours - Posterior Impact 4 feet

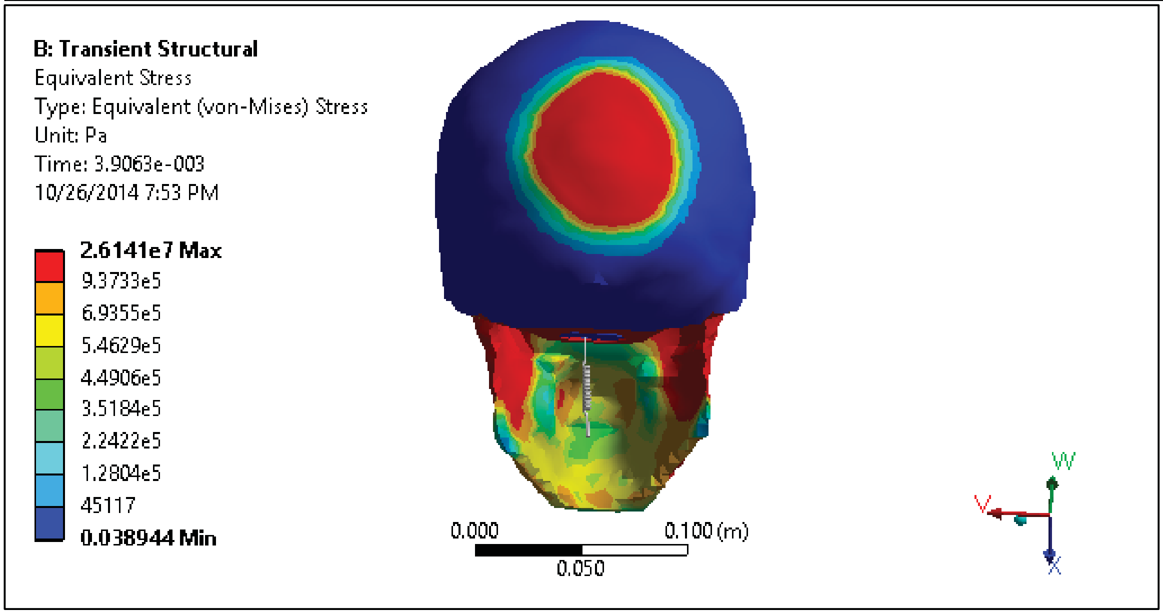

Figure 3.60 Von Mises Stress Distribution Contours - Posterior Impact 5 feet

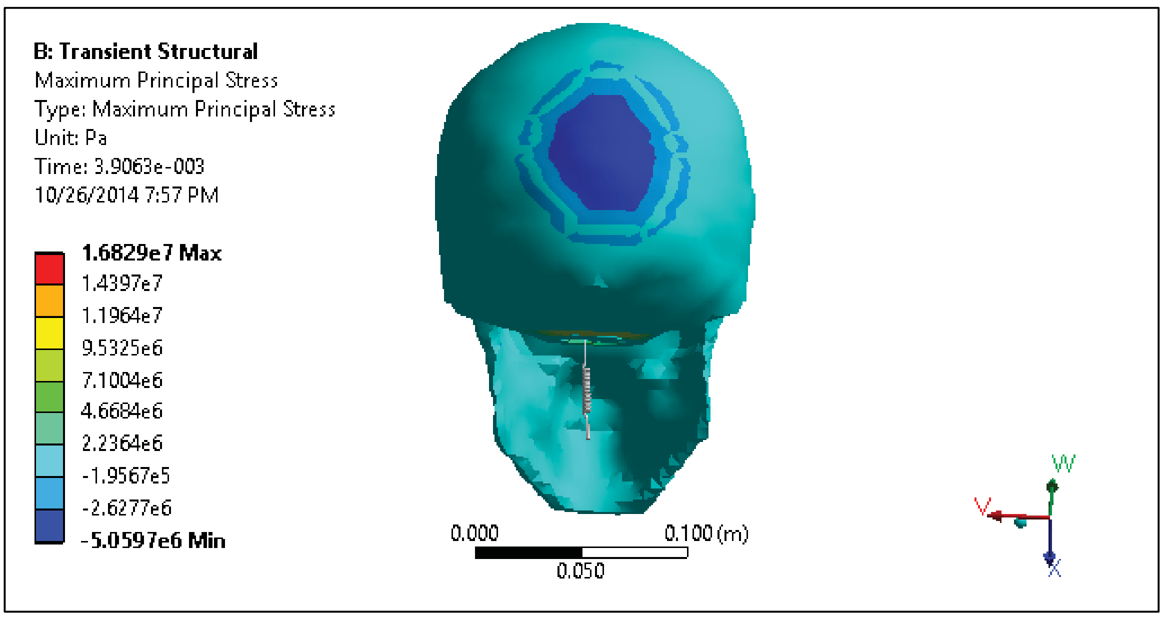

Figure 3.61 Maximum Principal Stress Distribution Contours - Posterior Impact 5 feet

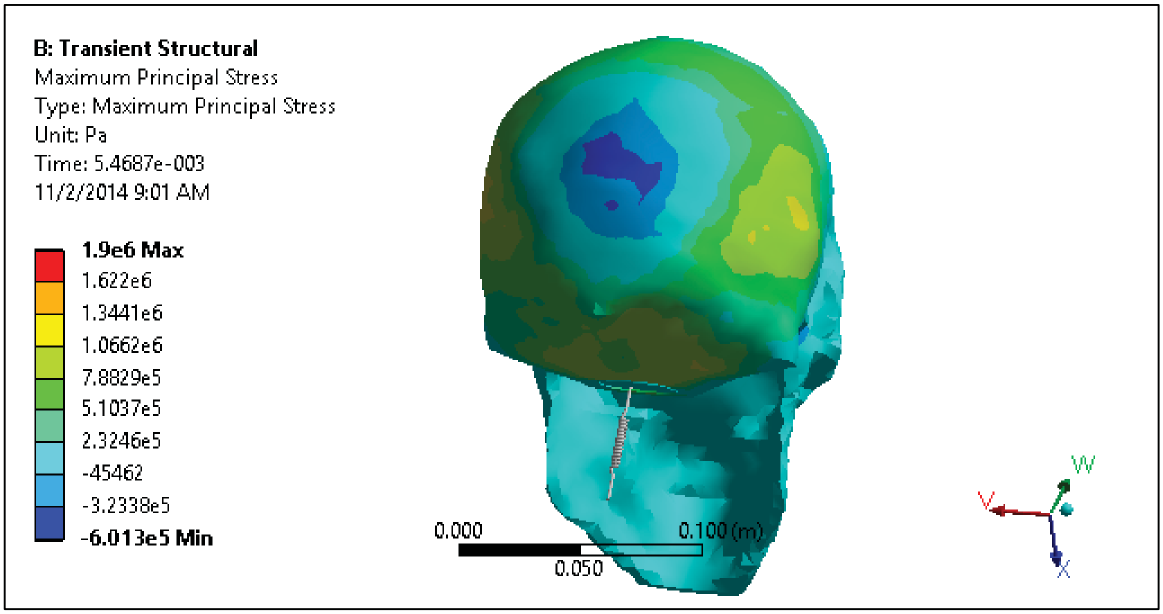

Figure 3.62 Location of peak value of Maximum Principal Stress on skull (without scalp) for Posterior 5 feet impact

3.3 Overall Result Discussions

Overall comparison between all impact regions and drop heights is presented in this section.

- Peak value of Von-Mises Stress (38 MPa) was observed for Lateral 5 feet Impact. The magnitude of Lateral 2 feet impact (25MPa) was closer to the Posterior 5 feet impact (26MPa) which was he next highest in the peak values of Von-Mises stress. This means that the lateral impact was the most detrimental even from a shorter height or lesser distance from the impacting body.
- Peak value of Maximum Principal Stress (tension) was also observed for Lateral 5 feet Impact (~25MPa). Lateral region was also the only region which showed tensile maximum principal stress travelling from one end of skull to the other end. Refer to Figures 3.47 and 3.48
- Peak value of Maximum Shear Stress was observed in Lateral 5 feet Impact (19.6MPa) followed by 45-to-frontal 5 feet (13.5MPa) impact and Posterior 5 feet (13.3 MPa) impact.
- Least values of Von-Mises (7.8MPa), Maximum Principal (4.46MPa) and Maximum Shear (4.2 MPa) stresses were observed for Frontal 2 feet impact.
- Thus, Lateral impacts for all drop heights were the most detrimental to human brain with greater probabilities of TBI whereas the Frontal impact of 2 feet drop height was the least detrimental amongst all regions and drop heights.

Thus, one can conclude various impacts are sensitive to impact regions.

4. Correlation between Head Kinematics and Brain Kinetics

Anna Oeur and her research team at University of Ottawa reconstructed and analyzed non-persistent concussions, persistent concussions and TBIs in their study. Non-persistent concussions are the ones that resolve in few weeks whereas the persistent ones remain for years. TBIs cause permanent damage to the brain. They found that linear and angular accelerations for TBIs were higher than the non-persistent or persistent concussions. They also found that dynamic responses of some individual persistent concussions overlapped with that of TBIs thus making persistent concussions equally hazardous to human brain [27].

Extracting some data from their published abstract we got linear acceleration tolerance level for TBI as 319 G and angular acceleration tolerance level for TBI as 23000 rad/s^2 [27] .This section uses linear acceleration data to determine drop heights for the TBI tolerance level. Von-Mises stress and Maximum Principal Stress values for those corresponding drop heights and various impact regions were also obtained. Angular acceleration TBI tolerance is not considered since NOCSAE drop test and FE simulation data is not available for the same.

Maximum linear acceleration values (in Gs) acquired from NOCSAE drop tests for frontal, 45-to-frontal, lateral and posterior impact regions were plotted on Y-axis as a function of drop heights (in feet) on X-axis. Linear acceleration curves were represented by dotted lines and colors were used to distinguish between the impact regions. Linear acceleration TBI tolerance value of 319G was marked horizontally in red color. The points where the red line intersected with the dotted curves were traced down to the X-axis to obtain drop heights for respective regions. Refer to Figure 4.1

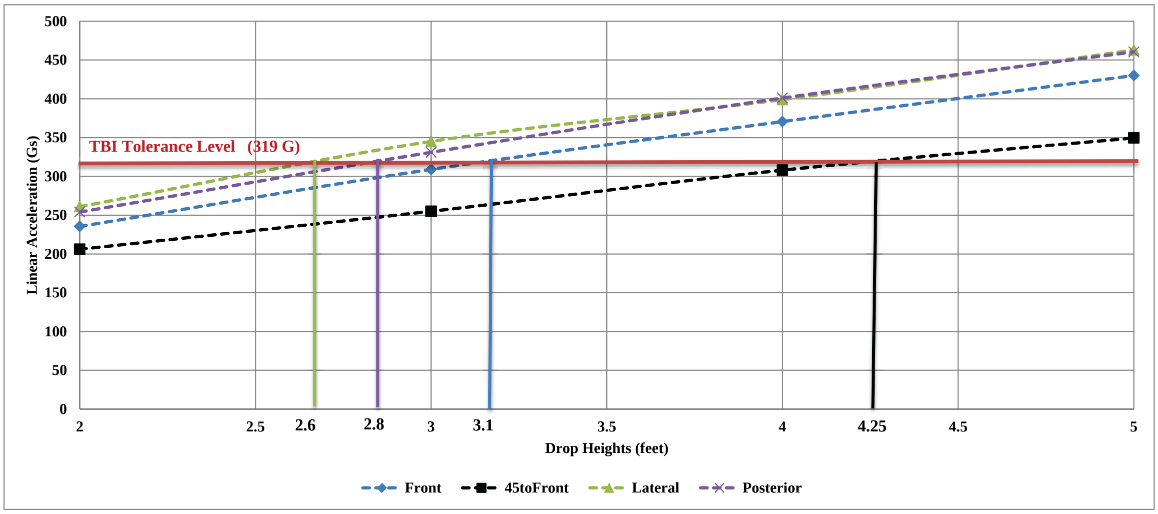

Figure 4.1 Plot of Linear Acceleration values for frontal, 45-to-frontal, lateral and posterior impact regions as a function of drop heights to determine TBI drop height for various regions from TBI Tolerance acceleration value

Extracting values from Figure 4.1, we got:

Table 4.1 Drop Heights for TBI tolerance level (linear acceleration)

Impact Region	TBI Tolerance Drop Height (feet)
Front	3.125
45-to-Frontal	4.25
Lateral	2.625
Posterior	2.825

These results are observed to be consistent with that of FE simulations.

- Lateral Impact has the least TBI Tolerance height followed by Posterior impact i.e. during lateral impacts higher TBI occurrences might be observed.

- Deviation in frontal and 45-to-frontal results might have occurred due to approximation in area measurements. However, it matches with the fact that those regions will have higher TBI tolerance heights i.e. frontal and 45-to-frontal impacts are less detrimental as compared to other impacts.

These TBI tolerance heights were plotted on Figures 3.6, 3.20, 3.34 and 3.49 mentioned in Chapter 3. These figures got modified as Figures 4.2, 4.3, 4.4 and 4.5

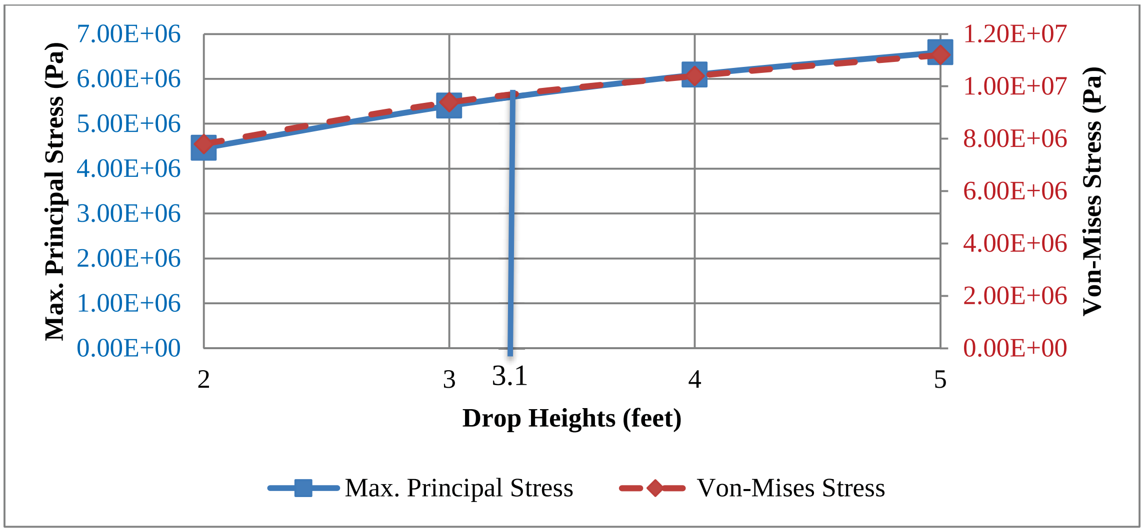

Figure 4.2 Linear-TBI drop height for Frontal impact region located on the plot of Maximum Principal Stress and Von-Mises Stress as a function of drop heights

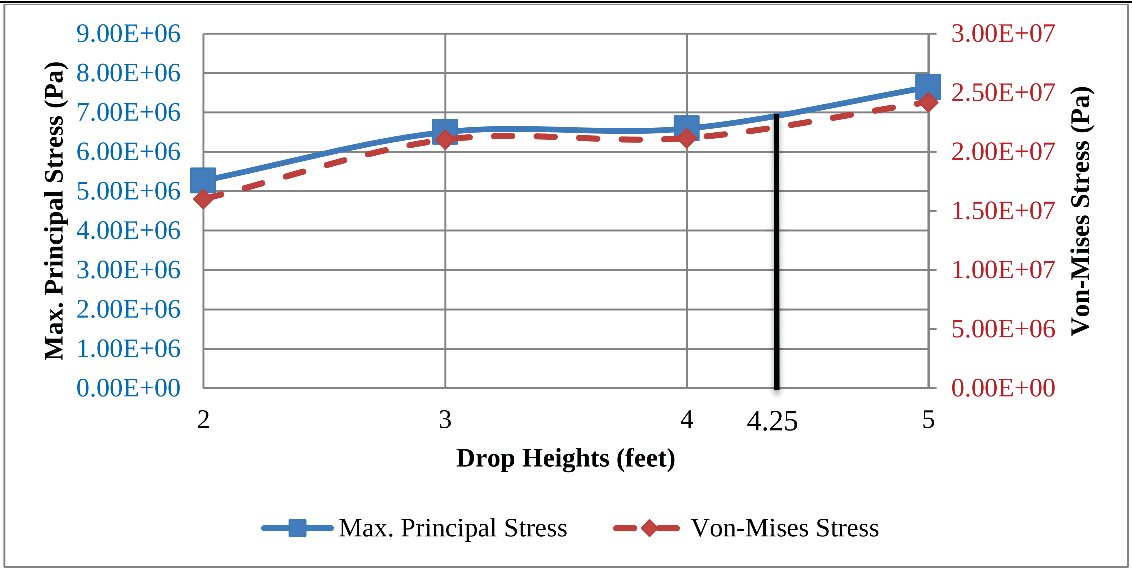

Figure 4.3 Linear-TBI drop height for 45-to-Frontal impact region located on the plot of Maximum Principal Stress and Von-Mises Stress as a function of drop heights

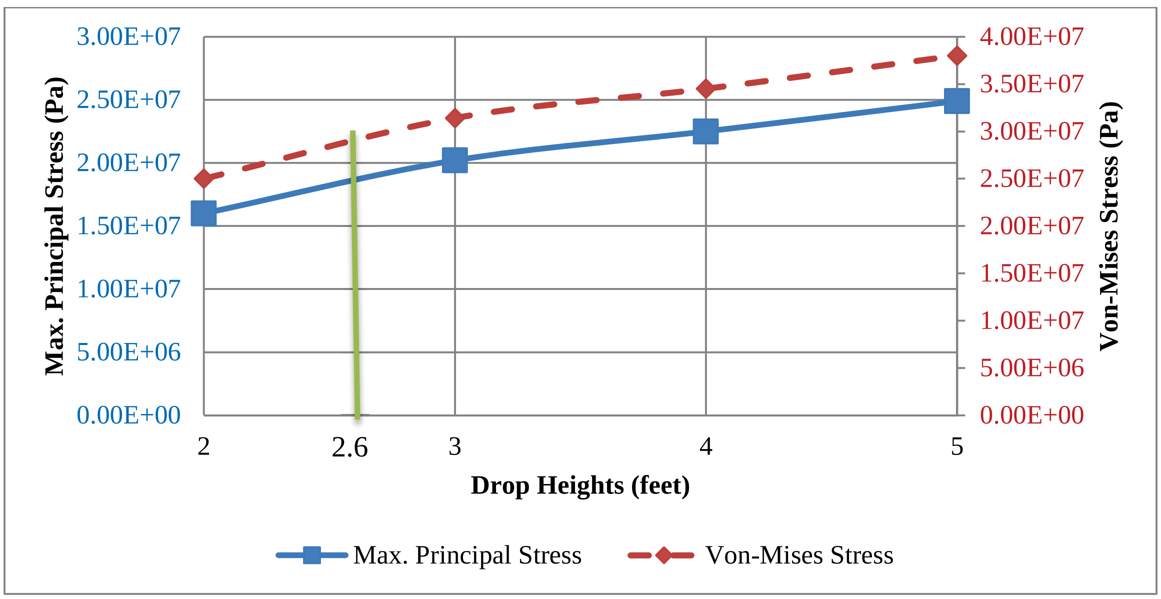

Figure 4.4 Linear-TBI drop height for Lateral impact region located on the plot of Maximum Principal Stress and Von-Mises Stress as a function of drop heights

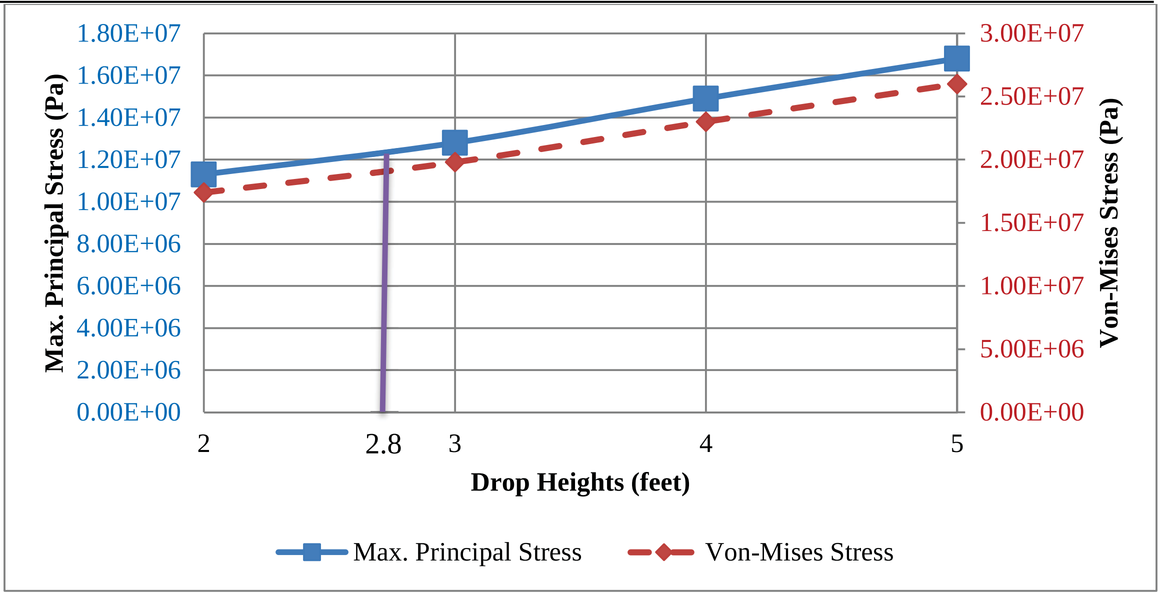

Figure 4.5 Linear-TBI drop height for Posterior impact region located on the plot of Maximum Principal Stress and Von-Mises Stress as a function of drop heights

Thus, the values of Von-Mises and Maximum Principal Stresses generated due to Linear-Acceleration TBI tolerance value are presented in Table 4.2

Table 4.2 Summary of Stresses corresponding to Linear-TBI Tolerance Drop Heights

Impact	Drop Height (feet)	Peak HICP (MPa)	Von-Mises Stress (MPa)	Max. Principal Stress (MPa)	Max. Principal Strain
Frontal	3.125 (~3)	4.9	9.5	5.6	0.14
45-to-Frontal	4.25 (~4)	4.0	22.5	6.8	0.34
Lateral	2.625 (~3)	2.9	30	18	0.19
Posterior	2.825 (~3)	4.1	19	12.5	0.17

Maximum Principal Strain was also recorded from the FE simulations so that it can be compared with mechanical properties of the brain tissue.

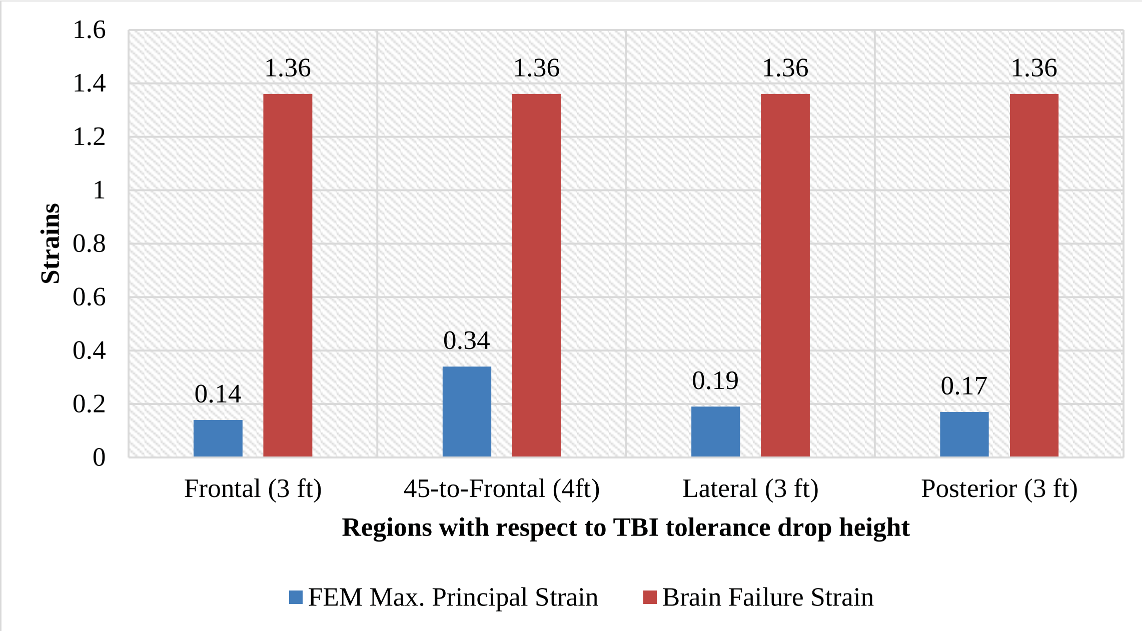

Figure 4.6 Bar plot of brain failure strain and maximum principal strain obtained from FE Simulations for Frontal, 45-to-Frontal, Lateral and Posterior impacts and their respective TBI-tolerant drop heights

Following observations can be deduced from above results (Table 4.2 and Figure 4.6):

1. Lateral Impact generates peak values of stresses at lower drop heights (2.625 feet). Thus, TBI tolerance value for lateral impacts is the least. Only 2 feet lateral impact was below TBI tolerance level whereas 3feet, 4 feet and 5 feet were above it. Peak Von-Mises and Maximum Principal Stress levels for lateral impact were observed at 3.7 msec for 5 feet drop and 3.49 MPa HICP.
2. Posterior impact is the next detrimental impact after lateral impact affecting not just the brain but cerebellum and spinal cord directly. This region is responsible for coordinating with other parts of brain and motor movements of the entire body. Damage in this region might lead to full-body paralysis. Only 2 feet impact was below TBI tolerance level whereas 3feet, 4 feet and 5 feet were above it. It causes

TBI beyond 2.825 feet drop height. Peak Von-Mises and Maximum Principal Stress levels for posterior impact were observed at 3.9 msec for 5 feet drop and 5.33 MPa HICP.

3. Frontal and 45-to-frontal impacts are least detrimental since those regions reach the peak tolerance stress values at higher heights. For frontal impact region, 2 and 3 feet impacts were below TBI tolerance level whereas 4 feet and 5 feet were above it, 3.125 feet was the threshold. For 45-to-frontal impact region, 2, 3 and 4 feet impacts were below TBI tolerance level whereas only 5 feet was above it, 4.25 feet was the threshold. Peak Von-Mises and Maximum Principal Stress levels for frontal impact were observed at 3.7 msec for 5 feet drop and 5.81 MPa HICP. Peak Von-Mises and Maximum Principal Stress levels for 45-to-frontal impact were observed at 3.7 msec for 5 feet drop and 4.65 MPa HICP.
4. The Maximum Principal Strain values of all impact regions are below the brain's failure strain values. This signifies that no structural damage will be detected in MRI or CT scans yet brain will experience TBI causing higher stress concentrations.

4.1 Formula Proposition

From above analysis it is evident that both Von-Mises and Max. Principal Stresses contribute towards causing TBIs. Thus, this research group is proposing a formula similar to acceleration criterion relating stress values to the TBI.

$$\frac{\sigma_{VM-regional}}{\sigma_{VM-TBI-max}} + \frac{\sigma_{MP-regional}}{\sigma_{MP-TBI-max}} \leq 1 \; then \; no \; TBI \qquad \ldots (E13)$$

Where,

$\sigma_{VM-regional}$ = Von-Mises Stress for a particular impact region and drop height in MPa

$\sigma_{VM-TBI-max}$= TBI tolerant Von-Mises Stress value in MPa (refer to Table 4.2)

$\sigma_{MP-regional}$ = Maximum Principal Stress for a particular impact region and drop height in MPa

$\sigma_{MP-TBI-max}$= TBI tolerant Maximum Principal Stress value in MPa (refer to Table 4.2)

Table 4.3 TBI stress criterion for frontal, 45-to-frontal, lateral and posterior regions based on equation E13

Frontal Impact								45-to-Frontal Impact							
Drop Height (feet)	Von-Mises Regional (MPa)	Von-Mises TBI max (MPa)	Von-Mises Ratio	Max. Principal Regional (MPa)	Max. Principal TBI max (MPa)	Max. Principal Ratio	TBI condition	Drop Height (feet)	Von-Mises Regional (MPa)	Von-Mises TBI max (MPa)	Von-Mises Ratio	Max. Principal Regional (MPa)	Max. Principal TBI max (MPa)	Max. Principal Ratio	TBI condition
2	7.8	9.5	0.82	4.46	5.6	0.80	1.62	2	16	22.5	0.71	2.27	6.8	0.33	1.04
3	9.39		0.99	5.4		0.96	1.95	3	21		0.93	6.5		0.96	1.89
4	10.4		1.09	6.09		1.09	2.18	4	21.2		0.94	6.59		0.97	1.91
5	11.2		1.18	6.59		1.18	2.36	5	24.2		1.08	7.64		1.12	2.20
Lateral Impact								Posterior Impact							
Drop Height (feet)	Von-Mises Regional (MPa)	Von-Mises TBI max (MPa)	Von-Mises Ratio	Max. Principal Regional (MPa)	Max. Principal TBI max (MPa)	Max. Principal Ratio	TBI condition	Drop Height (feet)	Von-Mises Regional (MPa)	Von-Mises TBI max (MPa)	Von-Mises Ratio	Max. Principal Regional (MPa)	Max. Principal TBI max (MPa)	Max. Principal Ratio	TBI condition
2	25	30	0.83	16	18	0.89	1.72	2	17.4	19	0.92	11.3	12.5	0.90	1.82
3	31.4		1.05	20.2		1.12	2.17	3	19.8		1.04	12.8		1.02	2.07
4	34.5		1.15	22.5		1.25	2.40	4	23		1.21	14.9		1.19	2.40
5	38		1.27	24.9		1.38	2.65	5	26		1.37	16.8		1.34	2.71

This formula has to be used only when $\frac{\sigma_{VM-regional}}{\sigma_{VM-TBI-max}}$ or $\frac{\sigma_{MP-regional}}{\sigma_{MP-TBI-max}}$ is less than one. When those values are greater than 1 then this formula is not required to determine which type of stress plays a prominent role in causing TBI. For example, consider case 1 of Frontal 4 and 5 feet impact. Von-Mises Stress TBI tolerance $\left(\frac{\sigma_{VM-regional}}{\sigma_{VM-TBI-max}}\right)$ values and Maximum Principal Stress TBI tolerance $\left(\frac{\sigma_{MP-regional}}{\sigma_{MP-TBI-max}}\right)$ values are greater than 1 (refer to Table 4.3) which signifies that both types of stresses will be responsible for TBI and above formula is not required. Now, consider case 2 of Frontal 2 and 3 feet impact. Von-Mises Stress TBI tolerance $\left(\frac{\sigma_{VM-regional}}{\sigma_{VM-TBI-max}}\right)$ values and Maximum Principal Stress TBI tolerance $\left(\frac{\sigma_{MP-regional}}{\sigma_{MP-TBI-max}}\right)$ values are less than 1 individually (refer to Table 4.3) which might be misconceived as no TBI. However, if their combined effect is observed then there is a risk of TBI.

Thus, Von-Mises Stress combined with Maximum Principal Stress can cause TBIs even though they won't cause TBI if experienced individually.

5. Conclusions

- Tolerance impact is sensitive to impact region
- A profound relation is observed between head kinematics and brain kinetics
- Linear and angular impact accelerations can be related to propose a TBI impact tolerance criteria or a formula (equation E12)

$$\frac{a_{regional}}{a_{TBI-max}} + \frac{\alpha_{regional}}{\alpha_{TBI-max}} \leq 1 \; then \; no \; TBI$$

Where,

$a_{regional}$ = linear impact accelerations for a particular impact region and drop height

$a_{TBI-max}$ = TBI tolerant linear impact acceleration measured individually (value = 318 G) [27]

$\alpha_{regional}$ = angular impact accelerations for a particular impact region and drop height

$\alpha_{TBI-max}$ = TBI tolerant angular impact acceleration measured individually (value = 23krad/s2) [27]

- Von-Mises Stresses and Maximum Principal Stresses can be related to propose a TBI impact tolerance criteria or a formula (equation E13)

$$\frac{\sigma_{VM-regional}}{\sigma_{VM-TBI-max}} + \frac{\sigma_{MP-regional}}{\sigma_{MP-TBI-max}} \leq 1 \; then \; no \; TBI$$

Where,

$\sigma_{VM-regional}$ = Von-Mises Stress for a particular impact region and drop height in MPa

$\sigma_{VM-TBI-max}$= TBI tolerant Von-Mises Stress value in MPa (refer to Table 4.2)

$\sigma_{MP-regional}$ = Maximum Principal Stress for a particular impact region and drop height in MPa

$\sigma_{MP-TBI-max}$= TBI tolerant Maximum Principal Stress value in MPa (refer to Table 4.2)

6. Recommendations

- Precise and instantaneous pressure-area measurements should be done to facilitate linear curves of Von-Mises and Max. Principal stresses.
- Measurement of angular acceleration through NOCSAE droptests can give stress distributions with respect to angular or rotational impact.
- Determination of inertial properties through experimental methods should be done in order to validate FE model values
- FE Brain model based on region-wise varying mechanical properties and strains should be done for more realistic simulations.
- On-field measurement of impact pressures with the help of pressure films in collegiate football games and practices will yield real time data of the games. This will help derive real time stress distributions in human head.
- Design of helmets can consider lateral impact region as design basis. A helmet providing cushioning effect against linear acceleration along with providing resistance to shear caused to angular acceleration can be designed based on this research.

Appendix A

Head Impact Contact Pressure (HICP) Calculations

Table A0.1 HICP for Frontal impact of 2 feet drop height

Impact	Front	Height (ft.)	2
Area measured (m2)	2.80E-03	Area on FE Model (m2)	2.29E-03
Mass of headform (kg)	4.917		
Time	G	Drop Test Acc (m/s2)	HICP
0.001562	0.62	6.11	1.07E+04
0.001757	1.44	14.13	2.48E+04
0.001953	7.33	71.94	1.26E+05
0.002148	20.63	202.33	3.55E+05
0.002343	40.23	394.54	6.93E+05
0.002539	65.96	646.89	1.14E+06
0.002734	96.19	943.33	1.66E+06
0.002929	129.69	1271.84	2.23E+06
0.003125	164.05	1608.79	2.83E+06
0.003320	193.11	1893.83	3.33E+06
0.003515	216.91	2127.19	3.74E+06
0.003710	233.26	2287.54	4.02E+06
0.003906	235.50	2309.48	4.06E+06
0.004101	225.90	2215.38	3.89E+06
0.004296	206.67	2026.76	3.56E+06
0.004492	177.79	1743.61	3.06E+06
0.004687	146.82	1440.42	2.53E+06
0.004882	118.39	1161.07	2.04E+06
0.005078	86.98	853.02	1.50E+06
0.005273	54.41	533.59	9.37E+05
0.005468	32.27	316.48	5.56E+05

Table A0.2 HICP for Frontal impact of 3 feet drop height

Impact	Front	Height (ft.)	3
Area	0.003062	Area on FE Model (m2)	2.29E-03
Mass of headform(m)	4.917		
Time	G	Drop Test Acc (m/s2)	HICP
0.001562	0.47	4.64	7.46E+03
0.001757	0.51	5.06	8.13E+03
0.001953	1.97	19.41	3.12E+04
0.002148	12.19	119.63	1.92E+05
0.002343	34.18	335.26	5.38E+05
0.002539	67.06	657.65	1.06E+06
0.002734	109.85	1077.31	1.73E+06
0.002929	156.71	1536.84	2.47E+06
0.003125	202.64	1987.30	3.19E+06
0.003320	246.96	2421.94	3.89E+06
0.003515	284.72	2792.22	4.48E+06
0.003710	305.98	3000.68	4.82E+06
0.003906	308.99	3030.22	4.87E+06
0.004101	295.20	2894.98	4.65E+06
0.004296	265.23	2601.07	4.18E+06
0.004492	226.31	2219.39	3.56E+06
0.004687	185.13	1815.56	2.92E+06
0.004882	137.88	1352.22	2.17E+06
0.005078	88.77	870.54	1.40E+06
0.005273	54.17	531.27	8.53E+05
0.005468	37.34	366.27	5.88E+05

Table A0.3 HICP for frontal impact of 4 feet drop height

Impact	Front	Height (ft.)	4
Area	0.00331	Area on FE Model (m2)	2.29E-03
Mass of headform(m)	4.917		
Time	G	Drop Test Acc (m/s2)	HICP
0.001562	0.40	4.00	5.96E+03
0.001757	0.49	4.85	7.21E+03
0.001953	0.51	5.06	7.52E+03
0.002148	4.92	48.31	7.18E+04
0.002343	23.94	234.83	3.49E+05
0.002539	59.07	579.37	8.61E+05
0.002734	108.84	1067.39	1.59E+06
0.002929	166.58	1633.68	2.43E+06
0.003125	223.34	2190.27	3.25E+06
0.003320	278.72	2733.36	4.06E+06
0.003515	331.17	3247.75	4.83E+06
0.003710	365.12	3580.69	5.32E+06
0.003906	370.63	3634.70	5.40E+06
0.004101	352.67	3458.53	5.14E+06
0.004296	316.20	3100.90	4.61E+06
0.004492	270.54	2653.18	3.94E+06
0.004687	222.74	2184.36	3.25E+06
0.004882	166.15	1629.46	2.42E+06
0.005078	106.19	1041.44	1.55E+06
0.005273	64.50	632.54	9.40E+05
0.005468	44.88	440.12	6.54E+05

Table A0.4 HICP for frontal impact of 5 feet drop height

Impact	Front	Height (ft.)	5
Area (m2)	0.003572	Area on FE Model (m2)	2.29E-03
Mass of headform(kg)	4.917		
Time	G	Drop Test Acc (m/s2)	HICP
0.001562	0.02	0.21	2.90E+02
0.001757	0.12	1.26	1.74E+03
0.001953	0.58	5.69	7.84E+03
0.002148	9.38	91.99	1.27E+05
0.002343	36.70	359.94	4.96E+05
0.002539	81.82	802.39	1.10E+06
0.002734	142.66	1399.06	1.93E+06
0.002929	213.06	2089.42	2.88E+06
0.003125	283.93	2784.42	3.83E+06
0.003320	352.37	3455.57	4.76E+06
0.003515	406.71	3988.53	5.49E+06
0.003710	430.25	4219.35	5.81E+06
0.003906	416.82	4087.70	5.63E+06
0.004101	375.77	3685.13	5.07E+06
0.004296	324.87	3185.93	4.39E+06
0.004492	267.19	2620.27	3.61E+06
0.004687	205.61	2016.42	2.78E+06
0.004882	140.81	1380.92	1.90E+06
0.005078	78.400	768.84	1.06E+06
0.005273	38.83	380.83	5.24E+05
0.005468	33.47	328.29	4.52E+05

Table A0.5 HICP for 45-to-frontal impact of 2 feet drop height

Impact	45	Height (ft.)	2
Area measured (m2)	3.02E-03	Area on FE Model (m2)	3.30E-03
Mass of headform (kg)	4.917		
Time	G	Drop Test Acc (m/s2)	HICP
0.001562	0.81	8.01	1.30E+04
0.001757	3.31	32.49	5.29E+04
0.001953	10.71	105.07	1.71E+05
0.002148	24.54	240.73	3.92E+05
0.002343	44.98	441.17	7.18E+05
0.002539	70.91	695.41	1.13E+06
0.002734	101.42	994.60	1.62E+06
0.002929	134.59	1319.94	2.15E+06
0.003125	165.19	1619.97	2.64E+06
0.003320	187.60	1839.82	2.99E+06
0.003515	200.54	1966.62	3.20E+06
0.003710	205.96	2019.79	3.29E+06
0.003906	204.19	2002.49	3.26E+06
0.004101	194.12	1903.75	3.10E+06
0.004296	176.76	1733.48	2.82E+06
0.004492	155.01	1520.17	2.47E+06
0.004687	130.03	1275.21	2.07E+06
0.004882	102.26	1002.83	1.63E+06
0.005078	73.98	725.59	1.18E+06
0.005273	48.43	474.92	7.73E+05
0.005468	28.27	277.23	4.51E+05

Table A0.6 HICP for 45-to-frontal impact of 3 feet drop height

Impact	45	Height (ft.)	3
Area measured (m2)	3.02E-03	Area on FE Model (m2)	3.02E-03
Mass of headform (kg)	4.917		
Time	G	Drop Test Acc (m/s2)	HICP
0.001562	0.51	5.06	8.24E+03
0.001757	2.88	28.27	4.60E+04
0.001953	11.05	108.44	1.76E+05
0.002148	27.23	267.11	4.35E+05
0.002343	51.97	509.74	8.29E+05
0.002539	84.03	824.12	1.34E+06
0.002734	121.12	1187.86	1.93E+06
0.002929	160.80	1577.14	2.57E+06
0.003125	198.06	1942.36	3.16E+06
0.003320	227.00	2226.14	3.62E+06
0.003515	246.15	2413.92	3.93E+06
0.003710	255.20	2502.75	4.07E+06
0.003906	251.61	2467.51	4.01E+06
0.004101	235.13	2305.89	3.75E+06
0.004296	209.46	2054.18	3.34E+06
0.004492	183.47	1799.31	2.93E+06
0.004687	155.68	1526.71	2.48E+06
0.004882	122.93	1205.59	1.96E+06
0.005078	92.29	905.14	1.47E+06
0.005273	61.61	604.27	9.83E+05
0.005468	32.42	317.96	5.17E+05

Table A0.7 HICP for 45-to-frontal impact of 4 feet drop height

Impact	45	Height (ft.)	4
Area measured (m2)	3.63E-03	Area on FE Model (m2)	3.02E-03
Mass of headform (kg)	4.917		
Time	G	Drop Test Acc (m/s2)	HICP
0.001562	0.27	2.74	3.72E+03
0.001757	0.83	8.22	1.12E+04
0.001953	5.72	56.12	7.61E+04
0.002148	21.02	206.13	2.79E+05
0.002343	49.93	489.70	6.64E+05
0.002539	92.40	906.19	1.23E+06
0.002734	144.51	1417.21	1.92E+06
0.002929	198.62	1947.85	2.64E+06
0.003125	247.01	2422.36	3.28E+06
0.003320	282.85	2773.87	3.76E+06
0.003515	302.32	2964.81	4.02E+06
0.003710	307.74	3017.98	4.09E+06
0.003906	300.15	2943.50	3.99E+06
0.004101	279.00	2736.10	3.71E+06
0.004296	246.02	2412.65	3.27E+06
0.004492	204.58	2006.29	2.72E+06
0.004687	163.06	1599.08	2.17E+06
0.004882	121.79	1194.40	1.62E+06
0.005078	77.53	760.40	1.03E+06
0.005273	41.13	403.41	5.47E+05
0.005468	20.65	202.54	2.75E+05

Table A0.8 HICP for 45-to-frontal impact of 5 feet drop height

Impact	45	Height (ft.)	5
Area measured (m2)	3.63E-03	Area on FE Model (m2)	3.02E-03
Mass of headform (kg)	4.917		
Time	G	Drop Test Acc (m/s2)	HICP
0.001562	0.27	2.74	3.72E+03
0.001757	0.43	4.21	5.72E+03
0.001953	3.67	36.07	4.89E+04
0.002148	17.85	175.12	2.37E+05
0.002343	48.45	475.14	6.44E+05
0.002539	95.87	940.16	1.27E+06
0.002734	156.15	1531.35	2.08E+06
0.002929	219.06	2148.28	2.91E+06
0.003125	276.72	2713.74	3.68E+06
0.003320	323.45	3172.00	4.30E+06
0.003515	348.75	3420.13	4.64E+06
0.003710	349.46	3427.09	4.65E+06
0.003906	334.31	3278.55	4.44E+06
0.004101	308.32	3023.68	4.10E+06
0.004296	272.93	2676.60	3.63E+06
0.004492	230.16	2257.16	3.06E+06
0.004687	183.71	1801.63	2.44E+06
0.004882	138.21	1355.39	1.84E+06
0.005078	91.18	894.17	1.21E+06
0.005273	45.46	445.81	6.04E+05
0.005468	17.25	169.21	2.29E+05

Table A0.9 HICP for lateral impact of 2 feet drop height

Impact	Side	Height (ft.)	2
Area measured (m2)	5.22E-03	Area on FE Model (m2)	4.74E-03
Mass of headform (kg)	4.917		
Time	G	Drop Test Acc (m/s2)	HICP
0.001562	1.24	12.23	1.15E+04
0.001757	4.86	47.68	4.49E+04
0.001953	11.85	116.25	1.10E+05
0.002148	25.58	250.86	2.36E+05
0.002343	47.99	470.71	4.43E+05
0.002539	76.98	754.91	7.11E+05
0.002734	116.99	1147.35	1.08E+06
0.002929	166.09	1628.83	1.53E+06
0.003125	212.48	2083.72	1.96E+06
0.003320	246.43	2416.69	2.28E+06
0.003515	261.23	2561.82	2.41E+06
0.003710	253.94	2490.30	2.35E+06
0.003906	225.32	2209.69	2.08E+06
0.004101	185.45	1818.72	1.71E+06
0.004296	149.80	1469.11	1.38E+06
0.004492	124.48	1220.78	1.15E+06
0.004687	99.50	975.82	9.19E+05
0.004882	65.814	645.41	6.08E+05
0.005078	37.88	371.55	3.50E+05
0.005273	24.44	239.68	2.26E+05
0.005468	18.41	180.60	1.70E+05

Table A0.10 HICP for lateral impact of 3 feet drop height

Impact	Side	Height (ft.)	3
Area measured (m2)	5.77E-03	Area on FE Model (m2)	4.74E-03
Mass of headform (kg)	4.917		
Time	G	Drop Test Acc (m/s2)	HICP
0.001562	0.58	5.69	4.85E+03
0.001757	1.01	9.91	8.45E+03
0.001953	5.63	55.27	4.71E+04
0.002148	15.98	156.76	1.34E+05
0.002343	36.23	355.30	3.03E+05
0.002539	68.91	675.79	5.76E+05
0.002734	111.76	1096.08	9.34E+05
0.002929	168.95	1656.89	1.41E+06
0.003125	237.43	2328.474	1.98E+06
0.003320	300.54	2947.30	2.51E+06
0.003515	340.43	3338.47	2.85E+06
0.003710	345.35	3386.79	2.89E+06
0.003906	315.27	3091.83	2.63E+06
0.004101	262.56	2574.90	2.19E+06
0.004296	205.76	2017.81	1.72E+06
0.004492	162.48	1593.38	1.36E+06
0.004687	130.26	1277.32	1.09E+06
0.004882	90.85	891.00	7.59E+05
0.005078	46.57	456.79	3.89E+05
0.005273	19.92	195.37	1.66E+05
0.005468	15.40	151.06	1.29E+05

Table A0.11 HICP for lateral impact of 4 feet drop height

Impact	Side	Height (ft.)	4
Area measured (m2)	6.04E-03	Area on FE Model (m2)	4.74E-03
Mass of headform (kg)	4.917		
Time	G	Drop Test Acc (m/s2)	HICP
0.001562	0.58	5.67	4.63E+03
0.001757	0.51	5.06	4.12E+03
0.001953	3.52	34.60	2.81E+04
0.002148	14.17	139.04	1.13E+05
0.002343	35.39	347.07	2.82E+05
0.002539	70.82	694.57	5.65E+05
0.002734	118.24	1159.59	9.43E+05
0.002929	180.23	1767.45	1.44E+06
0.003125	259.01	2540.09	2.07E+06
0.003320	338.25	3317.16	2.70E+06
0.003515	390.08	3825.44	3.11E+06
0.003710	398.64	3909.41	3.18E+06
0.003906	365.51	3584.49	2.92E+06
0.004101	301.50	2956.79	2.41E+06
0.004296	230.27	2258.21	1.84E+06
0.004492	179.15	1756.90	1.43E+06
0.004687	145.67	1428.60	1.16E+06
0.004882	106.49	1044.39	8.50E+05
0.005078	66.82	655.33	5.33E+05
0.005273	45.15	442.86	3.60E+05
0.005468	34.66	339.90	2.77E+05

Table A0.12 HICP for lateral impact of 5 feet drop height

Impact	Side	Height (ft.)	5
Area measured (m2)	6.41E-03	Area on FE Model (m2)	4.74E-03
Mass of headform (kg)	4.917		
Time	G	Drop Test Acc (m/s2)	HICP
0.001562	0.66	6.54	5.02E+03
0.001757	0.60	5.90	4.53E+03
0.001953	3.57	35.02	2.69E+04
0.002148	16.45	161.40	1.24E+05
0.002343	42.29	414.80	3.18E+05
0.002539	84.25	826.23	6.34E+05
0.002734	141.26	1385.35	1.06E+06
0.002929	214.65	2105.03	1.62E+06
0.003125	307.61	3016.72	2.32E+06
0.003320	400.45	3927.13	3.01E+06
0.003515	458.52	4496.59	3.45E+06
0.003710	463.08	4541.32	3.49E+06
0.003906	415.96	4079.26	3.13E+06
0.004101	332.51	3260.8	2.50E+06
0.004296	246.99	2422.15	1.86E+06
0.004492	190.72	1870.41	1.44E+06
0.004687	151.14	1482.19	1.14E+06
0.004882	106.88	1048.19	8.05E+05
0.005078	69.45	681.07	5.23E+05
0.005273	53.95	529.16	4.06E+05
0.005468	46.66	457.63	3.51E+05

Table A0.13 HICP for posterior impact of 2 feet drop height

Impact	Rear	Height (ft.)	2
Area measured (m2)	3.41E-03	Area on FE Model (m2)	2.92E-03
Mass of headform (kg)	4.917		
Time	G	Drop Test Acc (m/s2)	HICP
0.001562	0.33	3.58	5.18E+03
0.001757	0.92	9.07	1.31E+04
0.001953	3.63	35.65	5.15E+04
0.002148	11.96	117.30	1.69E+05
0.002343	29.15	285.89	4.13E+05
0.002539	55.70	546.25	7.88E+05
0.002734	89.26	875.39	1.26E+06
0.002929	126.22	1237.87	1.79E+06
0.003125	161.87	1587.48	2.29E+06
0.003320	193.67	1899.32	2.74E+06
0.003515	221.38	2171.07	3.13E+06
0.003710	242.62	2379.32	3.43E+06
0.003906	253.85	2489.45	3.59E+06
0.004101	251.01	2461.60	3.55E+06
0.004296	233.69	2291.76	3.31E+06
0.004492	208.47	2044.48	2.95E+06
0.004687	179.52	1760.49	2.54E+06
0.004882	148.06	1452.02	2.10E+06
0.005078	117.55	1152.84	1.66E+06
0.005273	88.64	869.27	1.25E+06
0.005468	59.29	581.48	8.39E+05

Table A0.14 HICP for posterior impact of 3 feet drop height

Impact	Rear	Height (ft.)	3
Area measured (m2)	3.89E-03	Area on FE Model (m2)	2.92E-03
Mass of headform (kg)	4.917		
Time	G	Drop Test Acc (m/s2)	HICP
0.001562	0.15	1.47	1.87E+03
0.001757	0.81	8.01	1.01E+04
0.001953	3.76	36.92	4.66E+04
0.002148	13.31	130.60	1.65E+05
0.002343	34.68	340.11	4.30E+05
0.002539	70.16	688.03	8.69E+05
0.002734	117.04	1147.78	1.45E+06
0.002929	169.90	1666.18	2.10E+06
0.003125	221.23	2169.59	2.74E+06
0.003320	265.06	2599.38	3.28E+06
0.003515	298.99	2932.11	3.70E+06
0.003710	322.76	3165.25	4.00E+06
0.003906	330.70	3243.11	4.10E+06
0.004101	317.19	3110.61	3.93E+06
0.004296	285.48	2799.61	3.54E+06
0.004492	243.26	2385.65	3.01E+06
0.004687	198.56	1947.21	2.46E+06
0.004882	158.37	1553.09	1.96E+06
0.005078	121.36	1190.18	1.50E+06
0.005273	81.75	801.75	1.01E+06
0.005468	42.72	419.02	5.29E+05

Table A0.15 HICP for posterior impact of 4 feet drop height

Impact	Rear	Height (ft.)	4
Area measured (m2)	4.06E-03	Area on FE Model (m2)	2.92E-03
Mass of headform (kg)	4.917		
Time	G	Drop Test Acc (m/s2)	HICP
0.001562	0.17	1.68	2.05E+03
0.001757	1.22	12.02	1.46E+04
0.001953	6.04	59.28	7.19E+04
0.002148	20.37	199.80	2.42E+05
0.002343	51.22	502.36	6.09E+05
0.002539	101.01	990.59	1.20E+06
0.002734	165.70	1625.03	1.97E+06
0.002929	237.13	2325.52	2.82E+06
0.003125	301.10	2952.79	3.58E+06
0.003320	351.38	3445.87	4.18E+06
0.003515	386.14	3786.83	4.59E+06
0.003710	400.09	3923.55	4.76E+06
0.003906	391.65	3840.84	4.66E+06
0.004101	361.17	3541.87	4.29E+06
0.004296	310.71	3047.10	3.69E+06
0.004492	246.41	2416.45	2.93E+06
0.004687	184.40	1808.38	2.19E+06
0.004882	140.27	1375.64	1.67E+06
0.005078	105.10	1030.68	1.25E+06
0.005273	64.54	632.96	7.67E+05
0.005468	27.88	273.44	3.31E+05

Table A0.16 HICP for posterior impact of 5 feet drop height

Impact	Rear	Height (ft.)	5
Area measured (m2)	4.16E-03	Area on FE Model (m2)	2.92E-03
Mass of headform (kg)	4.917		
Time	G	Drop Test Acc (m/s2)	HICP
0.001562	0.10	1.054	1.25E+03
0.001757	0.27	2.742	3.24E+03
0.001953	2.15	21.098	2.49E+04
0.002148	9.35	91.78	1.08E+05
0.002343	29.26	286.94	3.39E+05
0.002539	71.23	698.58	8.25E+05
0.002734	136.10	1334.71	1.58E+06
0.002929	217.45	2132.46	2.52E+06
0.003125	301.61	2957.85	3.49E+06
0.003320	373.26	3660.44	4.32E+06
0.003515	425.54	4173.15	4.93E+06
0.003710	456.02	4472.12	5.28E+06
0.003906	460.59	4516.85	5.33E+06
0.004101	437.46	4290.03	5.07E+06
0.004296	383.97	3765.52	4.45E+06
0.004492	303.68	2978.10	3.52E+06
0.004687	231.17	2267.07	2.68E+06
0.004882	176.31	1729.05	2.04E+06
0.005078	122.29	1199.26	1.42E+06
0.005273	77.47	759.77	8.97E+05
0.005468	53.61	525.78	6.21E+05

Appendix B

Simulations with detailed ANSYS features

B.1 FEModeler

Orphan Mesh in ABAQUS (.inp) format was imported in FEModeler of ANSYS 14.5

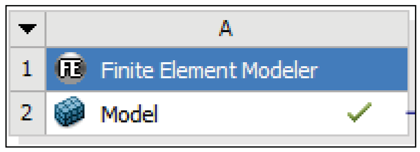

Figure B0.1 Finite Element Modeler module of ANSYS 14.5

The model was cleaned up and ‘Body Grouping’ was done with respect to ‘Components’ in order to get each layer of human head as a separate part instead of an entire body (refer to Figure 2.10)

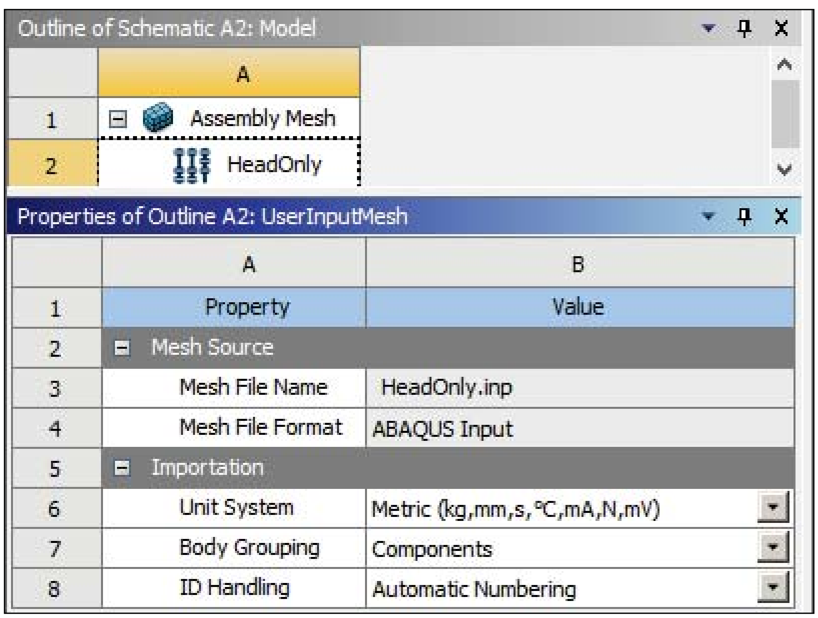

Figure B0.2 Screenshot of Body Grouping in Head assembly according to its Components (layers) in ANSYS 14.5

B.2 Engineering Data (Materials)

The materials were added in Engineering Data tab of the Transient Structural analysis type (explained further in Section 2.4.3). The materials considered for analysis are the same as specified in the data of validated model.

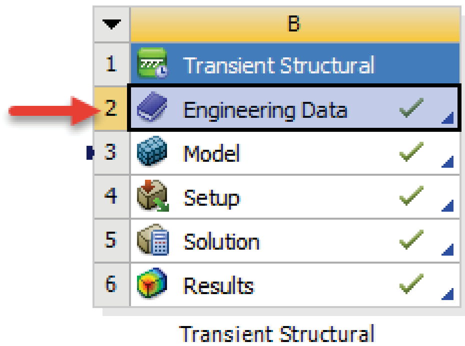

Figure B0.3 Screenshot of Transient Structural module highlighting Engineering data step (Materials) tab in ANSYS 14.5

B.3 Model

The model from FEModeler was directly imported in Model tab of Transient Structural module of ANSYS. The module was refreshed and updated to access the imported model.

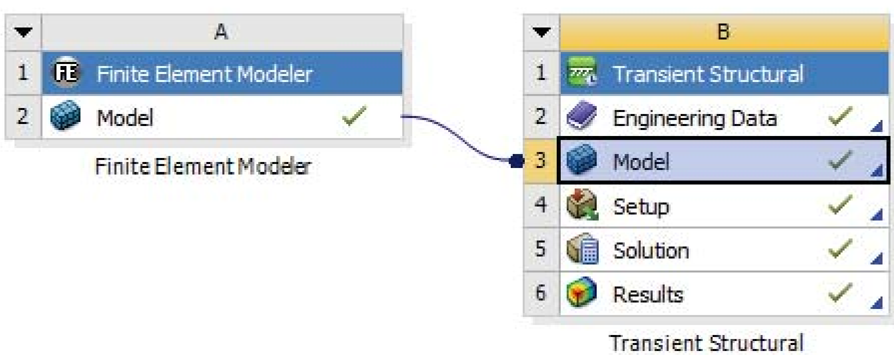

Figure B0.4 Screenshot of FE Model importing process in Transient Structural module

The imported model parts were named and assigned appropriate material properties (refer to Figure 2.14)

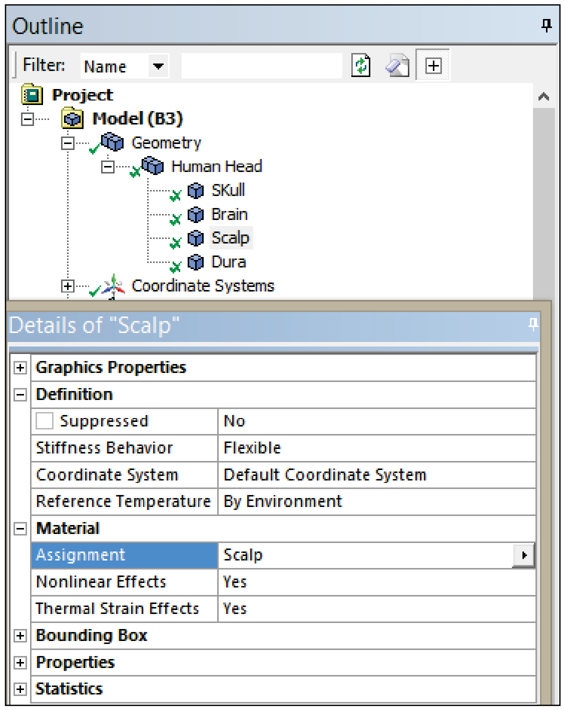

Figure B0.5 Screenshot of Material Assignment process to the Scalp

B.4 Analysis Settings

These are a group of settings that allow setting up of our simulation model according to the actual experimental conditions. Let us consider 45 to frontal region and drop height of 3 feet to understand various controls of Analysis Settings as displayed in Table 2.5

Table B0.17 Analysis Settings: Various Controls

Object Name	*Analysis Settings*
State	Fully Defined
Step Controls	
Number Of Steps	21.
Current Step Number	1.
Step End Time	1.5625e-003 s
Auto Time Stepping	Off
Define By	Substeps
Number Of Substeps	2.
Time Integration	On
Solver Controls	

Solver Type	Program Controlled
Weak Springs	Program Controlled
Large Deflection	On
Restart Controls	
Generate Restart Points	Program Controlled
Retain Files After Full Solve	No
Nonlinear Controls	
Force Convergence	Program Controlled
Moment Convergence	Program Controlled
Displacement Convergence	Program Controlled
Rotation Convergence	Program Controlled
Line Search	Program Controlled
Stabilization	Off
Output Controls	
Stress	Yes
Strain	Yes
Nodal Forces	No
Contact Miscellaneous	No
General Miscellaneous	No
Store Results At	All Time Points
Max Number of Result Sets	Program Controlled
Damping Controls	
Stiffness Coefficient Define By	Direct Input
Stiffness Coefficient	0.
Mass Coefficient	0.
Numerical Damping	Program Controlled
Numerical Damping Value	0.1
Analysis Data Management	
Solver Files Directory	D:\Ansys\final_0_v8_45_3ft_files\dp0\SYS-1\MECH\
Future Analysis	None
Scratch Solver Files Directory	
Save MAPDL db	No
Delete Unneeded Files	Yes
Nonlinear Solution	Yes
Solver Units	Active System
Solver Unit System	mks

- Step Controls:

This defines the number of steps in terms of time intervals that were considered for load input cycle on FE model. These are usually specified by putting 'end time' of each step or event in a load cycle. As explained earlier, the major impact event was also defined in terms of time steps which was inserted in the step controls as shown in Table 2.6. ‘Auto Stepping’ was toggled ‘off’ so that more user-controlled environment can be established however ‘Time Integration’ was toggled ‘on’ so that system can integrate time dependent variables without user inputs. The time cycle was defined based on ‘SubSteps’ instead of ‘Time’ so that uniform distribution of curve can be achieved. The numbers of substeps taken were 2 in order to reduce the processing time since these time steps were gained from data acquisition systems and hence did not need much convergence.

Table B0.18 Step Controls: Time Cycle and end time specifications

Step	Step End Time
1	1.5625e-003 s
2	1.7578e-003 s
3	1.9531e-003 s
4	2.1484e-003 s
5	2.3437e-003 s
6	2.5391e-003 s
7	2.7344e-003 s
8	2.9297e-003 s
9	3.125e-003 s
10	3.3203e-003 s
11	3.5156e-003 s
12	3.7109e-003 s
13	3.9063e-003 s
14	4.1016e-003 s
15	4.2969e-003 s
16	4.4922e-003 s
17	4.6875e-003 s
18	4.8828e-003 s
19	5.0781e-003 s
20	5.2734e-003 s
21	5.4687e-003 s

- Solver Controls:

As the name specifies, these control the way a solver processes solution options. This was set to default ‘Program Controlled’ and ‘Large deflection’ was toggled ‘on’

- Restart Controls:

  These define whether a new solution will start from some points of older solution versions. These were set to default 'Program Controlled' value and the restart files of older solutions were erased after every new run was initiated by setting 'Retains files after Full Solve' to 'No'. This was done in order to avoid log of simulation history files.

- Nonlinear Controls:

  Force, Moment, Displacement and Rotation convergences were set to default 'Program Controlled' values and Stabilization was inactivated in order to record any destabilized activity occurring due to load inputs during the simulation.

- Output Controls:

  A control was established over Stress and Strain results by toggling them to 'Yes' however nodal forces were not constrained by selecting 'No' option for them. Results were stored for 'All data points'. Other options for result storage included 'last time point', 'equally spaced points', 'specified recurrence rate'. Maximum number of result sets were set to default 'Program Controlled' option which was 1000 sets per run.

- Damping Controls:

Damping controls were set to default ‘Program Controlled’ controlled value. Stiffness coefficient was kept as a user input and numerical damping value was 0.1 by default.

- Analysis Data Management:

  Appropriate solver directory was selected facilitating effective book-keeping and well defined location for storage of all results’ log files. The unit system was defined as MKS system for the simulations.

Appendix C

Accelerations' Calculator

Please refer to A-3 (oversized) sheet attached at the end of this document.

Appendix D

Basic Anatomy of Human Head

A background on basic anatomy of head and its terminologies is also provided here to help understand the head injury mechanics better. Hair and facial skin form the outermost layers of the head. These are not considered in this study. As shown in Figure D0.6, scalp is the next layer made up of soft tissue approximately 5 to 7 mm thick and covering the outer surface of the skull. Skull or braincase is made up from bone and varies from 4 to 7 mm in thickness. The Dura matter, the arachnoid and the Pia matter form three membranes of 'the meninges': a protective and nutrition-providing covering of the brain. The subdural and subarachnoid spaces are filled with cerebrospinal fluid (CSF) which is responsible for nutrient supply and signal transportation. It also protects the brain against impacts and blows by providing a cushioning effect. These individual layers are not considered in this study however a layer of Dura matter is considered.

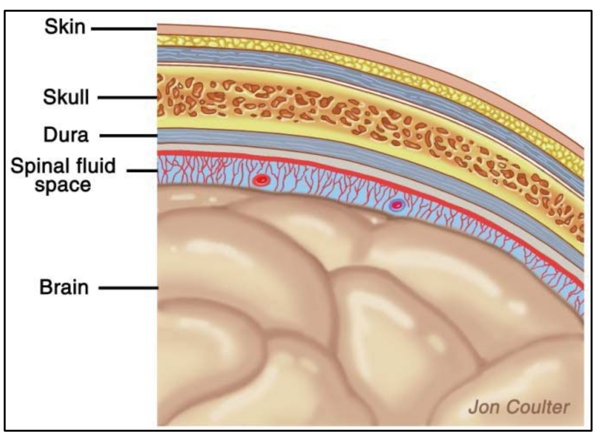

Figure D0.6 Layers of human head [31]

Brain: a huge network of nerve cells can be divided into cerebral hemispheres, cerebellum, midbrain, pons and medulla oblongata. As shown in Figure D0.7, the frontal lobe is located on the anterior side. Adjacent to the frontal lobe is the temporal lobe located on the lateral side of the head. The parietal lobe, located above the temporal lobe, forms the lateral and superior side of the brain. The occipital lobe, located on the posterior side of the head, forms the posterior portion of the cerebral hemispheres. The cerebellum, midbrain, pons, and medulla oblongata, which lie beneath the cerebral hemispheres, form the remaining portion of the brain. The cerebellum is located at the base of the skull below the occipital lobe and parietal lobes. Brain stem connects to the spinal cord.

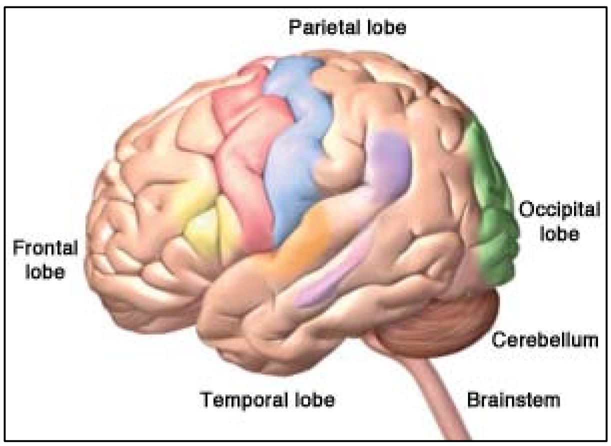

Figure D0.7 Structural differentiation of human brain [32]

References

[1] N. Collins, "The Telegraph," 20 Sep 2013. [Online]. Available: http://www.telegraph.co.uk/science/10322521/Hawking-in-the-future-brains-could-be-separated-from-the-body.html. [Accessed 1 November 2014].

[2] The Brain Preservation Foundation, "The Brain Preservation Foundation," [Online]. Available: http://www.brainpreservation.org/. [Accessed 1 November 2014].

[3] D. Itskov, Interviewee, *Russian entrepreneur Dmitry Itskov dreams of cybernetic immortality*. [Interview]. 8 June 2013.

[4] Neurovigil Inc, "Neurovigil," 2014. [Online]. Available: http://www.neurovigil.com/. [Accessed 2014].

[5] WhiteHouse, "Brain Initiative," 30 September 2014. [Online]. Available: http://www.whitehouse.gov/share/brain-initiative. [Accessed 1 November 2014].

[6] American Academy of Orthopaedic Surgeons, "A silent epidemic: Minor traumatic brain injury.," 10 October 2013. [Online]. Available: http://www.sciencedaily.com/releases/2013/10/131010124740.htm. [Accessed 9 September 2014].

[7] American Heart Association , "Traumatic brain injury linked with tenfold increase in stroke risk," 29 July 2011. [Online]. Available: http://www.sciencedaily.com/releases/2011/07/110728162622.htm. [Accessed 9 September 2014].

[8] The JAMA Network Journals, "Large increase seen in emergency departments visits for

traumatic brain injury," 13 May 2014. [Online]. Available: http://www.sciencedaily.com/releases/2014/05/140513161726.htm. [Accessed 9 September 2014].

[9] Centers for Disease Control and Prevention, National Center for Injury Prevention and Control, "Traumatic Brain Injury in the United States: Fact Sheet," 2 June 2014. [Online]. Available: http://www.cdc.gov/traumaticbraininjury/get_the_facts.html. [Accessed 9 September 2014].

[10] National Hospital Discharge Survey, "Rates of TBI-related Hospitalizations by Age Group — United States, 2001–2010," 24 February 2014. [Online]. Available: http://www.cdc.gov/traumaticbraininjury/data/rates_hosp_byage.html. [Accessed 9 September 2014].

[11] Radiological Society of North America, "Single concussion may cause lasting brain damage," 12 March 2013. [Online]. Available: http://www.sciencedaily.com/releases/2013/03/130312092642.htm. [Accessed 9 September 2014].

[12] McMaster University, "Concussions not taken seriously enough, researcher finds," 8 January 2010. [Online]. Available: http://www.sciencedaily.com/releases/2010/01/100118001721.htm. [Accessed 9 September 2014].

[13] Mary Ann Liebert, Inc., Publishers, "Is there a period of increased vulnerability for repeat traumatic brain injury?," 10 January 2013. [Online]. Available: http://www.sciencedaily.com/releases/2013/01/130110111321.htm. [Accessed 9 September

2014].

[14] Radiological Society of North America, "Concussion patients show Alzheimer's-like brain abnormalities," 18 June 2013. [Online]. Available: http://www.sciencedaily.com/releases/2013/06/130618101727.htm. [Accessed 9 September 2014].

[15] American Academy of Neurology (AAN), "Brain still injured from concussion after symptoms fade," 20 November 2013. [Online]. Available: http://www.sciencedaily.com/releases/2013/11/131120192149.htm. [Accessed 9 September 2014].

[16] American Academy of Neurology (AAN), "Have a brain injury? You may be at higher risk for stroke," 26 June 2013. [Online]. Available: http://www.sciencedaily.com/releases/2013/06/130626162618.htm. [Accessed 9 September 2014].

[17] Wikipedia Contributors, "Sports in the United States," 1 November 2014. [Online]. Available: http://en.wikipedia.org/w/index.php?title=Sports_in_the_United_States&oldid=631955788. [Accessed 1 September 2014].

[18] K. G. Harmon, J. A. Drezner, M. Gammons, K. M. Guskiewicz, M. Halstead, S. A. Herring and W. O. Roberts, "American Medical Society for Sports Medicine position statement: concussion in sport.," *British Journal of Sports Medicine,* pp. 47, 15-62.

[19] American Academy of Pediatrics, "Children with brain injuries nearly twice as likely to suffer from depression," 25 October 2013. [Online]. Available:

http://www.sciencedaily.com/releases/2013/10/131025091934.htm. [Accessed 9 September 2014].

[20] Journal of Neurosurgery Publishing Group, "Children with ADHD more likely to be moderately disabled after mild traumatic brain injury," 25 June 2013. [Online]. Available: http://www.sciencedaily.com/releases/2013/06/130625121146.htm. [Accessed 9 September 2014].

[21] American Academy of Neurology, "After a concussion, which teens will have emotional symptoms?," 10 July 2014. [Online]. Available: http://www.sciencedaily.com/releases/2014/07/140710161523.htm. [Accessed 9 September 2014].

[22] American Academy of Pediatrics, "High school athletes say concussions won't sideline them," 6 May 2013. [Online]. Available: http://www.sciencedaily.com/releases/2013/05/130506095407.htm. [Accessed 9 September 2014].

[23] University of Virginia Health System, "Could a 'trojan horse' better identify traumatic brain injury?," 23 October 2013. [Online]. Available: http://www.sciencedaily.com/releases/2013/10/131023100955.htm. [Accessed 9 September 2014].

[24] University of Rochester Medical Center, "On-field blood test can diagnose sports concussions," 9 January 2014. [Online]. Available: http://www.sciencedaily.com/releases/2014/01/140109004257.htm. [Accessed 9 September 2014].

[25] NFL, "George Mason researchers think saliva might unlock concussions," 29 October 2013. [Online]. Available: http://www.nfl.com/news/story/0ap2000000271940/printable/george-mason-researchers-think-saliva-might-unlock-concussions. [Accessed 29 October 2014].

[26] F. W. R. S, "Internal Head Injury Assessment," in *15th Stapp Car Crash Conference, The Society of Automotive Engineers*, 1971.

[27] O. Anna, K. Clara, P. Andrew, R. Philippe, H. Blaine, M. Shawn, B. Susan, S. Aynsley and C. Michael, "An Examination of Headform Dynamic Responsefor Concussive and Traumatic Brain Injury," in *1st International Conference on Helmet Performance and Design*, London, UK, 2013.

[28] SENSOR PRODUCTS INC., "Fujifilm Prescale® Tactile Pressure Indicating Sensor Film," SENSOR PRODUCTS INC., 2014. [Online]. Available: http://www.sensorprod.com/fuji-prescale.php. [Accessed 25 October 2014].

[29] D. M. Labyak, "Interpretation of Head Injuries Due to Oblique Impact by Finite Element Modeling," Michigan Technological University, Houghton, 2003.

[30] A. Inc, *ANSYS 14.5 Analysis Software*, 2014.

[31] Earsite.com, "Acoustic Neuroma," 2014. [Online]. Available: http://www.earsite.com/acoustic-neuroma-treatment. [Accessed 30 October 2014].

[32] ATrain Education, "Brain Anatomy and the Disorders Associated with Stroke," [Online]. Available: https://www.atrainceu.com/course-module/1473287-62_stroke-acute-care-and-rehab-module. [Accessed 31 October 2014].

Frontal Impact

Axes	X	Y	Z	
Centroid of FE Head model	0.013256	-0.058213	0.076937	Origin
Centroid of Frontal Impact Are	0.01225	0.027753	0.0011979	Point of impact

Frontal Impact : 2 feet

Linear Acceleration			Angular Acceleration	
			Analytical methods	
Topaq Accelerations				
Pressure from films (Pa)	2790000			
Area measured (m2)	0.0028			
Mass of headform (kg)	4.917		Ixx (axis out of nose)	0.0614
			Iyy (axis out of superior head region)	0.1070
Max. Acceleration (m/s2)	1588.773642		Izz (axis out of left ear)	0.0297
			Fx	-9829.5039
Drop Test / Analyser Accelerations			Fy	0.0000
	Gs	**m/s2**	Fz	0.0000
ar (resultant from Siglab)	235.50	2309.47	r(i)	0.0010
ax	203.85	1999.09	r(j)	-0.0860
ay	8.87	86.98	r(k)	0.0757
az	-80.57	-790.12	Mx	0
			My	-745
			Mz	-845.35
			(alpha)x	0.00
			(alpha)y	-6960.71
			(alpha)z	-28433.67
			(alpha)resultant	29273.280

3 feet

Linear Acceleration			Angular Acceleration	
			Analytical methods	
Topaq Accelerations				
Pressure from films (Pa)	2840000			
Area measured (m2)	0.0030615			
Mass of headform (kg)	4.917		Ixx (axis out of nose)	0.0614
			Iyy (axis out of superior head region)	0.1070
Max. Acceleration (m/s2)	1768.28554		Izz (axis out of left ear)	0.0297
			Fx	-12132.1960
Drop Test / Analyser Accelerations			Fy	0.0000
	Gs	**m/s2**	Fz	0.0000
ar (resultant from Siglab)	309.00	3030.22	r(i)	0.0010
ax	251.60	2467.40	r(j)	-0.0860
ay	12.04	118.07	r(k)	0.0757
az	-101.75	-997.84	Mx	0
			My	-918.8
			Mz	-1043.4
			(alpha)x	0
			(alpha)y	-8584.56
			(alpha)z	-35095.15
			(alpha)resultant	36129.83

Frontal Impact : Accelerations' Plot

Heights (feet)	LinearAcc_Topaq	LinearAcc_Drop Tests	AngularAcc_Analytical
2	1588.773642	2309.47	29273.28035
3	1768.28554	3030.22	36129.82997
4	2068.84279	3634.71	43318.60088
5	2483.099451	4219.36	47785.27484

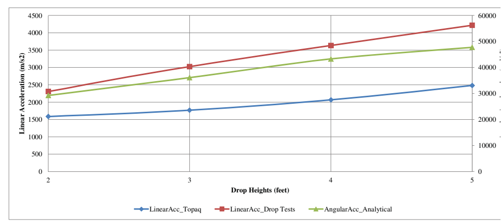

4 feet

Linear Acceleration			Angular Acceleration	
			Analytical methods	
Topaq Accelerations				
Pressure from films (Pa)	3250000			
Area measured (m2)	0.00313			
Mass of headform (kg)	4.917		Ixx (axis out of nose)	0.0614
			Iyy (axis out of superior head region)	0.1070
Max. Acceleration (m/s2)	2068.84279		Izz (axis out of ears)	0.0297
			Fx	-14546.14
Drop Test / Analyser Accelerations			Fy	0.0000
	Gs	**m/s2**	Fz	0.0000
ar (resultant from Siglab)	370.64	3634.71	r(i)	0.0010
ax	301.67	2958.34	r(j)	-0.0860
ay	10.27	100.76	r(k)	0.0757
az	-117.74	-1154.62	Mx	0
			My	-1101.7
			Mz	-1251
			(alpha)x	0
			(alpha)y	-10293.44
			(alpha)z	-42077.86
			(alpha)resultant	43318.60

5 feet

Linear Acceleration			Angular Acceleration	
			Analytical methods	
Topaq Accelerations				
Pressure from films (Pa)	3420000			
Area measured (m2)	0.00357			
Mass of headform (kg)	4.917		Ixx (axis out of nose)	0.0614
			Iyy (axis out of superior head region)	0.1070
Max. Acceleration (m/s2)	2483.099451		Izz (axis out of ears)	0.0297
			Fx	-16044.49
Drop Test / Analyser Accelerations			Fy	0.0000
	Gs	**m/s2**	Fz	0.0000
ar (resultant from Siglab)	430.25	4219.36	r(i)	0.0010
ax	332.74	3263.06	r(j)	-0.0860
ay	20.80	204.00	r(k)	0.0757
az	-154.73	-1517.37	Mx	0
			My	-1215.2
			Mz	-1380
			(alpha)x	0
			(alpha)y	-11353.90
			(alpha)z	-46416.82
			(alpha)resultant	47785.27

45deg to Frontal Impact

Axes	X	Y	Z	
Centroid of FE Head model	0.013256	-0.058213	0.076937	Origin
Centroid of 45 to Front Impact Area	0.06313	0.010446	0.087155	Point of impact

2 feet				
Linear Acceleration			Angular Acceleration	
			Analytical methods	
Topaq Accelerations				
Pressure from films (Pa)	3850000			
Area measured (m2)	0.00302			
Mass of headform (kg)	4.917		Ixx (axis out of nose)	0.0614
			Iyy (axis out of superior head region)	0.1070
Max. Acceleration (m/s2)	2364.653244		Izz (axis out of ears)	0.0297
			Fx	-7087.19
Drop Test / Analyser Accelerations			Fy	0.00
	Gs	**m/s2**	Fz	-7087.19
ar (resultant from Siglab)	205.96	2019.80	r(i)	-0.0499
ax	134.66	1320.57	r(j)	-0.0687
az	150.99	1480.73	r(k)	-0.0102
ay	-47.68	-467.62	Mx	487
a45		2038.4161	My	-281.4
F45		10022.892	Mz	-487
sin45 or cos45		0.7071	(alpha)x	7937.36
			(alpha)y	-2629.19
			(alpha)z	-16380.43
			(alpha)resultant	18391.11

3 feet				
Linear Acceleration			Angular Acceleration	
			Analytical methods	
Topaq Accelerations				
Pressure from films (Pa)	4040000			
Area measured (m2)	0.00302			
Mass of headform (kg)	4.917		Ixx (axis out of nose)	0.0614
			Iyy (axis out of superior head region)	0.1070
Max. Acceleration (m/s2)	2481.350417		Izz (axis out of ears)	0.0297
			Fx	-8576.92
Drop Test / Analyser Accelerations			Fy	0.00
	Gs	**m/s2**	Fz	-8576.92
ar (resultant from Siglab)	255.21	2502.75	r(i)	-0.0499
ax	167.90	1646.55	r(j)	-0.0687
az	180.58	1770.86	r(k)	-0.0102
ay	-49.80	-488.35	Mx	589.3
a45		2466.89	My	-340.5
F45		12129.7	Mz	-589.3
sin45 or cos45		0.7071	(alpha)x	9604.69
			(alpha)y	-3181.37
			(alpha)z	-19821.33
			(alpha)resultant	22254.36

45 to Front Impact : Accelerations' Plot			
Heights (feet)	LinearAcc_Topaq	LinearAcc_Drop Tests	AngularAcc_Analytical
2	2364.65	2019.80	18391.11
3	2481.35	2502.75	22254.36
4	3144.97	3017.99	26185.66
5	3418.12	3427.09	29433.38

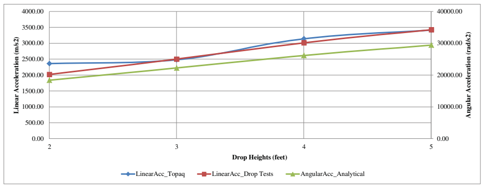

4 feet				
Linear Acceleration			Angular Acceleration	
			Analytical methods	
Topaq Accelerations				
Pressure from films (Pa)	4260000			
Area measured (m2)	0.00363			
Mass of headform (kg)	4.917		Ixx (axis out of nose)	0.0614
			Iyy (axis out of superior head region)	0.1070
Max. Acceleration (m/s2)	3144.966443		Izz (axis out of ears)	0.0297
			Fx	-10093.86
Drop Test / Analyser Accelerations			Fy	0.00
	Gs	**m/s2**	Fz	-10093.86
ar (resultant from Siglab)	307.75	3017.99	r(i)	-0.0499
ax	195.25	1914.77	r(j)	-0.0687
az	213.86	2097.26	r(k)	-0.0102
ay	-61.49	-603.05	Mx	693.4
a45		2903.1943	My	-400.7
F45		14275.006	Mz	-693.4
sin45 or cos45		0.7071	(alpha)x	11301.37
			(alpha)y	-3743.83
			(alpha)z	-23322.77
			(alpha)resultant	26185.66

5 feet				
Linear Acceleration			Angular Acceleration	
			Analytical methods	
Topaq Accelerations				
Pressure from films (Pa)	4630000			
Area measured (m2)	0.00363			
Mass of headform (kg)	4.917		Ixx (axis out of nose)	0.0614
			Iyy (axis out of superior head region)	0.1070
Max. Acceleration (m/s2)	3418.120805		Izz (axis out of ears)	0.0297
			Fx	-11345.04
Drop Test / Analyser Accelerations			Fy	0.00
	Gs	**m/s2**	Fz	-11345.04
ar (resultant from Siglab)	349.47	3427.09	r(i)	-0.0499
ax	220.15	2158.97	r(j)	-0.0687
az	240.04	2354.01	r(k)	-0.0102
ay	-68.03	-667.11	Mx	779.4
a45		3263.06	My	-450.4
F45		16044.5	Mz	-779.4
sin45 or cos45		0.7071	(alpha)x	12703.03
			(alpha)y	-4208.19
			(alpha)z	-26215.41
			(alpha)resultant	29433.38

Lateral / Side Impact

Axes	X	Y	Z	
Centroid of FE Head model	0.013256	-0.058213	0.076937	Origin
Centroid of Side Impact Area	-0.05059	-0.035948	0.04107	Point of impact

2 feet

Linear Acceleration			Angular Acceleration	
			Analytical methods	
Topaq Accelerations				
Pressure from films (Pa)	3320000			
Area measured (m2)	0.00522			
Mass of headform (kg)	4.917		Ixx (axis out of nose)	0.0614
			Iyy (axis out of superior head region)	0.1070
Max. Acceleration (m/s2)	3524.588164		Izz (axis out of ears)	0.0297
			Fx	0.0000
Drop Test / Analyser Accelerations			Fy	0.0000
	Gs	**m/s2**	Fz	-11557.44
ar (resultant from Siglab)	261.23	2561.83	r(i)	0.0638
ax	5.77	56.60	r(j)	-0.0223
ay	-14.96	-146.73	r(k)	0.0359
az	239.68	2350.51	Mx	257.7
			My	737
			Mz	0
			(alpha)x	4200.12
			(alpha)y	6885.96
			(alpha)z	0.00
			(alpha)resultant	8065.82

3 feet

Linear Acceleration			Angular Acceleration	
			Analytical methods	
Topaq Accelerations				
Pressure from films (Pa)	3490000			
Area measured (m2)	0.00577			
Mass of headform (kg)	4.917		Ixx (axis out of nose)	0.0614
			Iyy (axis out of superior head region)	0.1070
Max. Acceleration (m/s2)	4095.444377		Izz (axis out of ears)	0.0297
			Fx	0.0000
Drop Test / Analyser Accelerations			Fy	0.0000
	Gs	**m/s2**	Fz	-13365.98
ar (resultant from Siglab)	345.36	3386.80	r(i)	0.0638
ax	-8.72	-85.48	r(j)	-0.0223
ay	-8.13	-79.75	r(k)	0.0359
az	277.19	2718.32	Mx	298.1
			My	852.7
			Mz	0
			(alpha)x	4858.58
			(alpha)y	7966.98
			(alpha)z	0.00
			(alpha)resultant	9331.59

4 feet

Linear Acceleration			Angular Acceleration	
			Analytical methods	
Topaq Accelerations				
Pressure from films (Pa)	3550000			
Area measured (m2)	0.00604			
Mass of headform (kg)	4.917		Ixx (axis out of nose)	0.0614
			Iyy (axis out of superior head region)	0.1070
Max. Acceleration (m/s2)	4360.789099		Izz (axis out of ears)	0.0297
			Fx	0.0000
Drop Test / Analyser Accelerations			Fy	0.0000
	Gs	**m/s2**	Fz	-14689.20
ar (resultant from Siglab)	398.65	3909.42	r(i)	0.0638
ax	32.60	319.75	r(j)	-0.0223
ay	-4.12	-40.40	r(k)	0.0359
az	304.63	2987.43	Mx	327.5
			My	937.1
			Mz	0
			(alpha)x	5337.75
			(alpha)y	8755.55
			(alpha)z	0
			(alpha)resultant	10254.32

5 feet

Linear Acceleration			Angular Acceleration	
			Analytical methods	
Topaq Accelerations				
Pressure from films (Pa)	3640000			
Area measured (m2)	0.00641			
Mass of headform (kg)	4.917		Ixx (axis out of nose)	0.0614
			Iyy (axis out of superior head region)	0.1070
Max. Acceleration (m/s2)	4745.251169		Izz (axis out of ears)	0.0297
			Fx	0.0000
Drop Test / Analyser Accelerations			Fy	0.0000
	Gs	**m/s2**	Fz	-14910.07
ar (resultant from Siglab)	463.09	4541.33	r(i)	0.0638
ax	17.46	171.19	r(j)	-0.0223
ay	5.40	52.96	r(k)	0.0359
az	309.21	3032.35	Mx	332.5
			My	951.3
			Mz	0
			(alpha)x	5419.24
			(alpha)y	8888.22
			(alpha)z	0.00
			(alpha)resultant	10410.03

Side Impact : Accelerations' Plot

Heights (feet)	LinearAcc_Topaq	LinearAcc_Drop Tests	AngularAcc_Analytical
2	3524.588164	2561.83	8065.822588
3	4095.444377	3386.80	9331.585087
4	4360.789099	3909.42	10254.32454
5	4745.251169	4541.33	10410.02655

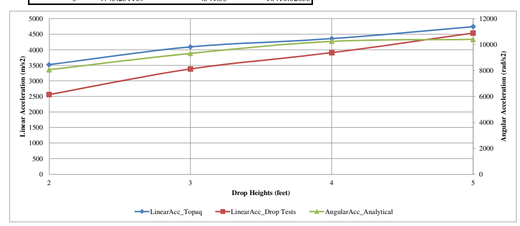

Posterior / Rear Impact

Axes	X	Y	Z	
Centroid of FE Head model	0.013256	-0.058213	0.076937	Origin
Centroid of Rear Impact Area	0.0073938	-0.11593	-0.0076186	Point of impact

2 feet

Linear Acceleration			Angular Acceleration	
			Analytical methods	
Topaq Accelerations				
Pressure from films (Pa)	2770000			
Area measured (m2)	0.00341			
Mass of headform (kg)	4.917		Ixx (axis out of nose)	0.0614
			Iyy (axis out of superior head region)	0.1070
Max. Acceleration (m/s2)	1921.029083		Izz (axis out of ears)	0.0297
			Fx	9007.13
Drop Test / Analyser Accelerations			Fy	0.0000
	Gs	**m/s2**	Fz	0.0000
ar (resultant from Siglab)	253.85	2489.46	r(i)	0.0059
ax	186.80	1831.84	r(j)	0.0577
ay	13.36	131.05	r(k)	0.0846
az	-139.28	-1365.82	Mx	0
			My	762
			Mz	-519.7
			(alpha)x	0
			(alpha)y	7119.55
			(alpha)z	-17480.31
			(alpha)resultant	18874.56

3 feet

Linear Acceleration			Angular Acceleration	
			Analytical methods	
Topaq Accelerations				
Pressure from films (Pa)	3900000			
Area measured (m2)	0.00389			
Mass of headform (kg)	4.917		Ixx (axis out of nose)	0.0614
			Iyy (axis out of superior head region)	0.1070
Max. Acceleration (m/s2)	3085.417938		Izz (axis out of ears)	0.0297
			Fx	11167.75
Drop Test / Analyser Accelerations			Fy	0.0000
	Gs	**m/s2**	Fz	0.0000
ar (resultant from Siglab)	330.71	3243.11	r(i)	0.0059
ax	231.60	2271.25	r(j)	0.0577
ay	12.78	125.28	r(k)	0.0846
az	-173.11	-1697.60	Mx	0
			My	944.2
			Mz	-644.4
			(alpha)x	0
			(alpha)y	8821.88
			(alpha)z	-21674.64
			(alpha)resultant	23401.19

Rear Impact : Accelerations' Plot			
Heights (feet)	LinearAcc_Topaq	LinearAcc_Drop Tests	AngularAcc_Analytical
2	1921.029083	2489.46	18874.56059
3	3085.417938	3243.11	23401.18704
4	3311.083994	3923.55	29268.14468
5	3553.386211	4516.85	31407.38246

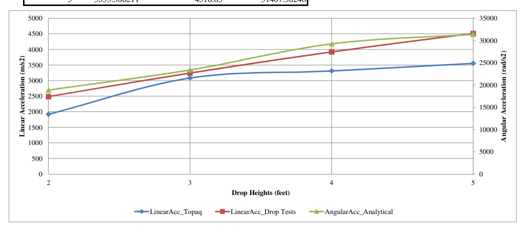

4 feet

Linear Acceleration			Angular Acceleration	
			Analytical methods	
Topaq Accelerations				
Pressure from films (Pa)	4010000			
Area measured (m2)	0.00406			
Mass of headform (kg)	4.917		Ixx (axis out of nose)	0.0614
			Iyy (axis out of superior head region)	0.1070
Max. Acceleration (m/s2)	3311.083994		Izz (axis out of ears)	0.0297
			Fx	13967.93
Drop Test / Analyser Accelerations			Fy	0.0000
	Gs	**m/s2**	Fz	0.0000
ar (resultant from Siglab)	400.09	3923.55	r(i)	0.0059
ax	289.68	2840.74	r(j)	0.0577
ay	8.26	80.98	r(k)	0.0846
az	-225.53	-2211.69	Mx	0
			My	1181
			Mz	-805.95
			(alpha)x	0
			(alpha)y	11034.36
			(alpha)z	-27108.43
			(alpha)resultant	29268.14

5 feet

Linear Acceleration			Angular Acceleration	
			Analytical methods	
Topaq Accelerations				
Pressure from films (Pa)	4200000			
Area measured (m2)	0.00416			
Mass of headform (kg)	4.917		Ixx (axis out of nose)	0.0614
			Iyy (axis out of superior head region)	0.1070
Max. Acceleration (m/s2)	3553.386211		Izz (axis out of ears)	0.0297
			Fx	14989.17
Drop Test / Analyser Accelerations			Fy	0.0000
	Gs	**m/s2**	Fz	0.0000
ar (resultant from Siglab)	460.59	4516.85	r(i)	0.0059
ax	310.85	3048.44	r(j)	0.0577
ay	9.60	94.17	r(k)	0.0846
az	-246.21	-2414.52	Mx	0
			My	1267.3
			Mz	-864.86
			(alpha)x	0
			(alpha)y	11840.68
			(alpha)z	-29089.89
			(alpha)resultant	31407.38